UNIVERSITÀ DEGLI STUDI DI PAVIA

DOTTORATO IN SCIENZE CHIMICHE E FARMACEUTICHE

XXIX CICLO

Coordinatore: Chiar.mo Prof. Mauro Freccero

MULTIFUNCTIONAL THERAPEUTIC SYSTEMS FOR TISSUE REPAIRING

Tutore

Chiar.ma Prof.ssa Silvia Rossi

Silvia Rossi

Tesi di Dottorato di

MARIKA TENCI

Marika Tenci

A.A. 2015- 2016

SUMMARY

Premise

Tissue-repairing is one of the most important challenges in biomedical field. The recovery of tissue damages is essential for slowing and reverting the progression of lesions and for restoring tissue functions, particularly when the tissue damage is concomitant to pathological conditions, such as diabetes and malignancies, persistent infections, or other patient related factors. The classical approach based on drug treatment has been recently combined with the use of technological platforms able to play an active role on repairing/regeneration mechanisms. This could provide important advancements in developing alternative, complementary and more efficacious treatments.

The aim of the research activity was the development of innovative systems for the treatment of chronic wounds and ulcerative colitis. As for skin lesions, powder formulations, based on biopolymers, and hybrid/polymers films intended for the delivery of natural bioactive agents (such as manuka honey and essential oils) as such or in association with platelet lysate, a hemoderivative well-known for its tissue repairing properties (Rossi et al., 2015; Mori et al., 2016a) were studied. Moreover, an *in situ* gelling system loaded with a plant extract rich in anthocyanins was developed for the treatment of ulcerative colitis.

The first year of the research was focused on the development of pectin (PEC) /chitosan (CS) particles for the combined delivery of manuka honey (MH) bioactive components and platelet lysate (PL) (**Chapter 1**). Manuka honey, obtained from the nectar of *Leptospermum scoparium*, is approved by FDA for clinical purposes (Boateng and Catanzano, 2015). Particles were prepared by ionotropic gelation by dropping a PEC aqueous solution in an aqueous mixture of $CaCl_2$ and CS glutamate and freeze-dried. In order to obtain particles characterized by optimal technological properties (low size, high hydration properties and suitable mechanical resistance), different experimental conditions ($CaCl_2$ and CS concentrations, rest time in the cationic solution) were considered. Two different fractions of MH were examined: one (Fr1), rich in polar substances (sugars, methylglyoxal (MGO), dicarbonyl compounds), the other (Fr2), rich in polyphenols. Particles, characterized by the best technological properties, were loaded with PL and Fr1, since only Fr1 proved to be able of enhancing *in vitro* fibroblast proliferation. *In vivo* results on a rat wound model demonstrated that Fr1-loaded particles improved significantly wound healing with a potency comparable to that observed for PL-loaded particles. It must be underlined that Fr1 is more easily recovered and manipulated than PL and its use does not determine problems related to a heterologous administration of hemoderivatives. Moreover, separation of Fr1 from other honey components is not expensive, thus resulting in an affordable therapy in terms of costs.

Given the promising results obtained for MH Fr1 as wound healing agent, the early six months of the second year of the research was devoted to the preparation and optimization of a vehicle able to deliver Fr1 and to improve its efficacy, thanks to the association with hyaluronic acid (HA), a

biopolymer known for its tissue repairing properties (Frenkel, 2012) (**Chapter 2**). In particular, PEC/CS/ HA mini-capsules were prepared by inverse ionotropic gelation which implied to drop a CS/$CaCl_2$/Fr1 aqueous solution in a PEC/HA aqueous solution. The optimization of mini-capsules formulation was assisted by a DoE approach. The experimental design consisted of a screening phase and an optimization one. In the screening phase, a "full factorial design" (FFD) was employed to investigate the effect of various factors (CS, PEC and HA concentrations) on the response variables (particle size, capability to absorb wound exudate and mechanical resistance). The expansion of FFD to a "central composite design" (CDD) permitted to find the optimal composition of mini-capsules. The experimental results obtained from the characterization of the optimized mini-capsules were in line with the predicted ones, confirming the predictive power of the model. Fr1-loaded mini-capsules were able to promote *in vitro* cell proliferation and showed antimicrobial activity against *S. aureus* and *S. pyogenes*. The *in vivo* results on a rat model proved the capability of Fr1-loaded mini-capsules to stimulate tissue growth, enhancing epithelization and minimizing scar formation.

During the second half of the same year, an innovative *in situ* gelling system was developed for the treatment of ulcerative distal colitis (**Chapter 3**). Three polymers, characterized by different functional properties, have been investigated: gellan (GG), able to gelify in presence of ions, methylcellulose (MC), capable of thermogelling at a temperature higher than the physiological one ($tg \geq 50°C$), and hydroxypropyl cellulose (HPC), a mucoadhesive agent. A DoE approach was used: a "simplex centroid design" was applied to find the optimal composition of the vehicle. The response variables considered were: vehicle viscosity at room temperature, increase in vehicle viscosity resulting from the increase in temperature (from room to physiological value) and the dilution with simulated colonic fluid (SCF), viscoelastic behavior, tixotropic area and mucoadhesion properties of the gel formed at 37°C upon dilution in SCF. Surprisingly, GG addition to MC solution resulted in a decrease of gelation temperature which occurred in the range 35-40°C. The vehicle developed was loaded with maqui berry extract (MBE), known for antioxidant and anti-inflammatory properties. MBE was obtained from the fruits of maqui berry (*Aristotelia chilensis*), a plant species cultivated in central and southern Chile (Tanaka et al., 2013). MBE loading (0.5% w/w) into the vehicle improved rheological and mucoadhesive properties, functional to a better spreading and a longer permanence of the formulation onto mucosa. Loaded formulation showed *in vitro* antioxidant activity on both human fibroblast (NHDF) and human colorectal adenocarcinoma (Caco-2) cell lines.

In the third year of the research, clay/carvacrol (CVR) hybrids were prepared and loaded into *in situ* gelifying viscoelastic films, intended for the treatment of infected skin lesions (**Chapter 4**). CRV, a

monoterpene phenolic compound, is the major component (up to 80%) of oregano essential oil. It possesses antioxidant, antifungal and antimicrobial properties (Tunç and Duman, 2011). The main disadvantage of essential oils (EOs) is their volatility. Several strategies were proposed to reduce EOs evaporation. One of these provides the inclusion of EOs in montmorrilonite and halloysite clays. Recently, some authors proposed the use of such clays as packaging materials and demonstrated their capability to enhance the thermal stability and to preserve the antimicrobial properties of EOs (Efrati et al., 2014; Gorrasi et al., 2015; Shemesh et al., 2015). So far, to the best of my knowledge, no papers have been published on the use of EOs/clay hybrids loaded into films for cutaneous application.

Given these premises, three different clays, commonly employed as pharmaceutical excipients, have been considered: montmorrilonite (MMT), halloysite (HAL) and a commercial palygorskite (PHC).

In a first phase of the research, CVR and CVR/clay hybrids were prepared using two different approaches: adsorption in saturated atmosphere and shear mixing. Hybrids were subjected to thermal analysis in order to study the effect of clay type and of preparation method on CRV volatility. The hybrid prepared with PHC using shear mixing method allowed the highest CRV loading (i.e. the lowest EO volatility) and was chosen for the continuation of the research. CRV/PHC hybrid (HYBD) was *in vitro* investigated for citocompatibility, antioxidant activity and antimicrobial properties against *S. aureus* and *E. coli*.

In the second phase, the research was devoted to the preparation and optimization of films to be used as vehicle for HYBD. Films should be characterized by suitable mechanical properties (high flexibility and resistance to rupture) and by the capability to absorb wound exudate forming a viscoelastic persistent gel, able to protect the lesion area without impairing CRV release.

Films, composed by poly(vinyl alcohol) (PVA), polyvinylpirrolidone (PVP) and chitosan glutamate (CS), were prepared by casting a HYBD suspension in the polymer mixture. Sericin (SER) was added to improve HYBD antioxidant properties (Mori et al., 2016b). A DoE approach was employed to obtain films of optimized composition. The experimental design provided a screening and an optimization phase. In the screening phase a FFD was used. The response variables considered were: film flexibility, mechanical strength, hydration capability and durability of the gel formed upon film hydration in a medium mimicking wound exudate. To find the formulation of optimized composition, the screening design was expanding to a CDD. The experimental results obtained for the optimized formulation were comparable to those predicted and confirmed the predictive power of the model. HYBD loaded film was able to improve cell proliferation and to control CRV release. It also showed *in vitro* antimicrobial activity against *E. coli* and *S. aureus.*

REFERENCES

Boateng, J., Catanzano, O., 2015. Advanced therapeutic dressings for effective wound healing - A review. J. Pharm. Sci. 104, 3653–3680.

Efrati, R., Natan, M., Pelah, A., Haberer, A., Banin, E., Dotan, A., Ophir, A., 2014. The combined effect of additives and processing on the thermal stability and controlled release of essential oils in antimicrobial films. J. Appl. Polym. Sci. 131, 40564-40574.

Frenkel, J.S., 2012. The role of hyaluronan in wound healing. Int. Wound J. 11, 159-163.

Gorrasi, G., 2015. Dispersion of halloysite loaded with natural antimicrobials into pectins: characterization and controlled release analysis. Carbohydrate Polymers. 127, 47–53.

Mori, M., Rossi, S., Ferrari, F., Bonferoni, M.C., Sandri, G., Riva, F., Tenci, M., Del Fante, C., Nicoletti, G., Caramella, C., 2016a. Sponge-like dressings based on the association of chitosan and sericin for the treatment of chronic skin ulcers. II. Loading of the hemoderivative platelet lysate. J. Pharm. Sci. 105, 1188–1195.

Mori, M., Rossi, S., Ferrari, F., Bonferoni, M.C., Sandri, G., Riva, F., Tenci, M., Del Fante, C., Nicoletti, G., Caramella, C., 2016b. Sponge-like dressings based on the association of chitosan and sericin for the treatment of chronic skin ulcers. II. Loading of the hemoderivative platelet lysate. J. Pharm. Sci. 105, 1188-1195.

Rossi, S., Ferrari, F., Sandri, G., Bonferoni, M.C., Del Fante, C., Perotti, C., Caramella, C., 2015. Wound healing: biopolymers and hemoderivatives, In: Mishra, M. (Ed.), Encyclopedia of Biomedical Polymers and Polymeric Biomaterials 1st ed., vol. 11. Taylor & Francis, New York, pp. 8280–8298.

Shemesh, R., Krepker, M., Natan, M., Danin-Poleg, Y., Banin, E., Kashi, Y., Nitzan, N., Vaxmanb, A., Segal, E, 2015. Novel LDPE/halloysite nanotube films with sustained carvacrol release for broad-spectrum antimicrobial activity. RSC Adv. 5, 87108 –87117.

Tanaka, J., Kadekaru, T., Ogawa, K., Hitoe, S., Shimoda, H., Hara, H., 2013. Maqui berry (*Aristotelia chilensis*) and the constituent delphinidin glycoside inhibit photoreceptor cell death induced by visible light. Food Chem. 139, 129-137.

Tunç, S., Duman, O., 2011. Preparation of active antimicrobial methyl cellulose/carvacrol/ montmorillonite nanocomposite films and investigation of carvacrol release. LWT - Food Sci. Tech. 44, 465-472.

Introduction

1 WOUNDS

According to the "Wound Healing Society" a wound consists of a disruption of the normal anatomic structure and functionality of a tissue (Lazarus et al., 1994). Based on the nature of the repair process wounds have been divided in two categories: acute and chronic wounds (Boateng and Catanzano, 2015).

Acute wounds are tissue injuries that completely heal within 12 weeks with minimal scar formation (Percival, 2002). These wounds arise from external factors and include: mechanical injuries, like abrasions and tears, caused by frictional contact of the skin with a hard surface; burns and chemical injuries (Boateng and Catanzano, 2015).

Chronic wounds, unlike acute ones, are injuries that normally do not heal beyond 12 weeks and often reoccur (Gurtner et al., 2008). Such wounds fail to heal due to repeated trauma to the lesion area, co-morbidities, like diabetes and malignancies, or bacteria contamination (Moore et al., 2006). All these causes provide a disruption of the orderly sequence of events during the wound healing process (Broderick, 2009). Depending on pathogenesis, chronic wounds have been mainly divided into 3 groups: leg ulcers, including venous, ischemic and traumatic ulcers, diabetic ulcers and pressure ulcers (Boateng et al., 2008).

Another wound classification is based on the number of skin layers and area involved (Bolton and van Rijswijk, 1991). An injury that concerns only the epidermal skin surface is considered as a superficial wound. A partial thickness wound is defined as an injury compromising the integrity of both epidermis and dermal layers, including blood vessels, sweat glands and hair follicles. Full thickness wounds occur when the damage is not only located to the epidermis and dermal layers, but also to the subcutaneous fat and/or deeper tissues (Boateng et al., 2008).

2 WOUND HEALING

Wound healing is a complex dynamic process, relating to growth and tissue regeneration. Such process involves several inter-related cellular, humoral and molecular mechanisms to reestablish the anatomic and function integrity of the damaged tissue and to replace lost tissue. The wound healing process comprises five interdependent and overlapping stages (Figure 1): hemostasis, inflammation, migration, proliferation and remodelling or maturation (Boateng et al., 2008).

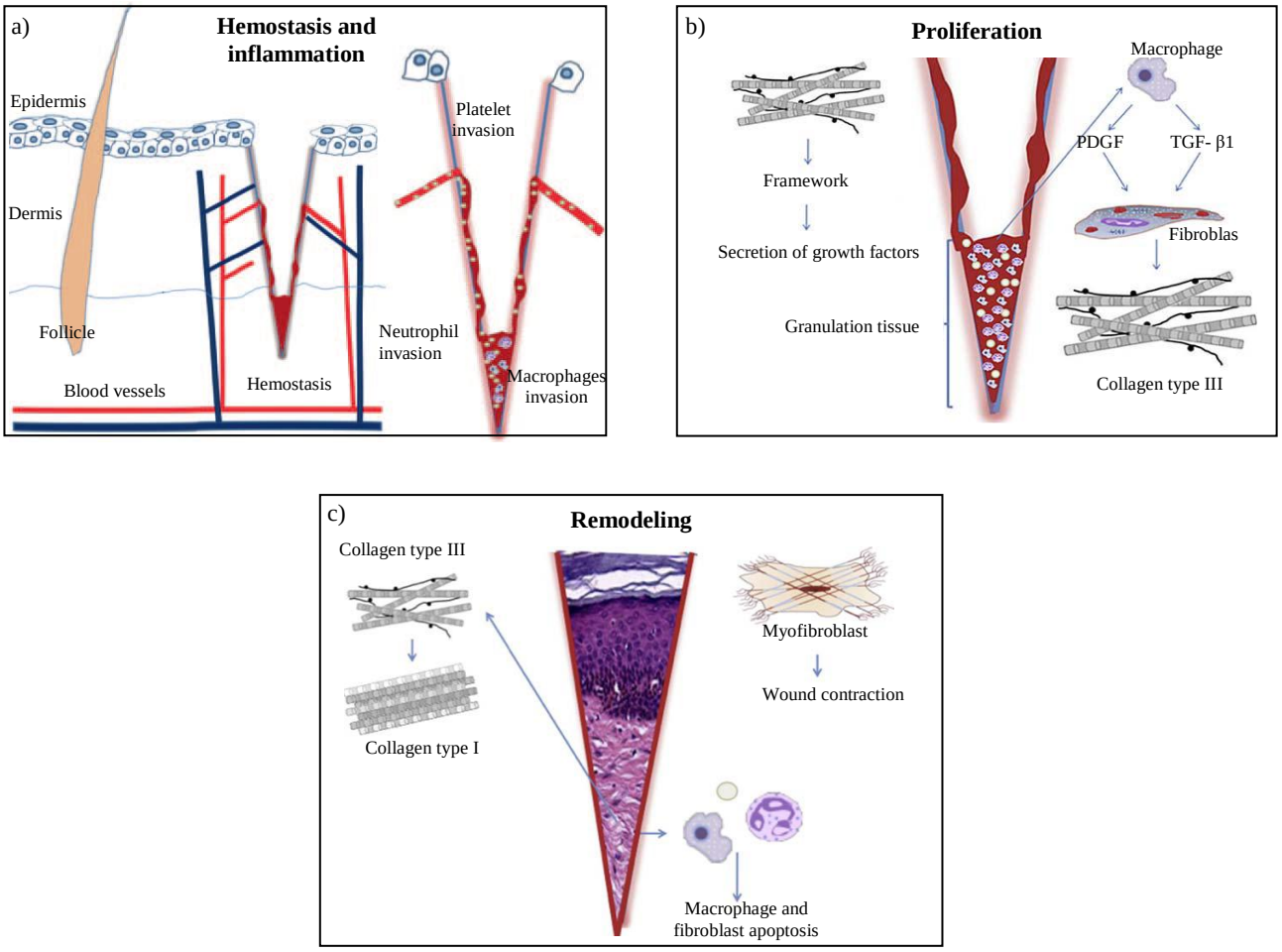

Figure 1 - Schematic representation of the phases of wound healing: (a) neutrophils invade wound area; (b) organization of the thrombus, secretion of growth factors and synthesis of collagen III; (c) reorganization of the connective tissue and wound contraction (modified from Reinke and Sorg, 2012).

2.1 Hemostasis and coagulation

As a result of tissue injury, bleeding usually occurs to remove bacteria and/or antigens from the lesion area. Afterward, haemostasis through the involvement of exudate components (i.e. clotting factors) begins. Many clotting factors, like fibrinogen, and thrombocytes are able to activate the

clotting cascade, resulting in clot formation (Singer and Clark, 1999; Reinke and Sorg, 2012). Furthermore, haemostasis triggers the inflammatory process, which involves both cellular and vascular responses (Reinke and Sorg, 2012).

Platelets play an important role in the wound healing process. In fact, they not only trigger vasoconstriction, reducing bleeding, but also secrete several relevant mediators, like growth factors (i.e. PDGF and TGF-β), as chemotactic agents, which affect the infiltration of leukocytes in the wound area (Singer and Clark, 1999; Reinke and Sorg, 2012). Moreover, the blood clot is rich in growth factors and in some constituents, such as fibrin molecules, fibronectin, vitronectin and thrombospondins, of the temporary extracellular matrix (ECM), able to induce the migration of leukocytes, keratinocytes, fibroblasts and endothelial cells (Boateng et al., 2008; Reinke and Sorg, 2012).

In addition, both platelets and leukocytes release cytokines and growth factors, which have been recognized as activators of the inflammatory process (Reinke and Sorg, 2012).

2.2 Inflammation

The inflammatory phase can be divided into an early step, focused on neutrophil role, and a late step with the appearance and transformation of monocytes. In the first days after injuries, neutrophils are recruited to the lesion area due to their ability in phagocytosis and protease secretion. Neutrophils are chemoattractants for other cells involved in the inflammatory phase, they also release mediators, including growth factors (i.e. TNF-α) and cytokines (i.e. IL-1β and IL-6), which amplify the inflammatory response (Eming et al., 2007).

Approximately 3 days after injury, macrophages invade wound site, activate phagocytosis of pathogens and cell debris, and secrete chemokines and cytokines (Tziotzios et al., 2012; Profyris et al., 2012). Some of these molecules are able to trigger the proliferative phase of wound healing (Gurtner et al., 2008).

2.3 Migration

Such phase consists in the migration of epithelial cells and fibroblasts to the lesion area (Boateng et al., 2008).

2.4 Proliferation

This phase, occuring approximately 3-10 days after injury, is focused on three different processes: reepithelialization, angiogenesis and granulation tissue formation.

Cytokines, such as IFN-γ and TGF-β, induce fibroblasts to produce collagen, fibronectin and other basic substances needed for wound healing. The role of cytokines is very important to allow the formation of a new matrix of connective tissue and consequently to provide the closure of tissue gap and to restore tissue functionality. Subsequently, an increase in collagen synthesis occurs, while fibroblasts proliferation declines, a balance between synthesis and degradation of ECM is reached (Reinke and Sorg, 2012).

2.4.1 Reepithelization

The reepithelization process is activated by signalling pathways of epithelial and non-epithelial cells at the wound edges, associated with the release of a variety of cytokines and growth factors (Werner and Grose, 2003).

Furthermore, cells at the wound edges undergo marked phenotypic alterations, such as retraction and reorganization of their intracellular tonofilaments in the direction of migration (Singer and Clark, 1999; Reinke and Sorg, 2012). The enzymatic loosening of the intercellular desmosomes via collagenase and elastase allow keratinocytes migration (also called "shuffling") along the preformed fibrin filaments in the granulation tissue (Jacinto et al. 2001).

Moreover, keratinocytes secrete the plasminogen activator, which is able to activate plasmin and collagenase, and therefore facilitates the degradation of collagen and proteins of ECM (Singer and Clark, 1999).

2.4.2 Angiogenesis

Angiogenesis is a complex process, involving a variety of cellular, humoral and molecular mechanisms to re-establish a suitable nutritive perfusion. It is initiated by growth factors, like VEGF, PDGF, bFGF, and thrombin, a serine protease that dissolves the basal lamina. After their proliferation and migration into the wound area, the endothelial cells release matrix metalloproteinases. New small tubular canals grow forming a vessel loop. Thereafter, the differentiation of the new vessels into arteries and venules occurs and the angiogenic process is completed (Reinke and Sorg, 2012).

2.4.3 Granulation Tissue Formation

The proliferation phase has been concluded developing a granulation tissue, and at the same time the remodelling phase starts. The granulation tissue is transitional; it replaces the provisional wound matrix, containing fibrin and fibronectin, and finally produces a scar (Reinke and Sorg, 2012). Simultaneously, fibroblasts, granulocytes, macrophages, capillaries and loosely organized collagen

bundles move into the wound site (Singer and Clark, 1999; Reinke and Sorg, 2012). The granuation tissue is highly vascularized, it appears with a classic redness and might be easily damaged. In this phase fibroblasts represent the dominating cells; they are responsible for the synthesis of collagen and ECM components (i.e. fibronectin, glycosaminoglycans, proteoglycans and hyaluronic acid), and also for the deposition and remodelling of ECM (Singer and Clark, 1999; Reinke and Sorg, 2012). The new ECM constitutes a scaffold for cell adhesion, regulates and organizes the growth, movement and differentiation of the cells inside itself (Eckes et al., 2010; Barker, 2011).
At the end of this phase the matureed fibroblasts are subjected to myofibroblast differentiation and afterward to apoptosis (Hinz, 2007).

2.5 Remodeling

This phase, also called maturation, is characterized by the formation of cellular connective tissue and by the strengthening of the new epithelium. During wound remodelling the components of ECM undergo some changes. Collagen III, produced in the proliferative phase, has been replaced by collagen I, with a higher strength. Subsequently, the myofibroblasts determine wound contractions, helpful to the decrease of the surface of the developing scar (Gurtner, 2000; Boateng et al. 2008).

3 FACTORS AFFECTING WOUND HEALING

Factors, that impair wound healing, may be divided in two major categories: local and systemic factors. Local factors are those that directly affect the environment around the lesion during the wound healing, while systemic factors are the overall health or disease state of the patient that determine the disruption of one or more stages of the healing process. Normally, a wound fails to heal due to multiple inter-related factors (Nawaz and Bentley, 2011).
In chronic wounds, an excessive secretion of exudate, rich in proteinase enzymes, inhibits or delays wound healing, causing maceration of the healthy tissues around the wound. Therefore, exudate produces a bad smell and has a negative impact on quality of life (QoL) (Boateng et al., 2008).
The presence of foreign bodies inside the wound area can induce a chronic inflammatory response and can also determine the formation of granuloma or abscess, resulting in healing delay (Boateng et al., 2008).
Commonly, bacteria contamination can interfere with the ordely sequence of events during the wound healing. Among these bacteria, *P. aeruginosa and S. aureus* have been recognized to reduce healing rate of ulcers or to cause the wound reappearance (Boateng et al., 2008).

Old age, malnutrition or specific nutrient deficiencies reduce the ability to fight infection and can prolong wound healing after a traumatic event or surgery. In particular, protein, vitamin (e.g. vitamin C) and mineral deficiencies can affect the healing process, impairing the inflammatory stage and collagen synthesis (Arnold and Barbul, 2006).

In the case of underlying pathological diseases, including diabetes and anaemia, the healing time is prolonged due to an inadequate blood circulation, nutrients and oxygen supply (Boateng et al., 2008). Oxygen is an essential nutrient for cell methabolism. A chronic hypoxic damage affects the proliferative phase of the wound healing. In particular, hypoxia reduces the production of granulation tissue and delays the re-epithalization (Tandara and Mustoe, 2004).

Some drugs, that affected coagulation, inflammatory or proliferative phase, have a significant impact on healing. Among these, systemic glucocorticoid steroids, that are commonly used as anti-inflammatory agents, have been known to inhibit fibroblast proliferation, collagen synthesis and keratynocite growth factor (KGF). In this way, glucocorticoids produce an incomplete granulation tissue and reduced wound contration (Franz et al., 2007; Boateng et al., 2008). Such therapeutic agents also increase the risk of wound infections (Wagner et al., 2008).

4 WOUND DRESSINGS

Wound dressings have been classified on the basis of their function (debridement, antibacterial, occlusive, absorbent, adherence), type of material employed in their manufactoring (e.g. hydrocolloid, alginate, collagen) and their physical form (ointment, film, foam, gel). Other classification criteria include: primary dressings that are directely in contact with wound surface; secondary ones, which are used to cover the primary dressings; and island dressings, which are characterized by the presence of a central absorbent region, surrounding by an adhesive portion. Wound dressings can also divide in traditional and modern dressings (Boateng et al., 2008).

4.1 Traditional dressings

Traditional wound dressings are commonly used to protect wounds against foreign contamination (i.e. bacteria) but also to deliver bioactive molecules to lesion sites (Jones et al., 2006; Boateng and Catanzano, 2015).

Traditional topical formulations, including liquid (solutions, suspensions and emulsions) and semi-solid (ointments and creams) preparations, rapidly absorb exudate, losing their rheological properties (Boateng et al., 2008).

On the contrary, in the case of exudative wounds, solid dressings provide a better exudate management and a prolonged permanence at the wound site. They may be employed as primary or

secondary dressings, or form part of a composite of many layers, each one of them exerting a specific function (Boateng and Catanzano, 2015). Such dressings can protect wounds against some bacterial contamination until their outer surface becomes moistened (Powers et al., 2013).
They provide only a poor occlusion and allow evaporation of exudate, resulting in a dehydrated wound bed. As a result of their adherence to wounds, they are painful to remove (Boateng and Catanzano, 2015).
To improve their properties, solid traditional dressings can be impregnated with some bioactive compounds (like topical antimicrobials and antiseptic agents) to obtain functional dressings (Boateng and Catanzano, 2015).

4.2 Modern dressings

Unlike traditional dressings, modern ones are designed and developed to play an active role in the wound healing process and to deliver bioactive compounds (Boateng et al., 2008). These dressings provide a moist environment around the wound to improve healing. They are classified, dependently on the materials used in their preparation (hydrocolloid, alginate and hydrogel dressings) or on their physical form (gels, thin films and foam sheets) (Boateng et al., 2008). Hereafter current available modern dressings are described.

Hydrocolloid dressings

Hydrocolloid dressings, using in wound management, are obtained from colloidal materials associated with other ones, like elastomers and adhesives. Among colloidal materials, carboxymethyl cellulose (CMC), gelatin and pectin are largely employed for their capability to gelify (Boateng et al., 2008). Thanks to their properties, hydrocolloid dressings are able to adhere to both moist and dry wound beds (Heenan, 1998) and have been used in the treatment of light to moderately exuding wounds, including pressure sores, minor burns and traumatic injuries (Boateng et al., 2008).
Upon contact with wound exudate, a change in physical state occurs inside the hydrocolloid dressing, resulting in the formation of a gel permeable to air (Thomas, 1992).

Alginate dressings

Alginate dressings, obtaining from calcium and sodium salts of alginic acid, include freezed-dried porous sheets and flexible fibres. They are able to gelify upon contact with wound exudate and to minimize bacterial contamination (Heenan, 1998).

In particular, alginate fibres provide the formation of protective gels due to the exchange of calcium or sodium ions with those containing in exudates and/or blood. Such gels create a moist environment around the wound (Thomas, 2000).

Hydrogel dressings

Hydrogels are threedimensional network of hydrophilic polymers; they are obtained from a variety of water-soluble polymers with different chemical and physical properties. The presence of hydrophilic polymer chains allows to absorb high volumes of water and to swell maintaining their typical gelatinous nature (Boateng et al., 2008).

They can be used on dry, sloughy, or necrotic wounds but usually are combined with secondary dressings (Watson and Hodgkin, 2005).

Hydrogels are non-particulate, non-toxic, and non-adherent dressings (Ahmed, 2015); they can be subjected to gamma radiation sterilization to obtain sterile hydrogels (Rosiak and Olejniczak, 1993).

Hydrogels can be prepared with natural polymers, like gelatin and agar, and synthetic ones, including polyvinylpyrrolidone and poly (vinyl alcohol).

Intrasite™, Nu-gel™, Kikgel, Aqua-gel, and Aquaform™ are some of the most common commercial hydrogel dressings currently available (Boateng and Catanzano, 2015).

Film dressings

The first film dressings were made from nylon derivatives supported by an adhesive polyethylene frame, which attributed an occlusive function to the dressing. They possessed a limited capability to absorb wound exudate, resulting in the accumulation of exudate at the wound site with risk of infections (Debra and Cheri, 1998; Boateng et al., 2008). Subsequently, the use of polyurethane was proposed in the development of semi-permeable film dressings, characterized by a higher porosity and permeability to water vapour and gases with respect to the original films (Boateng et al., 2008).

Foam dressings

These dressings comprise porous polyurethane foam or polyurethane foam film and sometimes additional adhesive borders (Morgan, 2002). They create a moist environment around the wound and provide thermal insulation (Wound care guidelines, 2005).

Thanks to porous structure, high absorbent ability and moisture vapour permeability, foam dressings are suitable for the treatment of granulating wounds, partial or full thickness wounds with minimal or moderate drainage (Young, 1997).

Bioactive dressings

Bioactive dressings, based on biomaterials, include tissue engineered products from natural or artificial sources (Barlett, 1981).

Biomaterials are well-known for their biocompatibility, biodegradability and atoxicity. Among these, collagen, hyaluronic acid, chitosan, alginates and elastin are largely employed to prepare bioactive dressings (Boateng et al., 2008). They are constituents of the natural tissue matrix and can also play an active role in wound healing (Ueno et al., 1999).

Such dressings have been used as delivery systems for bioactive compounds, like antimicrobials and growth factors (Boateng et al., 2008).

5 ULCERATIVE COLITIS

Inflammatory bowel disease (IBD) is an idiopathic chronic inflammation of the intestinal mucosa and comprises primarily 2 disorders: Crohn's disease and ulcerative colitis (Baumgart et al., 2012).
Crohn's disease (CD) is a transmural inflammation of the gastrointestinal mucosa; the several manifestations of such disease can affect the entire gastrointestinal tract from mouth to anus (Baumgart and Sandborn, 2007).
Unlike CD, ulcerative colitis (UC) is a restricted non-transmural inflammation of the colon. UC is most commonly classified for anatomic localization or for disease activity (Silverber et al., 2005). Three UC groups can be defined: ulcerative proctitis, restricted to the rectum; left-sided colitis, also called distal colitis, extended from the distal colorectum to the splenic flexure; and pancolitis (Figure 2), which involve the anatomic area from proximal to the splenic flexure (Silverber et al., 2005; Baumgart and Sandborn, 2007).

a)  b) 

Figure 2 - Common features of ulcerative colitis: a) transverse colon in a patient in remission; b) descending colon in a patient affected by pancolitis (modified from Baumgart and Sandborn, 2007).

Some studies suggested a possible relationship between mortality in UC patients and an increasing extent of colitis (Ekbom et al., 1992; Winther et al., 2003); other ones, however, did not evidence a significant correlation (Probert et al., 1993; Farrokhyar et al., 2001).

5.1 Epidemiology and etiology

UC was first seen and described in 1859 by the British physician Samuel Wilks (Baumgart and Carding, 2007). The highest incidence of UC has been reported from industrialized countries, like United States, United Kingdom and Scandinavia. A dramatical increase of such pathology occurred during the 20th century, in particular between the 1960s and 1980s (Loftus and Sandborn, 2003; Hanauer, 2006; Baumgart and Carding, 2007). Evidences support the theory that environmental factors provide a contribution to UC development (Krishnan and Korzenik, 2003).

The onset of UC and its clinical diversity are verifiably related to a complex interaction between genetic and environmental factors. In this perspective, many studied were performed (Danese et al., 2004; Khor et al. 2011). One of these demonstrated the influence of race and ethnic origin on UC characteristics, in particular on disease location and extra-intestinal disease complications (Nguyen et al., 2006).

5.1.1 Genetic factors

Considerable epidemiological data, including the family frequency, concordance rate in twins, and ethnic differences, demonstrate the role of genetic factors on the pathogenesis of UC (Hanauer, 2006; Baumgart and Carding, 2007). Moreover, the association between UC and other syndromes with genetic predisposition confirm the genetic factors contribution to susceptibility of UC. However, due its complexity UC cannot be explained by a single gene model (Satsangi et al., 2003).

5.1.2 Environmental factors

"Westernization"

UC is more prevalent in the North America and northern Europe; on the contrary the lowest incidence for such disease is reported from South America, southeast Asia, Africa (with the exception of South Africa), and Australia (Loftus, 2004). Moreover, several epidemiological studies in developing countries evidenced a higher UC incidence in urban compared with rural communities (Baumgart and Carding, 2007). An increasing incidence in third-world countries and among migrants from low-incidence regions moving to industrialized ones occurred as a result of "westernization" of lifestyle, including diet (Hanauer, 2006; Baumgart and Carding, 2007).

Sanitation

UC is known as a disease of cleanliness, consequently of socioeconomic changes. In fact, an excessive hygiene alters the intestinal bacteria flora by reducing the exposure to environmental antigens, like bacteria and viruses (Guarner et al., 2006; Hanauer, 2006; Baumgart and Carding, 2007).

Psychological stress

Adverse life events, chronic stress and depression have been reported to increase activity of UC, suggesting the interplay role of the nervous and immune systems (Mawdsley et al., 2005).

Diet

Diet has been considered as a possible risk factor for UC, especially for westernized lifestyle that often consists of high dietary carbohydrate, protein and fatty acid (Riordan et al., 1998; Wang et al., 2016). Daily fruit, in particular citrus fruit, intake shows a protective action against UC (Niewiadomski et al., 2016). Some authors demonstrated that frequent fast-food intake, more than once a week, confers a risk for UC, due to the high levels of monounsaturated (MUFA) and polyunsaturated fatty acids (PUFA) (Persson et al. 1992; Geerling et al., 2000; Sakamoto et al., 2005). Geerling et al. suggested that vitamin B6 may enhance the onset of UC (Geerling et al., 2000). High caffeine and/or tea intake was recently defined to be protective against UC (Niewiadomski et al., 2016).

Tobacco smoking

Smoking is a strong environmental risk factor for IBD and exerts an opposite effect on UC and CD, underlying that these forms of IBD are characterized by different pathogenesis (Thomas et al. 1998; Mahid et al., 2006). Some studies demonstrated that current smoke could protect against UC; in particular, the decreasing risk for UC appeared to be dose-dependent (Lindberg et al., 1988). On the contrary, cigarette smoking constitutes a relevant risk factor for CD (Danese et al., 2004). Although the mechanisms relating to different effects of smoking on such diseases are unknown, it has been recognized that smoking affect systemic and mucosal immunity with consequent alteration of immune functions (Sopori, 2002). Evidences suggest that the relationship between IBD and smoking is very complex and that genetic factors prevail on environmental ones (Danese et al., 2004).

Appendectomy

Similarly to tobacco smoking, appendectomy shows different effects on CD and UC. Several clinical studies suggested the inverse relation between an early appendectomy (before 20 years age) for an inflammatory condition, like appendicitis and lymphadenitis, and UC (Andersson et al., 2001; Naganuma et al., 2001). Such relation could be explained by the different mediators involved in the peculiar inflammatory processes of these diseases. In particular, UC is mediated by type 2 helper T cells, whereas appendicitis is related to type 1 helper T cells, also recognized for their role in CD incidence (Andersson et al., 2001).

An understanding of the complex interplay of specific genetic, environmental and immunologic mechanisms will results in novel strategies for UC with targeted efficacy (Hanauer, 2006).

5.2 Management of UC

To establish efficient treatment strategies for UC, different factors have been considered: disease location and severity; stage of disease, induction or maintenance; and steroid-dependence. The choice of route of administration (oral, parenteral or rectal) depends on UC anatomic location and severity (Isaacs et al., 2005).

The available and well-established pharmacological tools for UC include: 5-aminosalicylates (5-ASA), corticosteroids and immunomodulatory agents (Taylor and Irving, 2011).

5-ASA, like mesalamine and olsalazine, are used in the treatment of mild to moderate UC forms and represent the first-line therapy for both induction and maintenance of disease remission (Irvine, 2008; Taylor and Irving, 2011). Such anti-inflammatory agents have been regarded as safe and well-tolerated in the majority of patients (Taylor and Irving, 2011).

Corticosteroids were employed as UC therapeutic agents for the first time in 1955, changing the landscape of UC treatment (Truelove and Witts, 1955). Steroids introduction in UC therapy constituted a big challenge for their clinical benefits, but also produced the development of steroid dependence in some patients. However, corticosteroids also represent the mainstay of therapy for moderate and severe UC (Isaacs et al., 2005; Irvine, 2008).

Immunomodulators, such as azathioprine and 6-mercaptopurine, have been used for more than 40 years in UC therapy, thanks to their efficacy to induce and maintain the remission in moderate-to-severe UC (Isaacs et al., 2005; Ardizzone et al., 2006; Timmer et al., 2007; Prefontaine et al., 2009). Azathioprine and 6-mercaptopurine are recommended in the treatment of steroid-refractory and steroid-dependent diseases (Hogenauer et al., 2003; Ardizzone et al., 2006).

Recently biological agents, including monoclonal antibodies (i.e. infliximab) and fusion proteins, have been proposed as new therapeutic tools for UC, in particular for patients intolerant or not responsive to other drugs (Taylor and Irving, 2011).

5.2.1 Conventional therapeutic strategies

Medical guidelines suggest that the success of therapeutic strategies for IBD depends on the choice of bioactive agents and on administration route (parenteral, peroral and rectal). Among these, peroral and rectal ones are the most common (Isaacs et al., 2005). Rectal administration, providing high concentrations of the bioactive agents to the target site, is associated to lower adverse drug-related effects in comparison to drug systemic absorption (Klotz, M. Schwab, 2005). In general, rectal formulations, like enemas, foams, and suppositories, are used for the local and topical treatment of moderate distal colitis and proctitis; while for extensive disease management drug

systems for rectal administration have been associated with peroral or parenteral dosage forms (Mowat et al., 2011). The conventional dosage forms currently used in the management of CD and UC are summarized in Table 1.

Table 1 - Active agents and conventional commercial dosage forms for the therapy of CD and UC (modified from Lautenschläger et al., 2014).

PARENTERAL DOSAGE FORMS	RECTAL DOSAGE FORMS
pH-dependent dosage forms Budenosid: Entecort®; Budenofalk®; Targit® Mesalazin: Claversal®; Salofalk®; Pentasa®; Asacol®; Apriso® Sulfasalazine: Azulfidine®; Colo-Plean® Technology: CODES™ **Time-dependent dosage forms** Technology: TIME CLOCK®; Pulsicap® (no products on the market) **Enzyme-controlled dosage forms** No products on the market **Pressure-controlled dosage forms** No products on the market **Osmotic-controlled dosage forms** Technology: OROS CT™ (no products on the market)	**Enemas** Budenosid: Entecort® Betamethasone: Betnesol® Mesalazin: Claversal®; Pentasa® **Rectal foam** Budenosid: Budenofalk®; Entocort® Hydrocortisone: Colifoam® Mesalazine: Salofalk® **Suppositors** Mesalazine: Pentasa®; Salofalk®

5.2.2 Innovative therapeutic strategies

Innovative drug delivery systems have been developed to maximize the therapeutic efficacy, to reduce drug side effects, and finally to improve patient acceptability (Lautenschläger et al., 2014). A healthy intestinal barrier is constituted by three layers: a secreted mucus layer, an epithelial cell layer and a non-epithelial mucosal cell (like gut-associated lymphatic cells) layer (Lautenschläger et al., 2014).

The mucus layer constitutes a physical and chemical barrier, providing a high protection against microorganisms, toxins, viruses and other environmental antigens (Corazziari, 2009).

Mucus has a complex and not fully understood structure. Mucin glycoproteins have been recognized to exert a protective action on the entire gastrointestinal tract. In particular, mucin

glyproteins are characterized by the presence of hydrophobic domains and of negative surface charges, able to create a polyvalent adhesive barrier, hindering the passage of pathogens through the mucus layer (Cone, 2009).

The epithelial cells are considered the control centre of the intestinal barrier and separate the external environment from the gut-associated lymphoid tissue (Bamias et al., 2005). The underlying mucosal cells, such as goblet cells and Paneth cells, are able to secrete some specific components of the intestinal barrier and to control the functionality of the epithelial cells as well as the entire intestinal secreted barrier (McGuckin et al., 2009).

The onset of UC is accompanied by the loss of the integrity of the intestinal barrier structure. A significant reduction in secretory cells, an increase in intestinal permeability, a loss of the epithelial cell layer and a decrease of mucus layer occur (Balfour Sartor and Muehlbauer, 2007; Fyderek et al., 2009; Lautenschläger et al., 2014). An excessive mucosal immune response, associated to an intestinal inflammation, is consequent to the disruption and the loss of functionality of the intestinal barrier (Kleessen et al., 2002).

A variety of polymeric drug carriers are designed and developed to allow a drug specific targeting to inflamed tissues in UC. Such systems, like micro- and nanoparticles, can exert their action with different mechanism: muco-adhesion, bioadhesion, mucopenetration and uptake by M cells (Lautenschläger et al., 2014). In particular mucoadhesive polymeric systems able to interact with mucin glycoproteins by means of hydrogen bonds, van der Waals interactions, polymer chain interpenetration, hydrophobic forces, and electrostatic/ionic interactions (Smart, 2005), represent a promising therapeutic approach.

5.3 *In situ* gelling systems

Rectal drug administration can be effectively employed for the local treatment of UC. Actually, solid dosage forms such as suppositories are commercially available; their main disadvantage is a low patient compliance (Lautenschläger et al., 2014). Therefore, innovative rectal dosage forms like responsive hydrogels have been studied to improve patients compliance affected by UC (Yuan et al., 2012). Responsive hydrogels are liquids able to gelify upon contact with physiological fluids or as a result of temperature or pH changes. Thanks to such characteristics, responsive hydrogels allow an easy rectal administration, a prolonged permanence on action site with a consequent reduction in drug administration frequency, and a sustained drug release (Yuan et al., 2012; Özgüney et al., 2014)

Many attempts have been made to develop thermoresponsive and mucoadhesive *in situ* gelling systems (Choi et al., 1998; Han-Gon et al., 1998; Chul-Soon et al., 2004). Among these, a

promising association between poloxamer, as thermosensitive polymer, and sodium alginate, as mucoadhesive agent, was investigated for the delivery of nimesulide after rectal administration (Yuan et al., 2012).

6 REFERENCES

Abreu, M.T., 2002. The pathogenesis of inflammatory bowel disease: translational implications for clinicians. Curr. Gastroenterol. Rep. 4, 481-489.

Ahmed, E.M., 2015. Hydrogel: Preparation, characterization and applications: A review. J. Adv. Res. 6, 105–121.

Andersson, R.E., Olaison, G., Tysk, C., Ekbom, A., 2001. Appendectomy and protection against ulcerative colitis. N. Engl. J. Med. 344, 808-814.

Ardizzone, S., Maconi, G., Russo, A., Imbesi, V., Colombo, E., Bianchi Porro, G., 2006. Randomised controlled trial of azathioprine and 5-aminosalicylic acid for treatment of steroid dependent ulcerative colitis. Gut. 55, 47-53.

Arnold, M., Barbul, A., 2006. Nutrition and wound healing. Plast. Reconstr Surg. 117, 42S-58S.

Balfour Sartor, R., Muehlbauer, M., 2007. Microbial host interactions in IBD: implications for pathogenesis and therapy. Curr. Gastroenterol. Rep. 9, 497-507.

Bamias, G., Nyce, M.R., De La Rue, S.A., Cominelli, F., 2005. New concepts in the pathophysiology of inflammatory bowel disease. Ann. Intern. Med. 143, 895-904.

Barker, T.H., 2011. The role of ECM proteins and protein fragments in guiding cell behavior in regenerative medicine. Biomaterials. 32, 4211–4214.

Barlett, R.H., 1981. Skin substitutes. J. Trauma 21: S731.

Baumgart, D.C., Carding, S.R., 2007. Inflammatory bowel disease: cause and immunobiology. Lancet. 369, 1627-1640.

Baumgart, D.C., Sandborn, W.J, 2007. Inflammatory bowel disease: clinical aspects and established and evolving therapies. Lancet. 369, 1641-1657.

Baumgart, D.C., Sandborn, W.J, 2012. Chron's disease. Lancet. 380, 1590-1605.

Boateng, J., Catanzano, O., 2015. Advanced therapeutic dressings for effective wound healing - A review. J. Pharm. Sci. 104, 3653–3680.

Boateng, J.S., Matthews, K.H., Stevens, H.N., Eccleston, G.M., 2008.Wound healing dressings and drug delivery systems: A review. J. Pharm. Sci. 97, 2892–2923.

Bolton, L., van Rijswijk, L., 1991. Wound dressings: meeting clinical and biological needs. Dermatol. Nurs. 3, 146–161.

Broderick, N., 2009. Understanding chronic wound healing. Nurse Practitioner. 34, 16–22.

Choi, H.G., Jung, J.H., Ryu J.M., Yoon, S.J., Oh, Y.K., Kim C.K., 1998. Development of *in situ*-gelling and mucoadhesive acetaminophen liquid suppository. Int. J. Pharm. 165, 33-44.

Choi, H.G., Oh, Y.K., Kim, C.K., 1998. *In situ* gelling and mucoadhesive liquid suppository containing acetaminophen: Enhanced bioavailability. Int. J. Pharm. Sci. 165, 23-32.

Cone, R.A., 2009. Barrier properties of mucus. Adv. Drug Deliv. Rev. 61, 75-85.

Corazziari, E.S., 2009. Intestinal mucus barrier in normal and inflamed colon. J. Pediatr. Gastroenterol. Nutr. 48, S54–S55.

Danese, S., Sans, M., Fiocchi, C., 2004. Inflammatory bowel disease: the role of environmental factors. Autoimmun. Rev. 3, 394–400.

Debra, J.B., Cheri, O., 1998. Wound healing: technological innovations and market overview. 2, 1–185

Eckes, B., Nischt, R., Krieg, T., 2010. Cell-matrix interactions in dermal repair and scarring. Fibrogenesis Tissue Repair. 3:4.

Ekbom, A., Helmick, C.G., Zack, M., Holmberg, L., Adami, H.O., 1992. Survival and causes of death in patients with inflammatory bowel disease: a population-based study. Gastroenterology. 103, 954-960.

Eming, S.A., Krieg, T., Davidson, J.M., 2007. Inflammation in wound repair: molecular and cellular mechanisms. J. Invest. Dermatol. 127, 514–525.

Farrokhyar, F., Swarbrick, E.T., Grace, R.H., Hellier, M.D., Gent, A.E., Irvine, E.J., 2001. Low mortality in ulcerative colitis and Crohn's disease in three regional centers in England. Am. J. Gastroenterol. 96, 501-507.

Franz, M.G., Steed, D.L., Robson, M.C., 2007. Optimizing healing of the acute wound by minimizing complications. Curr. Probl. Surg. 44, 691-763.

Fyderek, K., Strus, M., Kowalska-Duplaga, K., Gosiewski, T., Wedrychowicz, A., Jedynak-Wasowicz, U., Sladek, M., Pieczarkowski, S., Adamski, P., Kochan, P., Heczko, P.B., 2009. Mucosal bacterial microflora and mucus layer thickness in adolescents with inflammatory bowel disease. World J. Gastroenterol. 15, 5287-5294.

Geerling, B.J., Dagnelie, P.C., Badart-Smook, R.D., Russel, M.G., Stockbrugger, R.W., Brummer, R.J., 2000. Diet as a risk factor for the development of ulcerative colitis. Am. J. Gastroenterol. 95, 1008-1012.

Guarner, F., Bourdet-Sicard, R., Brandtzaeg, P., Gill, H.S., McGuirk, P., van Eden, W., Versalovic, J., Weinstock, J.V., Rook, G.A., 2006. Mechanisms of disease: the hygiene hypothesis revisited. Nat. Clin. Pract. Gastroenterol. Hepatol. 3, 275-284.

Gurtner, G.C., Evans, G.R.D., 2000. Advances in head and neck reconstruction. Plast. Reconstr. Surg. 106, 672–682.

Gurtner, G.C., Werner, S., Barrandon, Y., Longaker, M.T., 2008. Wound repair and regeneration. Nature. 453, 314 –321.

Gurtner, G.C., Werner, S., Barrandon, Y., Longaker, M.T., 2008. Wound repair and regeneration. Nature. 453, 314–321.

Hanauer, S.B., 2006. Inflammatory bowel disease: epidemiology, pathogenesis, and therapeutic opportunities. Inflamm. Bowel Dis. 12, S6-S9.

Heenan, A., 1998. Alginates: Frequently asked questions. World Wide Wounds. 1, 1–7.

Heenan, A., 1998. Hydrocolloids: frequently asked questions. World Wide Wounds. 1, 1–17.

Hinz, B., 2007. Formation and function of the myofibroblast during tissue repair. J. Invest. Dermatol. 127, 526–537.

Hogenauer, C., Wenzl, H.H., Hinterleitner, T.A., Petritsch, W., 2003. Effect of oral tacrolimus (FK 506) on steroid-refractory moderate/severe ulcerative colitis. Aliment. Pharmacol. Ther. 18, 415-423.

Irvine, E.J., 2008. Quality of life of patients with ulcerative colitis: past, present, and future. Inflamm. Bowel Dis. 14, 554-565.

Isaacs, K.L., Lewis, J.D., Sandborn, W.J., Sands, B.E., Targan, S.R., 2005. State of the art: IBD therapy and clinical trials in IBD. Inflamm. Bowel Dis. 11, S3–S12.

J.D. Smart, The basics and underlyingmechanisms ofmucoadhesion, Adv. Drug Deliv. Rev. 57, 1556-1568.

Jacinto, A., Martinez-Arias, A., Martin, P., 2001. Mechanisms of epithelial fusion and repair. Nat. Cell. Biol. 3, E117–E123.

Jones, V., Grey, J.E., Harding, K.G., 2006. Wound dressings. Br. Med. J. 332, 777–780.

Kamaratos, A.V., Tzirogiannis, K.N., Iraklianou, S.A., Panoutsopoulos, G,I., Kanellos, I.E., Melidonis, A.I., 2014. Manuka honey-impregnated dressings in the treatment of neuropathic diabetic foot ulcers. Int. Wound J. 11, 259-263.

Kleessen, B., Kroesen, A., Buhr, H., Blaut, M., 2002. Mucosal and invading bacteria in patients with inflammatory bowel disease compared with controls. Scand. J. Gastroenterol. 37, 1034-1041.

Klotz, U., Schwab, M., 2005. Topical delivery of therapeutic agents in the treatment of inflammatory bowel disease. Adv. Drug Deliv. Rev. 57, 267–279.

Krishnan, A., Korzenik, J.R., 2002. Inflammatory bowel disease and environmental influences. Gastroenterol. Clin. North Am. 31, 21-39.

Lautenshläger, C., Schmidit, C., Fischer, D., Stallmach, A., 2014. Drug delivery strategies in the therapy of inflammatory bowel disease. Adv. Drug Deliver. Rev. 71, 58-76.

Lazarus, G.S., Cooper, D.M., Knighton, D.R., Percoraro, R.E., Rodeheaver, G., Robson, M.C., 1994. Definitions and guidelines for assessment of wounds and evaluation of healing. Wound Repair Regen. 2, 165–170.

Lindberg, E., Tysk, C., Andersson, K., Järnerot, G., 1988. Smoking and inflammatory bowel disease: a case control study. Gut. 29, 352-357.

Loftus, E.V., 2004. Clinical epidemiology of inflammatory bowel disease: incidence, prevalence, and environmental influences. Gastroenterology. 126, 1504- 1517.

Loftus, E.V., Sandborn, W.J., 2003. Epidemiology of inflammatory bowel disease. Gastroenterol. Clin. North Am. 31, 1-20.

Mahid, S.S., Minor, K.S., Soto, R.E., Hornung, C.A., Galandiuk, S., 2006. Smoking and inflammatory bowel disease: a meta-analysis. Mayo Clin. Proc. 81, 1462-1471.

Mawdsley, J.E., Rampton, D.S., 2005. Psychological stress in IBD: new insights into pathogenic and therapeutic implications. Gut. 54, 1481-1491.

McGuckin, M.A., Eri, R., Simms, L.A., Florin, T.H.J., Radford-Smith, G., 2009. Intestinal barrier dysfunction in inflammatory bowel diseases, Inflamm. Bowel Dis. 15, 100–113.

Moore, K., McCallion, R., Searle, R.J., Stacey, M.C., Harding, K.G., 2006. Prediction and monitoring the therapeutic response of chronic dermal wounds. Int. Wound J. 3, 89–96.

Morgan, D.A., 2002. Wounds—What should a dressing formulary include? Hosp. Pharmacist. 9, 261–266.

Mowat, C., Cole, A., Windsor, A., Ahmad, T., Arnott, I., Driscoll, R., Mitton, S., Orchard, T., Rutter, M., Younge, L., Lees, C., Ho, G.T., Satsangi, J., Bloom S., 2011. Guidelines for the management of inflammatory bowel disease in adults. Gut. 60, 571–607.

Naganuma, M., Iizuka, B., Torii, A., Ogihara, T., Kawamura, Y., Ichinose, M., Kojima, Y., Hibi, T., 2001. Appendectomy protects against the development of ulcerative colitis and reduces its recurrence: results of a multicenter case-controlled study in Japan. Am. J. Gastroenterol. 96, 1123-1126.

Nawaz, Z., Bentley, G., 2011.Surgical incisions and principles of wound healing. Surgery. 29, 59-62.

Nguyen, G.C., Torres, E.A., Regueiro, M., Bromfield, G., Bitton, A., Stempak, J., Dassopoulos, T., Schumm, P., Gregory, F.J., Griffiths, A.M., Hanauer, S.B., Hanson, J., Harris, M.L., Kane, S.V., Orkwis, H.K., Lahaie, R., Oliva-Hemker, M., Pare, P., Wild, G.E., Rioux, J.D., Yang, H., Duerr, R.H., Cho, J.H., Steinhart, A.H., Brant, S.R., Silverberg, M.S., 2006. Inflammatory bowel disease characteristics among African Americans, Hispanics, and non-Hispanic Whites: characterization of a large North American cohort. Am. J. Gastroenterol. 101, 1012–23.

Özgüney, I., Kardhiqi, A., Yıldız, G., Ertan, G., 2014. *In vitro–in vivo* evaluation of *in situ* gelling and thermosensitive ketoprofen liquid suppositories. Eur. J. Drug Metab. Pharmacokinet. 39, 283-291.

Percival, J.N., 2002. Classification of wounds and their management. Surgery. 20, 114–117.

Powers, J.G., Morton, L.M., Phillips, T.J., 2013. Dressings for chronic wounds. Dermatol. Ther. 26, 197–206.

Prefontaine, E., Sutherland, L.R., Macdonald, J.K., Cepiou, M., 2009. Azathioprine or 6-mercaptopurine for maintenance of remission in Crohn's disease. Cochrane Database Syst. Rev. 1, CD000067.

Probert, C.S., Jayanthi, V., Wicks, A.C., Mayberry, J.F., 1993. Mortality in patients with ulcerative colitis in Leicestershire, 1972-1989. An epidemiological study. Dig. Dis. Sci. 38, 538-541.

Profyris, C., Tziotzios, C., Do Vale, I., 2012. Cutaneous scarring: pathophysiology, molecular mechanisms, and scar reduction therapeutics Part I. The molecular basis of scar formation. J. Am. Acad. Dermatol. 66, 1–10.

Reinke, J.M., Sorg, H., 2012. Wound repair and regeneration. Eur. Surg. Res. 49, 35–43.

Riordan, A.M., Ruxton, C.H., Hunter, J.O., 1998. A review of associations between Crohn's disease and consumption of sugars. Eur. J. Clin. Nutr. 52, 229-238.

Rosiak, J.M., Olejniczak, J., 1993. Medical application of radiation formed hydrogels. Radiat. Phys. Chem. 42, 903-906.

Sakamoto, N., Kono, S., Wakai, K., Fukuda, Y., Satomi, M., Shimoyama, T., Inaba, Y., Miyake, Y., Sasaki, S., Okamoto, K., Kobashi, G., Washio, M., Yokoyama, T., Date, C., Tanaka, H., 2005. Dietary risk factors for inflammatory bowel disease: a multicenter case–control study in Japan. Inflamm. Bowel. Dis. 11, 154-163.

Satsangi, J., Morecroft, J., Shah, N.B., Nimmo, E., 2003. Genetics of inflammatory bowel disease: scientific and clinical implications. Best Pract. Res. Clin. Gastroenterol. 17, 3-18.

Silverberg, M.S., Satsangi, J., Ahmad, T., Arnott, I.D., Bernstein, C.N., Brant, S.R., Caprilli, R., Colombel, J.F., Gasche, C., Geboes, K., Jewell, D.P., Karban, A., Loftus, E.V., Peña, A.S., Riddell, R.H., Sachar, D.B., Schreiber, S., Steinhart, A.H., Targan, S.R., Vermeire, S., Warren, B.F., 2005.

Sopori, M., 2002. Effects of cigarette smoke on the immune system. Nat. Rev. Immunol. 2, 372-377.

Tandara, A.A., Mustoe, T.A., 2004. Oxygen in wound healing - More than a nutrient. World J. Surg. 28, 294-300.

Thomas, G.A, Rhodes, J., Green, J.T., 1998. Inflammatory bowel disease and smoking - a review.Am. J. Gastroenterol. 93, 144-149.

Thomas, S., 1992. Hydrocolloids. J. Wound Care 1. 27–30.

Thomas, S., 2000. Alginate dressings in surgery and wound management—Part 1. J. Wound Care. 9, 56–60.

Timmer, A., McDonald, J.W., Macdonald, J.K., 2007. Azathioprine and 6-mercaptopurine for maintenance of remission in ulcerative colitis. Cochrane Database Syst. Rev. 1, CD000478.

Toward an integrated clinical, molecular and serological classification of inflammatory bowel disease: report of a working party of the 2005 Montreal World Congress of Gastroenterology. Can. J. Gastroenterol. 19 (Suppl A):5A –36A.

Truelove, S., Witts, L., 1955. Cortisone in ulcerative colitis: final report on a therapeutic trial. Br. Med. J. 2:1041-1048.

Tziotzios, C., Profyris, C., Sterling, J., 2012. Cutaneous scarring: pathophysiology, molecular mechanisms, and scar reduction therapeutics Part II. Strategies to reduce scar formation after dermatologic procedures. J. Am. Acad. Dermatol. 66, 13–24.

Ueno, H., Yamada, H., Tanaka, I., Kaba, N., Matsuura, M., Okumura, M., Kadosawa, T., Fujinaga, T., 1999. Accelerating effects of chitosan for healing at early phase of experimental open wound in dogs. Biomaterials. 20, 1407–1414.

Wagner, A.E., Huck, G., Stiehl, D.P., Jelkmann, W., Hellwig-Bürgel, T., 2008. Dexamethasone impairs hypoxia-inducible factor-1 function. Biochem. Biophys. Res. Commun. 2008;372:336–340.

Watson, N.F.S., Hodgkin, W., 2005. Wound dressings. Surgery 23, 52–55.

Werner, S., Grose, R., 2003. Regulation of wound healing by growth factors and cytokines. Physiol. Rev. 83, 835–870.

Winther, K.V., Jess, T., Langholz, E., Munkholm, P., Binder, V., 2003. Survival and cause-specific mortality in ulcerative colitis: follow-up of a population-based cohort in Copenhagen County. Gastroenterology. 125, 1576-1582.

Wound care guidelines, 2005. Medicines management committee report. pp 1–33.

Yong, C.S., Oh, Y.K., Jung, S.H., Rhee, J.D., Kim, H.D., Kim C-K., Choi, H.G., 2004. Preparation of ibuprofen-loaded liquid suppository using eutectic mixture system with menthol. Eur. J. Pharm. Sci. 23, 347-353.

Young, T., 1997. Matching the dressing to the wound. Community Nurse. 3, 31–35.

Yuan, Y., Cui, Y., Zhang, L., Zhu, H.P., Guo, Y.S., Zhong, B., Hu, X., Zhang, L., Wang, X.H., Chen, L., 2012. Thermosensitive and mucoadhesive *in situ* gel based on poloxamer as new carrier for rectal administration of nimesulide. Int. J. Pharm. 430, 114-119.

Chapter 1

Particulate systems based on pectin/chitosan association for the delivery of manuka honey components and platelet lysate in chronic skin ulcers

International Journal of Pharmaceutics (2016) 509, 59-70.

Tenci, M., Rossi, S., Bonferoni, M.C., Sandri, G., Boselli, C., Di Lorenzo, A., Daglia, M., Icaro Cornaglia, A., Gioglio, L., Perotti, C., Caramella, C., Ferrari, F.

Corresponding author: Silvia Rossi

1.1 ABSTRACT

The aim of the present work was the development of a powder formulation for the delivery of manuka honey (MH) bioactive components and platelet lysate (PL) in chronic skin ulcers. In particular pectin (PEC)/chitosan (CS) particles were prepared by ionotropic gelation in the presence of calcium chloride and subsequently characterized for particle size, hydration properties and mechanical resistance. Different experimental conditions (calcium chloride and CS concentrations; rest time in the cationic solution) were considered in order to obtain particles characterized by optimal size, hydration properties and mechanical resistance. Two different fractions of MH were examined: one (Fr1), rich in methylglyoxal and the other (Fr2), rich in polyphenols.

Particles were loaded with Fr1, fraction able to enhance *in vitro* proliferation of human fibroblasts, and with PL. The presence of CS in Fr1-loaded particles produced an improvement in cell proliferation. Moreover, PL loading into particles did not affect the biological activity of the hemoderivative. *In vivo* efficacy of PL- and Fr1-loaded particles was evaluated on a rat wound model. Both treatments markedly increased wound healing to the same extent.

1.2 INTRODUCTION

Chronic skin lesions are defined as tissue injuries resulting from the disruption of normal anatomic structure and function, that do not heal within 12 weeks and often reoccur. The wound healing process fails or delays due to repeated tissue insults or to concomitant pathological conditions, such as diabetes and malignancies, persistent infections, poor primary treatment and other patient related factors. Such wounds include decubitus ulcers and leg ulcers (venous, ischemic or of traumatic origin) (Boateng et al., 2008).

Wound healing is a biological process related to the general phenomenon of tissue regeneration, that involves different and complex biochemical and cellular mechanisms (Boateng et al., 2008; Boateng and Catanzano, 2015). It starts immediately after injury, when the release of a pool of growth factors, cytokines, and low-molecular weight compounds from the serum and degranulating platelets occurs (Werner et al., 2003). The repair process consists of a cascade of events including haemostasis, inflammation, migration, proliferation and maturation (Werner et al., 2003; Boateng, et al., 2008).

Growth factors and cytokines modulate cell function, through direct physical interactions with extracellular domains of transmembrane receptors and are able to mediate and control wound healing phases. The role of all the growth factors involved in tissue regeneration is only partially elucidated, even if the potential benefits of many of them have been demonstrated (Anitua et al., 2007). Among these, the most extensively investigated are PDGF (platelet derived growth factor), TGF-beta (transforming growth factors beta), PDEGF (platelet derived epidermal growth factor), EGF (epidermal growth factor), VEGF (vascular endothelial growth factor), FGF (fibroblast growth factor), IGF (insulin-like growth factor), and TNF-alpha (tumor necrosis factor alpha) (Mazzucco et al., 2010). In the last decade some authors suggested the therapeutic use of hemoderivatives, in particular of platelet lysate (PL) in wound treatment (Crovetti et al., 2004; Ranzato et al., 2008). This hemoderivate, rich in growth factors and other biologically active substances, has proved to be capable of promoting tissue regeneration.

Recently our research group has developed different formulations loaded with PL for the treatment of skin, ophthalmic and mucosa lesions (Sandri et al., 2011a; Sandri et al, 2011b; Del Fante et al., 2011; Caramella et al., 2011; Sandri et al., 2012; Rossi et al., 2013; Mori et al., 2014; Dellera et al., 2014; Rossi et al., 2015; Sandri et al., 2015; Mori et al., 2016a, 2016b). In particular, a powder formulation for the combined delivery of PL and of a model antibiotic drug, vancomycin hydrochloride (VCM), was developed (Mori et al., 2014). Powder particles were prepared by freeze-drying calcium alginate beads obtained by ionic gelation. A powder formulation clearly shows advantages with respect to gauzes and semisolid preparations in the treatment of skin ulcers:

easier and less painful administration and the possibility to load active substances of different nature in the same dosage form, thereby avoiding eventual incompatibility problems.

Pectin (PEC) and chitosan are reported in literature as natural polymers, capable of enhancing wound healing. Pectin constitutes the cell walls of most plants and is usually extracted from several types of fruits, by means of chemical or enzymatic methods. The use of pectin in wound dressings, for example, gels, permits removal of exudates, creates an acid environment, not suitable for bacterial growth. It is also able to bind active molecules such as drugs or growth factors to promote wound healing (Munarin et al., 2012). Chitosan, a linear polysaccharide obtained from chitin deacetylation, possesses antibacterial and antioxidant properties useful in avoiding the onset of infections (Rossi et al., 2007; Rossi et al., 2010; Zheng et al., 2003). It is able to inhibit bacterial growth due to the presence of positively charged amino groups, that bind negatively charged bacteria cell walls (Rabea et al., 2003). Evidence has been reported in the literature that chitosan acts as a chemo-attractant for neutrophils, stimulates granulation and tissue formation or re-epithelization and inhibits metalloproteinases (Muzzarelli, 2009).

Given these premises, it seemed interesting to develop a powder formulation based on bioactive polymers such as PEC and chitosan glutamate (CS) for the delivery of manuka honey (MH) and PL for the treatment of skin ulcers. MH, obtained from *Leptospermum scoparium*, is well known in literature for its antibacterial properties and potential capability of enhancing wound healing. The antibacterial activity is attributed to the high concentration of methylglyoxal (MGO) (Mavric et al., 2008), whereas, to our knowledge, no information about the MH components responsible for its capability to enhance cell proliferation is available (Molan and Rhodes, 2015). In the present work, two different fractions of MH were examined: one (Fr1), rich in polar substances such as methylglyoxal, the other (Fr2), rich in non-polar substances such as polyphenols. Their capability to enhance cell proliferation was investigated *in vitro* on fibroblast cell lines.

PEC/CS particles were prepared by ionotropic gelation and characterized for particle size, hydration properties and mechanical resistance. Particles with the best functional properties were subsequently loaded with PL and the MH fraction which had shown the best cell proliferation properties.

The capability of PL- and MH- loaded particles to promote wound healing was evaluated *in vitro* on human fibroblast cells and *in vivo* on a rat model.

1.3 MATERIALS AND METHODS

1.3.1 Materials

The following materials were used: $CaCl_2$ (Sigma Chimica, Milan, I); chitosan low MW (deacetylation degree: 80%) (Sigma Chimica, Milan, I); Dulbecco's Modified Eagles Medium (DMEM, Lonza, BioWhittaker, B); Dulbecco's Phosphate Buffer Solution (Sigma Aldrich, Milan, I); Genu® Pectin type LM-18 CG (PEC, Giusto Faravelli S.p.a, Milan, I); formic acid 1M (Fluka Analytical, D); glutamic acid (Sigma Chimica, Milan, I); Hank's balance salt solution (HBSS) (Sigma Aldrich, Milan, I); inactivated foetal calf bovine serum (Euroclone, Pero, I); manuka honey (MH, Marica Natura, Trezzano Rosa, I); methanol HiPerSolv CHRONANORM, HPLC-grade (VWR International, Milan, I); MTT (3-(4,5-dimethylthiazol-2-yl)-2,5-diphenyltetrazolium bromide) (Sigma Aldrich, Milan, I); $NaH_2PO_4 \cdot H_2O$ (Carlo Erba, Milan, I); $Na_2HPO_4 \cdot H_2O$ (Carlo Erba, Milan, I); NaCl (Carlo Erba, Milan, I); penicillin streptomycin 100× (pen/strep)/amphoteric 100× (Sigma Aldrich, Milan, I); PTA-blocking solution (PBS/Tween20/Albumin) (Sigma Aldrich, Milan, I); trypan blue solution (Sigma Aldrich, Milan, I); trypsin–EDTA solution (Sigma Aldrich, Milan, I).

Platelet lysate (PL) was supplied by the Immunohaematology and Transfusion Service and Cell Therapy Unit of Fondazione IRCCS, S. Matteo Hospital, Pavia, I. A pooled sample prepared from platelet rich plasma (containing 500×10^3 platelets/μl) obtained from eight different blood donors was used.

1.3.2 Solid phase extraction (SPE) of manuka honey (MH)

Native MH was subjected to SPE (Oelschlaegel S., 2012), with some modifications. In brief, a tC18 Sep-Pak Vac 6cc cartridge (Waters, Milford, Ma, USA) containing 1 g of stationary phase was conditioned with methanol (10 ml) and formic acid 0.1 % (% v/v, 10 ml). Two grams of MH were dissolved in 3 ml of 0.1% formic acid and then poured into the cartridge at a flow rate of 1 ml/min. After loading the honey solution, the polar substances (sugars, methylglyoxal (MGO), dicarbonyl compounds, ...) were recovered with 1 ml formic acid 0.1% v/v (Fraction 1, Fr1), and the non-polar substances (Fraction 2, Fr2) were eluted with a 1 ml mixture of methanol/0.1% v/v formic acid (75/25, % v/v).

Fr1 and Fr2, after removal of methanol under a nitrogen stream and reconstitution of the initial volume with HPLC-grade water, were freeze-dried at $8x10^{-1}$ mbar and -50°C (Modulyo® Edwards Freeze-Drier, Kingston, NY).

1.3.3 *In vitro* evaluation

1.3.3.1 Assessment of cell viability properties of manuka honey (MH) and pectin (PEC)

NHDF (normal human dermal fibroblasts from foreskin) (Promocell GmbH, Heidelberg, G) 6th to 16th passage were used (Mori et al, 2014).

To assess biocompatibility of the samples, a cell viability test was performed. This *in vitro* assay was used to estimate the number of viable cells after contact with the samples considered.

$3.5 \cdot 10^4$ cell/well (0.35 cm^2 area) were seeded in 96-well plates with complete medium (CM) and grown to confluence.

In vitro NHDF fibroblast viability was investigated upon cell contact with PEC, Fr1, Fr2, freeze-dried MH and native MH for 24 h. PEC aqueous solution (2% w/w), diluted 1:20 w/w in medium without serum (M (w/s)), was considered. Fr1, Fr2, freeze-dried MH and native MH were dissolved in M (w/s) to final concentrations equal to 7.5 mg/ml. CM and M (w/s) were used as references. 200 μl of each sample was put in contact with cells for 24 h. Then samples were removed from the wells and 50 μl of 7.5 μM MTT (3-(4,5-dimethylthiazol-2-yl)-2,5-diphenyltetrazolium bromide) in 100 μl of HBSS (pH 7.4) was added to each well and incubated for 3 h. Afterwards, the solution absorbance was determined at a wavelength of 570 nm, with a 690 nm reference wavelength, by means of an IMark® Microplate reader (Bio-Rad Laboratories S.r.l., Segrate, Milan, I) after 60 s shaking. Results were expressed as % viability, calculated by normalizing the absorbance measured after contact with samples with that measured after contact with M (w/s).

1.3.3.2 Assessment of cell proliferation properties of PL mixtures with PEC and Fr1

A cell proliferation test was performed to assess the capability of PL/PEC and PL/Fr1 mixtures to improve NHDF fibroblast growth in comparison with the pure components.

$2 \cdot 10^4$ cell/well (0.35 cm^2 area) were seeded in 96-well plates together with the samples and incubated for 24 h after seeding. The samples tested were: PL, PEC, Fr1, PL/PEC mixture, PL/Fr1 mixture and PL/PEC/Fr1 mixture. The concentration of PEC aqueous solution was 2% w/w. PL and PEC were mixed in a 1:1 weight ratio. Each sample was diluted 1:20 w/w in M (w/s). The final concentration of Fr1 upon dilution was 7.5 mg/ml. CM and M (w/s) were used as references.

After dilution, 200 μl of each sample was put in contact with cells for 24 h. Then a MTT test was performed (as described in section 1.3.3.1).

1.3.4 Preparation of unloaded particles

Unloaded particles were prepared by ionic gelation in different experimental conditions as regards $CaCl_2$ and CS concentrations and rest time in the cationic solution. In particular, 1 ml of a 3% (w/w)

aqueous PEC solution was dropped through a syringe needle (32 G: 0,26 mm Ø x 4 mm) into 30 ml of a $CaCl_2$ solution (0.5, 0.75, 1, 2% w/w), containing CS (0, 0.5, 0.75, 1% w/w). The rest time in the cationic solution varied from 10 min to 12 h. Particles were separated by vacuum filtration, freeze-dried overnight (Heto DRY WINNER®, Analitica De Mori, Milan, I) and characterized.
Characterization of unloaded particles

1.3.4.1 Particle size

Particle size was evaluated by an optical microscope (Leica DMI 3000B), equipped with internal camera and PC Leica Application Suite EZ V1.8.1 program (Leica Microequipments, Milan, I).

1.3.4.2 Hydration properties

The hydration properties of unloaded particles were evaluated by means of Franz cells, using PBS (phosphate buffer saline, $NaH_2PO_4 \cdot H_2O$ 0.036%, w/w, $Na_2HPO_4 \cdot H_2O$ 0.137%, w/w, NaCl 0.85%, w/w), as medium mimicking wound exudates. Donor and receptor chambers of Franz cells were separated by a previously hydrated dialysis membrane (cut-off 12000-14000 Da). 10 mg of unloaded particles were layered on a paper disc and in turn, placed on the dialysis membrane. After different times (1, 2, 4 and 6 h) the weight increase of hydrated with respect to dry particles was measured (Mori et al., 2014). The normalized parameter amount of PBS absorbed by unit weight (gPBS/g) was then calculated.

1.3.4.3 Mechanical resistance

The mechanical resistance of the particles was determined by means of TA.XTplus apparatus (ENCO, Spinea, I), equipped with a conical probe (P/10C). The probe was lowered into particles at a rate of 0.1 mm/s up to a depth of 0.5 mm. The work of penetration, calculated as the area under the penetration force vs distance curve, was recorded.

1.3.5 Preparation of particles loaded with PL and Fr1

1.3.5.1 PL-loaded particles

1 ml of a 1:1 w/w mixture of a 6% w/w aqueous PEC solution with PL was dropped through a syringe needle (32 G: 0,26 mm Ø x 4 mm) in 30 ml of a 0.5% (w/w) $CaCl_2$ solution, with or without CS (1% w/w). After a prefixed rest time (10 min) in the cationic solution, particles were separated by vacuum filtration, freeze-dried overnight (Heto DRY WINNER®, Analitica De Mori, Milan, I) and characterized.

1.3.5.2 Fr1-loaded particles

1 ml of a 6% w/w aqueous PEC solution containing Fr1 (50 mg/ml) was dropped through a syringe needle (32 G: 0,26 mm Ø x 4 mm) into 30 ml of a 0.5% (w/w) $CaCl_2$ solution containing Fr1 (50 mg/ml), in presence or absence of CS (1% w/w). After a prefixed rest time (10 min) in the cationic solution, particles were separated by vacuum filtration, freeze-dried overnight (Heto DRY WINNER®, Analitica De Mori, Milan, I) and characterized.

1.3.6 Characterization of loaded particles

PL- and Fr1- loaded particles were characterized for size and mechanical resistance as previously described for unloaded particles.

Assessment of PDGF-AB (heterodimer platelet derived growth factor-AB) and Fr1 loaded into particles

Particles loaded with PL and Fr1 were dissolved in 1.5 ml sodium citrate aqueous solution (50 mM).

The amounts of PDGF-AB loaded into particles and present in fresh PL (same amount employed for the preparation of particles) were assessed by means of an ELISA test (Human PDGF-AB Quantikine PharmPak, R&D Systems, Minneapolis, MN, USA; assay range: 31.2-2000 pg/ml) (Rossi et al., 2013). %PDGF-AB loaded was calculated according to the following equation:

%PDGF AB= (PDGF AB amount into sample/ PDGF AB amount in fresh PL) x 100

The amount of Fr1 loaded into particles was evaluated by means of an RP-HPLC-DAD method, previously developed and validated (Daglia et al., 2013). In detail, the analyses were performed using an Agilent 1200 HPLC system (Agilent, Waldbronn, D), equipped with a quaternary pump and diode array detector. The Agilent Chemstation software was used for acquiring and processing data. The separation was achieved on a Zorbax Eclipse XDB-C18 column (150 x 4.6 mm i.d., 5 μm particle size), equipped with the corresponding guard column, both maintained at 25°C. The mobile phase consisted of water acidified with 0.1% formic acid (eluent A) and acetonitrile (eluent B), eluted with the following gradients at a flow rate of 0.3 ml/min: 0 min, 10% B; 0−5 min, 15% B; 5−30 min, 15% B; 30−45 min, 30% B; 45−50 min, 50% B; 50−60 min, 100% B; 60−65 min, 100% B; 65−70 min, 10% B; 70−80 min, 10% B. The injection volume was 5 μl. Spectral data were collected within the range of 200-800 nm for all peaks and chromatograms were processed at 314 nm. The amount of Fr1 loaded was expressed as % of loaded MGO. Before HPLC analysis, MGO,

contained in Fr1 samples, was derivatized with 6 mg of *o*-phenylenediamine (OPD) and kept at 37°C for 1 h under constant stirring, to obtain the corresponding and UV-detectable quinoxaline.
1 h later, the samples were centrifuged at 8000 rpm for 10 min at room temperature. The supernatant was collected and submitted to HPLC analysis.

1.3.7 Assessment of cell proliferation properties

Cell proliferation properties of PL- and Fr1-loaded particles were assessed as described in section 1.3.3.2. Particles were dissolved in 1.5 ml 50 mM sodium citrate aqueous solution and then diluted 1:20 w/w in M (w/s). CM and M (w/s) were used as references. The cell proliferation test was also performed on fresh PL, Fr1 and on unloaded particles, subjected to the same treatment of PL-loaded particles (addition of 50 mM sodium citrate solution and subsequent dilution 1:20 in M (w/s)).

1.3.8 *In vivo* efficacy on rat wound model

All animal experiments were carried out in full compliance with the standard international ethical guidelines (European Communities Council Directive 86/609/EEC) approved by Italian Health Ministry (D.L. 116/92). The study protocol was approved by the Local Institutional Ethics Committee of the University of Pavia for the use of animals. Male rats (Wistar 200-250 g) were anesthetized with equitensine (3 ml/kg) and shaved to remove all hair from the site of injury. Three full thickness burns, having a circular diameter of 4 mm, were produced on the backs of the animals by contact with a brass rod (105 °C for 40 s). The day after, three 6-mm full-thickness excisional wounds were outlined using a punch biopsy tool on each animal back. Wounds were photographed with a digital camera (Sigma SD 14) and treated with PL-loaded particles (25 mg) wetted with physiological solution (25 μl), Fr1-loaded particles (25 mg) wetted with physiological solution (25 μl), and physiological solution (25 μl) (reference). Wounds were covered with a sterile gauze and the rat's back was wrapped with a surgery stretch (Safety, Monza, I), to keep particles or physiological solution into lesions. At prefixed times after treatment (3, 7, 10, 14 and 18 days) the three lesions were photographed with a digital camera (Sigma SD 14) and wetted with 25 μl of physiological solution. The analysis of the photographs was carried out using UTHSCSA Image Tool v. 3.0 software. 18 days after the treatment full thickness biopsies were obtained and immunohistochemical analysis of the excised tissues was carried out. A wound healing > 70% was considered the endpoint.

1.3.8.1 Microscopic analysis

A histological examination of the wounds was performed 18 days after the treatment. The animals were sacrificed and tissue samples were bisected along the widest line of the wound, then fixed in 4% w/v neutral buffered paraformaldehyde for 48 h, dehydrated with gradient alcohol series, cleared in xylene and embedded in paraffin. Sections (8 μm) were obtained using a Leitz microtome (Wetzlar, G) and were stained with haematoxylin and eosin (H&E). The slices were examined at the magnification of 5X under a light microscope Axiophot Zeiss (Oberkochen, G) equipped with a digital camera.

1.3.9 Statistical analysis

Whenever possible, experimental values of the various types of measures were subjected to statistical analysis. In particular, Anova one way, multiple range test (MRT) was used (Statgraphics 5.0, Statistical Graphics Corporation, Rockvillle, MD, USA).

1.4 RESULTS AND DISCUSSION

1.4.1 Cell viability properties of MH and PEC

Figure 1 shows % viability values of MH fractions, freeze-dried MH and native MH. It can be observed that Fr1 was characterized by a % viability value higher than that observed for M (w/s); it indicates that Fr1 didn't show cytotoxicity and was able to induce fibroblast proliferation. Fr2, freeze-dried MH and native MH were characterized by % viability values higher than M (w/s) but lower than Fr1, meaning that Fr2 also supported cell proliferation, but at a lower extent in comparison with Fr1. These results point out that polar components are the major factors responsible for MH proliferation properties. For this reason, Fr1 was chosen for further investigation.

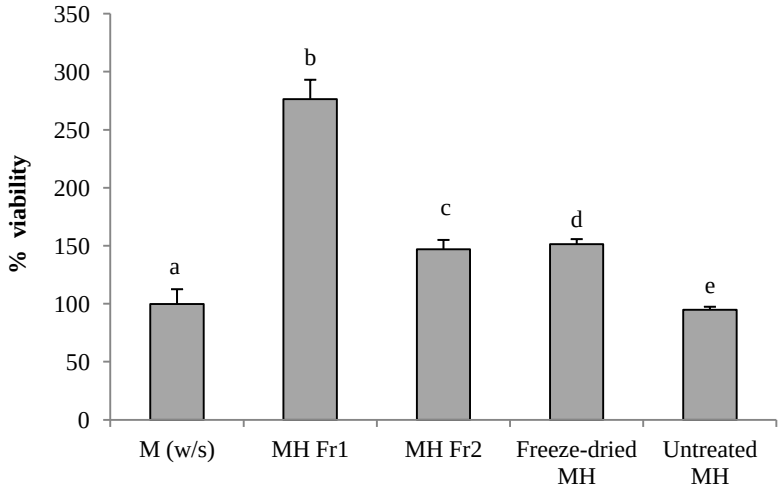

Figure 1 - % viability values of Fr1 and Fr2 in comparison with freeze-dried MH and native MH, tested at the same concentration (7.5 mg/ml). M (w/s) was used as reference (mean values ± s.e.; n=8). Anova one way, MRT ($p<0.05$): a *vs* b/c/d; b *vs* c/d/e.

In Figure 2 % viability values of PEC aqueous solution (2% w/w) diluted with M (w/s) in different ratios are reported. It can be observed that 1:40 and 1:20 w/w dilutions showed % viability values significantly higher ($p < 0.05$) than that obtained for M (w/s), whereas 1:10 w/w dilution was characterized by a % viability comparable to that of the medium. A decrease in % viability values was observed on increasing polymer concentration. This is likely due to the increase in sample viscosity, that could hinder a correct exchange of nutrients between medium and cells. On the basis of these results, 1: 20 w/w dilution was chosen for cell proliferation tests.

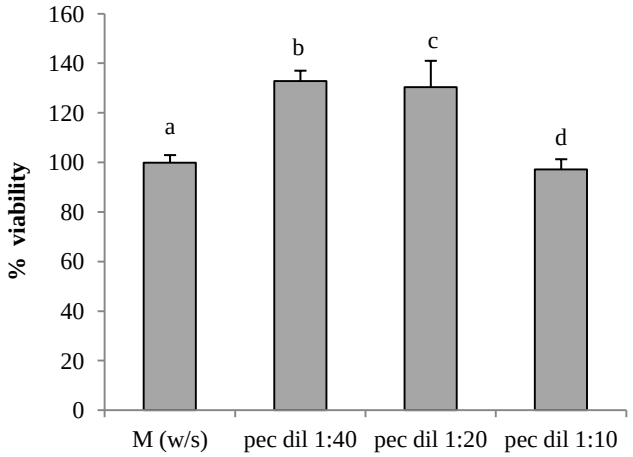

Figure 2 - % viability values of PEC aqueous solution (2% w/w) diluted in M (w/s) (1:40, 1:20 and 1:10 w/w ratio). M (w/s) was used as reference (mean values ± ds; n=8). Anova one way, MRT ($p<0.05$): a *vs* b/c.

1.4.2 Cell proliferation properties of PL mixtures with PEC and Fr1

In Figure 3 % proliferation values of the binary mixture PL/PEC and PL/Fr1 and of the ternary mixture PL/PEC/Fr1 are reported in comparison with those of the single components (PL, PEC and Fr1).

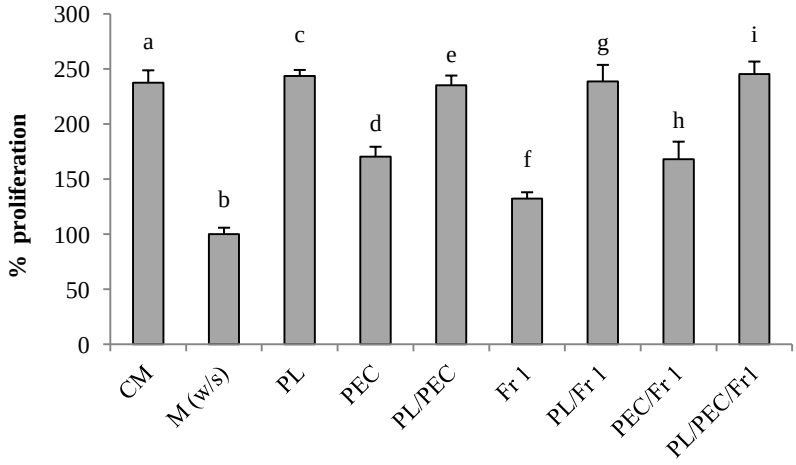

Figure 3 - % proliferation values of the binary mixtures PL/PEC and PL/Fr1 and of the ternary mixture PL/PEC/Fr1 in comparison with those of the single components (PL, PEC and Fr1). Anova one way, MRT ($p < 0.05$): a *vs* b; b *vs* c/d/e/f/g/h/i; d *vs* e; f *vs* g/h/i; d *vs* i.

It can be observed that M (w/s) was characterized by a % proliferation significantly lower ($p < 0.05$) than that obtained for CM; this indicates the discriminating power of the test.

PL showed a % proliferation comparable to CM and significantly ($p < 0.05$) higher than M (w/s).

This result is attributable to the bioactive substances contained in PL, which were able to promote cell proliferation. PEC and Fr1 showed % proliferation values significantly higher than M (w/s), indicating their capability to induce cell proliferation. The presence of PEC and/or Fr1 did not modify the biological properties of PL. In fact, the PL/Fr1, PL/PEC and PL/PEC/Fr1 mixtures were characterized by % proliferation values comparable to that of PL.

1.4.3 Characterization of unloaded particles

1.4.3.1 Particle size

In Figure 4 (a-b) the size of unloaded particles as a function of preparation conditions ($CaCl_2$ and CS concentrations, rest time in cationic solution) is reported. In the case of particles prepared in absence of CS (Figure 4a) and with rest times of 10 and 30 min, $CaCl_2$ concentration did not affect particle size. A significant ($p<0.05$) increase in particle size was observed after a rest time of 1 h for 0.5 and 0.75% w/w $CaCl_2$ concentrations and after a rest time of 18 h for $CaCl_2$ concentrations higher than 0.75% w/w. A longer permanence of PEC drops in the cationic solution was responsible for a greater polymer gelation, that determined an increase in particle size. The higher the Ca ion concentration, the longer the time required for PEC-Ca ion interaction.

The addition of 0.5 % w/w CS to 0.5% $CaCl_2$ solution was responsible for an increase in particle size for rest times of 10 and 30 min (Figure 4b). The same effect was observed for 10 min rest time also in presence of 0.75% w/w CS. On the contrary, the addition of CS 1% (w/w) to 0.5% $CaCl_2$ solution, independently of rest time, did not affect particle size significantly. Such a result indicates that PEC/CS interaction depends on both PEC/CS ratio and contact time. For high PEC/CS ratio (i.e. low CS concentrations) and short contact time, PEC/CS interaction was shallow and superficial and determined an increase in particle size. The higher the contact time, the greater the interpolymer diffusion and interaction. Such interaction determined a reduction of particle volume that resulted in no variation in size of PEC/CS particles with respect to those CS-free.

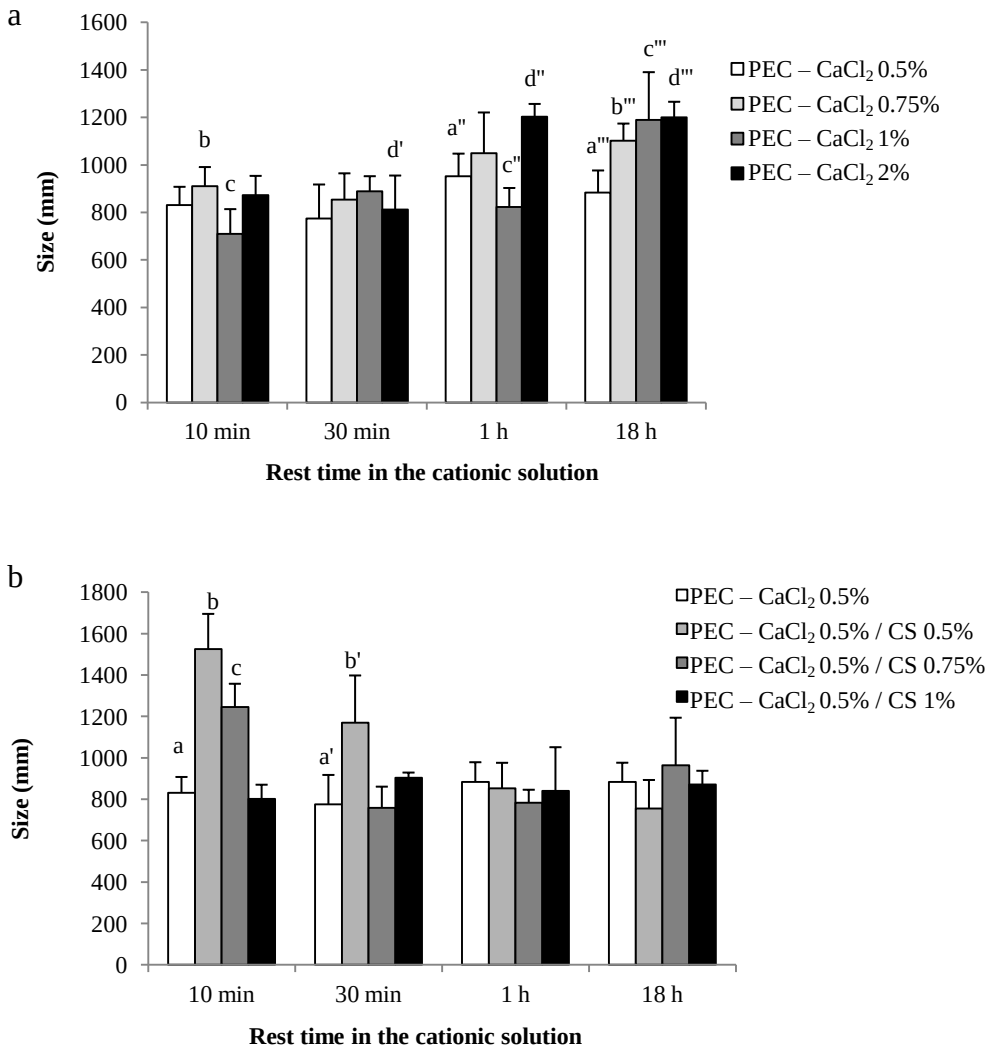

Figure 4 - Influence of preparation conditions on size of unloaded particles (mean values ± s.d.; n = 3): (a) particle size as a function of $CaCl_2$ concentrations and rest time in $CaCl_2$ solution. Anova one way, MRT ($p < 0.05$): a″ *vs* d″; c″ *vs* d″; a‴ *vs* b‴/d‴; b *vs* b‴; c *vs* c‴; d′ *vs* d″/d‴; (b) particle size as a function of CS concentration and rest time in $CaCl_2$/CS solution. Anova one way, MRT ($p < 0.05$): a *vs* b; a *vs* c; a′ *vs* b′.

1.4.3.2 Hydration properties

In Figure 5 (a-b) the normalized parameter PBS absorbed by unit weight (gPBS/g) of unloaded particles is reported as a function of preparation conditions ($CaCl_2$ and CS concentrations, rest time in cationic solution). All particles were able to hydrate and gelify when in contact with PBS (medium mimicking wound exudate); this behavior was attributable to the exchange of the Ca ions of the particles with the Na ions contained in the buffer.

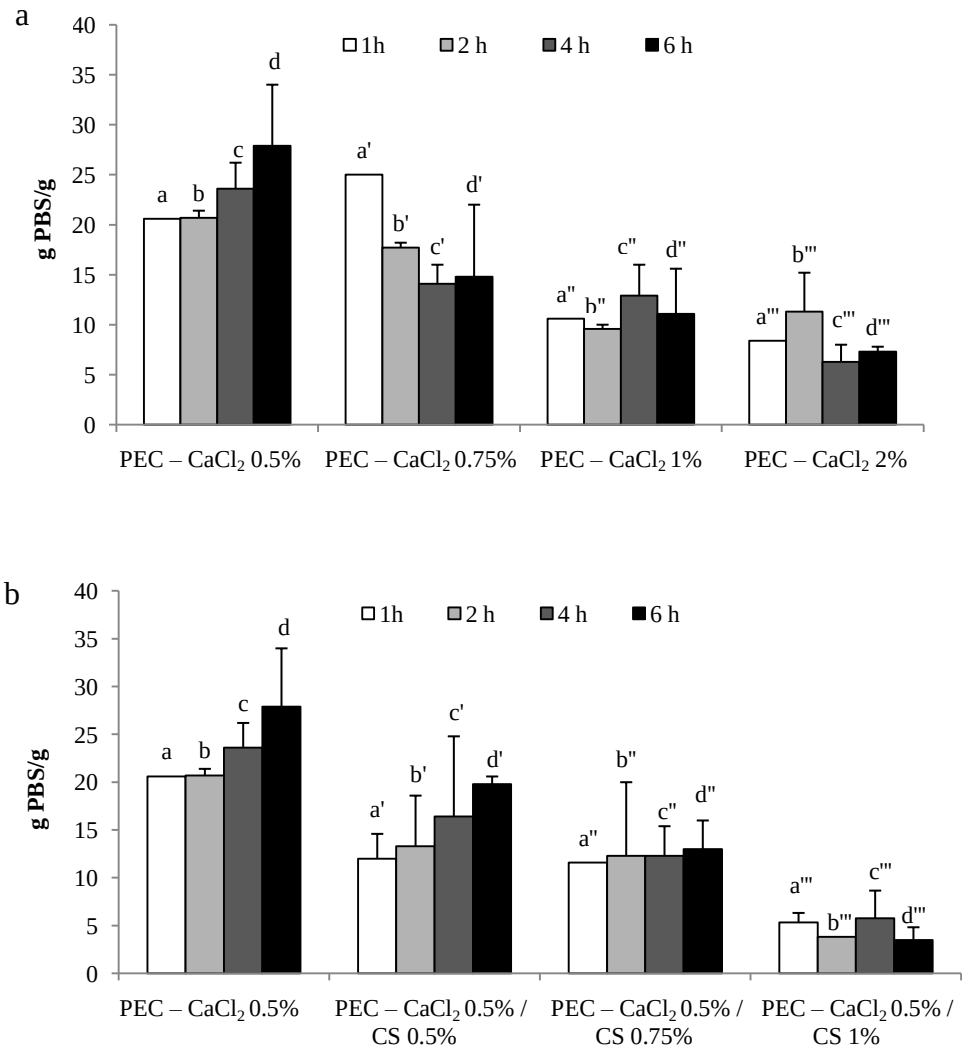

Figure 5 - Influence of preparation conditions on hydration properties of unloaded particles (mean values ± s.d.; n = 3): (a) PBS amount absorbed/ unit weight as a function of $CaCl_2$ concentrations. Anova one way, MRT ($p < 0.05$): a *vs* a′/a″/a‴; b *vs* b′/b″/b‴; c *vs* c′/c″/c‴; d *vs* d″/d‴; a′ *vs* a″/a‴/b′/c′; b′ *vs* c′; a″ *vs* a‴/b″; a‴ *vs* d‴; (b) PBS amount absorbed/ unit weight as a function of CS concentrations. Anova one way, MRT ($p < 0.05$): a *vs* a′/a″/a‴; b *vs* b‴; c *vs* c″/c‴; d *vs* d″/d‴; a′ *vs* a‴/d′; b′ *vs* b‴; a″ *vs* a‴; b″ *vs* b‴.

The capability to absorb wound exudate should quicken healing because the exudate of chronic wounds is rich in metalloproteinases and polimorphonuclear elastases, that are tissue destructive proteinase enzymes. For this reason an important characteristic of modern dressings is the capability to absorb excess wound exudate to maintain skin moisture more functional to healing (Boateng et al., 2008).

Particle capability to absorb buffer depended on $CaCl_2$ and CS concentrations. As expected, an increase in $CaCl_2$ concentration produced a decrease in the amount of PBS absorbed. This was due to a higher cross-linking degree of pectin chains due to Ca ions. In particular, particles prepared

with $CaCl_2$ 0.5% (w/w) were able to absorb PBS to an extent 20-fold higher than their weight (Figure 5a).

In presence of CS, lower hydration properties were observed; absorbed PBS amount decreased on increasing CS concentration (Figure 5b), probably due to the formation of a packed polymeric structure based on ionic interactions between CS and PEC. Particles prepared with the highest CS concentration were able to absorb PBS about three times their weight.

For all the conditions considered, no variation in absorbed PBS amount was observed on increasing hydration time up to 6 h; this was due to the formation, within the first hour, of a very viscous gel able to protect the area of the lesion.

1.4.3.3 Mechanical resistance properties

Figure 6 (a and b) shows the results of penetrometry measurements performed on unloaded particles prepared with and without CS. In particular, force and work of penetration normalized for particle volume were used as parameters of particle mechanical resistance.

An increase in $CaCl_2$ concentration (1% e 2% (w/w)) caused a significant ($p<0.05$) increase in penetration parameters (Figure 6a). Mechanical resistance properties were also affected by CS concentration (Figure 6b). In particular, the highest values of both parameters were observed in presence of CS 1% (w/w), again indicating a packed polymeric structure based on ionic interactions between CS and PEC.

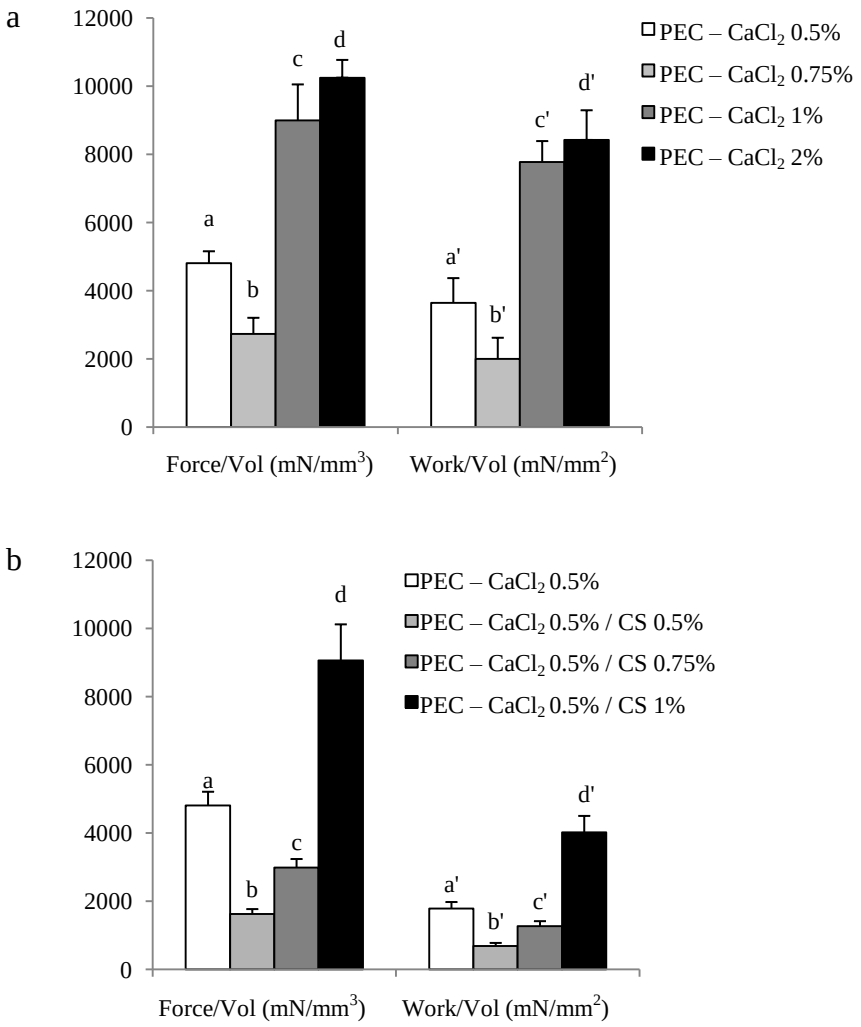

Figure 6 - Influence of preparation conditions on mechanical properties of unloaded particles (mean values ± s.e.; n = 3): (a) penetration force and area/unit volume as a function of $CaCl_2$ concentration. Anova one way, MRT ($p < 0.05$): a *vs* b/c; b *vs* d; a′ *vs* b′; b′ *vs* c′/d′; (b) force and area as a function of CS concentrations. Anova one way, MRT ($p < 0.05$): a *vs* b/c/d; b *vs* c/d; c *vs* d; a′ *vs* b′/d′; b′ *vs* c′/d′; c′ *vs* d′.

On the basis of the results obtained, $CaCl_2$ 0.5% (w/w) and CS 1% (w/w) concentrations were chosen as optimal conditions for particle preparation. Such conditions were used for the preparation of particles loaded with PL and Fr1.

1.4.4 Characterization of loaded particles

1.4.4.1 Particle size

In Figure 7 (a and b) size of PL- and Fr1-loaded particles are reported. Whereas PL loading caused a significant ($p < 0.05$) increase in particle size, it did not change after the addition of Fr1. This result could be attributed to the high increase in viscosity of PEC solution after mixing with PL; such an increase was responsible for bigger drops and, consequently, for greater particles. On the other hand, a slight increase in PEC solution viscosity was observed after addition of Fr1 (data not shown).

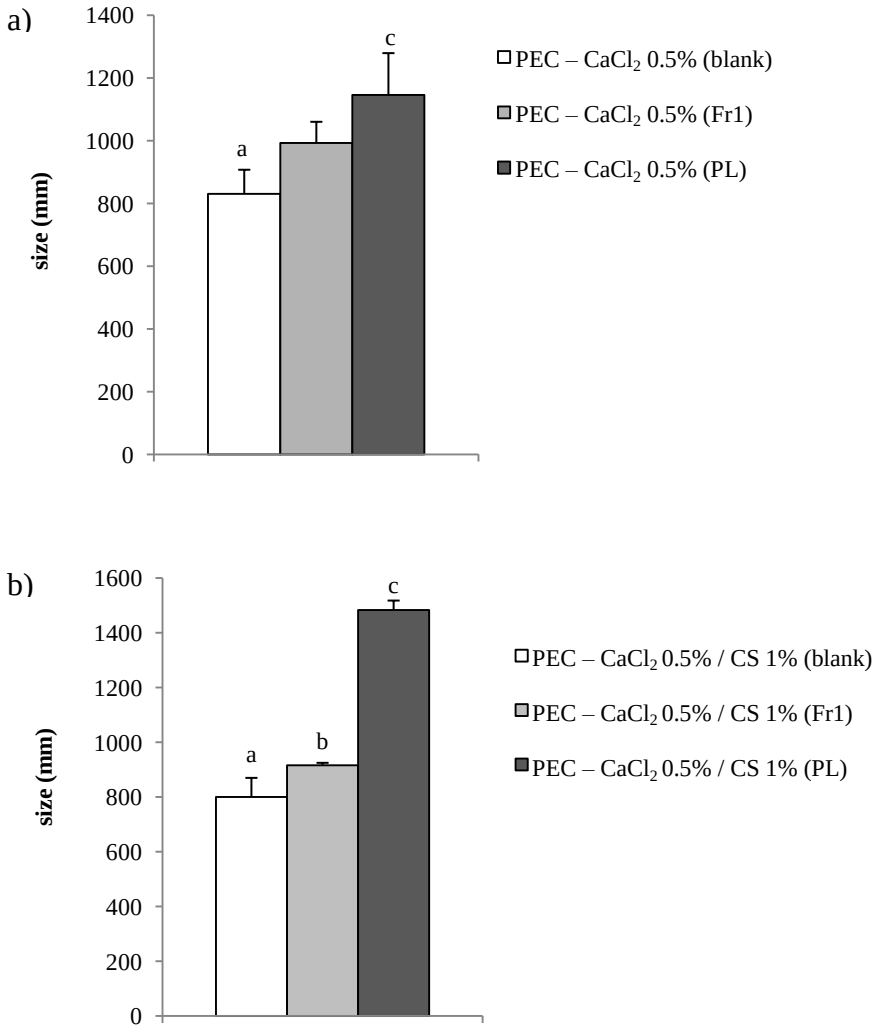

Figure 7 - Influence of PL and Fr1 loading on particle size (mean values ± s.d.; n = 3). (a) particles prepared using $CaCl_2$ 0.5% (w/w) solution. Anova one way, MRT ($p < 0.05$): a *vs* c; (b) particles prepared using $CaCl_2$ 0.5% (w/w)/CS 1% (w/w) mixture. Anova one way, MRT ($p < 0.05$): a *vs* b/c; b *vs* c.

1.4.4.2 Mechanical resistance properties

Figure 8 (a and b) shows the results of the penetrometry measurements carried out on loaded particles prepared with and without CS (1% w/w). The presence of both PL and Fr1 produced a decrease of mechanical resistance in comparison with unloaded particles, probably due to a disturbing effect to the particle packed structure. Such a decrease was stronger in the presence of PL and corresponded to an increase in particle size (see Figure 7).

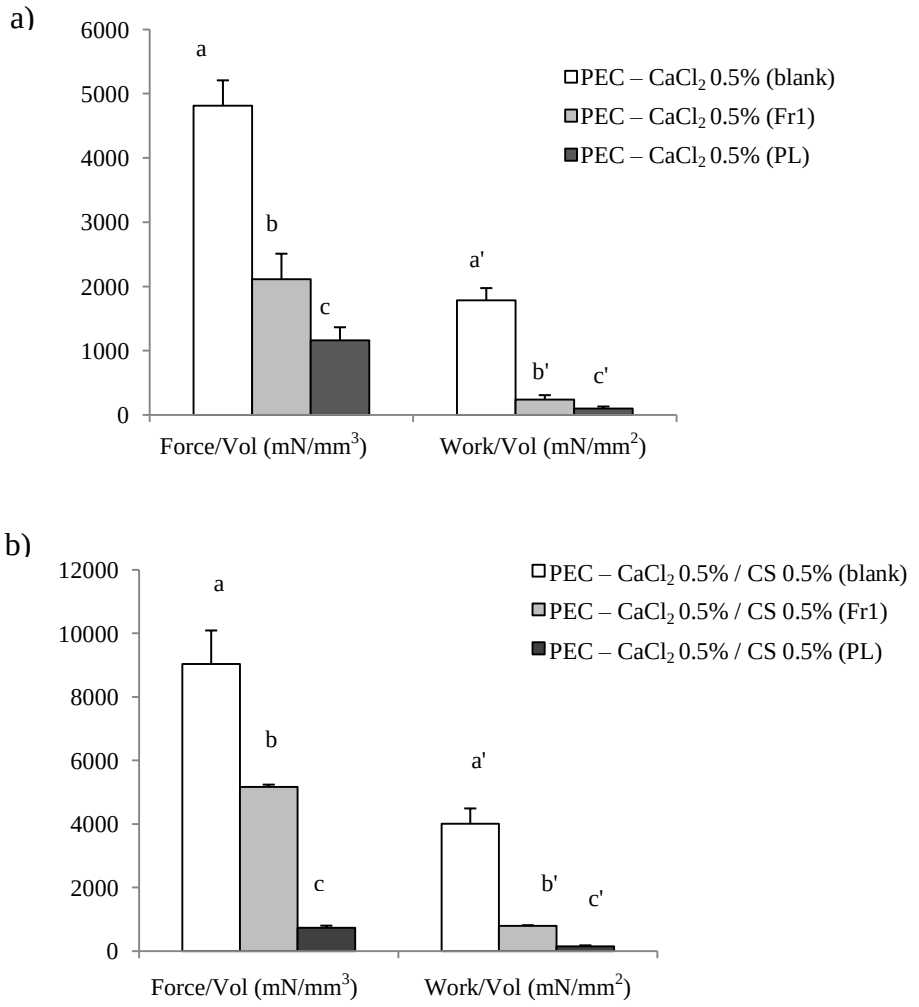

Figure 8 - Influence of PL and Fr1 loading on particle mechanical properties (mean values ± s.e.; n = 3). (a) Particles prepared using $CaCl_2$ 0.5% (w/w) solution. Anova one way, MRT ($p < 0.05$): a vs b/c; a′ vs b′/c′; (b) particles prepared using $CaCl_2$ 0.5% (w/w)/CS 1% (w/w) mixture. Anova one way, MRT ($p < 0.05$): a *vs* b/c; b *vs* c; a′ *vs* b′/c′; b′ *vs* c′.

1.4.4.3 PDGF-AB and Fr1 loaded into particles

In Table 1, %PDGF-AB and Fr1 loaded into particles are reported. The results showed that particles based on $CaCl_2$ 0.5% (w/w) were characterized by %PDGF-AB and Fr1 values equal to the

theoretical ones. The presence of CS produced a slight decrease in particle loading capacity. However, % PDGF-AB Fr1 values higher than 85% were obtained.

No significantly different results were obtained when particles were tested after 15 days storage at ambient temperature in hermetically sealed containers.

Table 1 - % PDGF AB and Fr1 loaded into particles (mean values ± s.d.; n = 4).

Beads	**% PL loaded**	**% Fr1 loaded**
PEC - $CaCl_2$ 0.5%	111.92 ± 6.69	100 ± 4.0
PEC - $CaCl_2$ 0.5%/CS 1%	87.40 ± 1.50	92 ± 10.0

1.4.5 Cell proliferation properties

In Figure 9, % proliferation values of loaded and unloaded particles diluted in M (w/s) are reported. On the basis of the results obtained for the mixture PEC/PL/ Fr1 (Figure 3), a 1:20 w/w dilution was chosen for the experiments on loaded and unloaded particles.

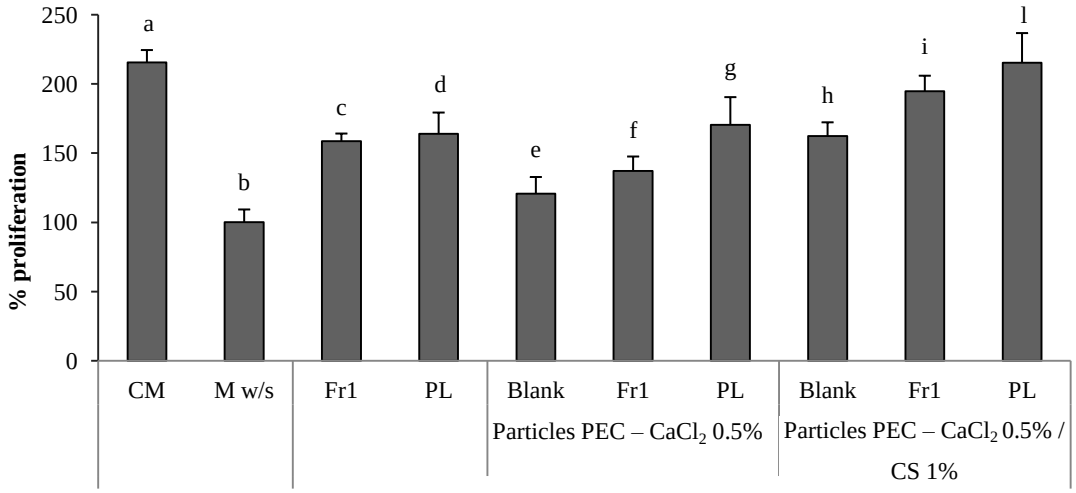

Figure 9 - % proliferation values of particles loaded with PL and Fr1. Unloaded formulations (blank), PL, Fr1, CM and M w/s were used as references (mean values ± s.e.; n=8). Anova one way-MRT: b *vs* a/c/d/f/g/h/i/l; c *vs* i; f *vs* i.

Both PL and Fr1 were characterized by % proliferation values significantly higher than M (w/s), to indicate that sodium citrate did not affect the biological activity of PL and Fr1.

Unloaded and Fr1-loaded particles, in absence of CS, showed % proliferation values comparable to M (w/s). The presence of CS in unloaded and Fr1-loaded particles produced an improvement of cell proliferation. Various mechanisms are reported in literature for chitosan activity on wound healing (Rossi. et al., 2015). It acts as a chemo-attractant for neutrophils and stimulates granulation tissue

formation or re-epithelization. Results reported in the literature prove that enzymes of wound bed are able to degrade chitosan, to form chitooligomers, involved in the synthesis of hyaluronan that, in turn, promotes cell motility, adhesion and proliferation and plays an important role in wound repair (Muzzarelli, 2009). Moreover, chitosan possesses a stimulatory effect on macrophages and antimicrobial properties that are beneficial in healing infected wounds. Moreover, it is able to inhibit metalloproteinases (Muzzarelli, 2009).

Both of the two formulations loaded with PL showed % proliferation values comparable with that of fresh PL. It indicates that the loading of PL into particles did not disturb the biological activity of the hemoderivative.

On the basis of the results obtained, particles prepared in presence of CS were chosen for *in vivo* efficacy tests.

1.4.6 *In vivo* efficacy on a rat wound model

Figure 10 shows full-thickness excisional wounds obtained 24 h after thermal injury on the back of male rats and 18 days after treatment with different formulations (PL-loaded particles, panel a, b; Fr1-loaded particles, panel c, d; physiological solution, panel e, f).

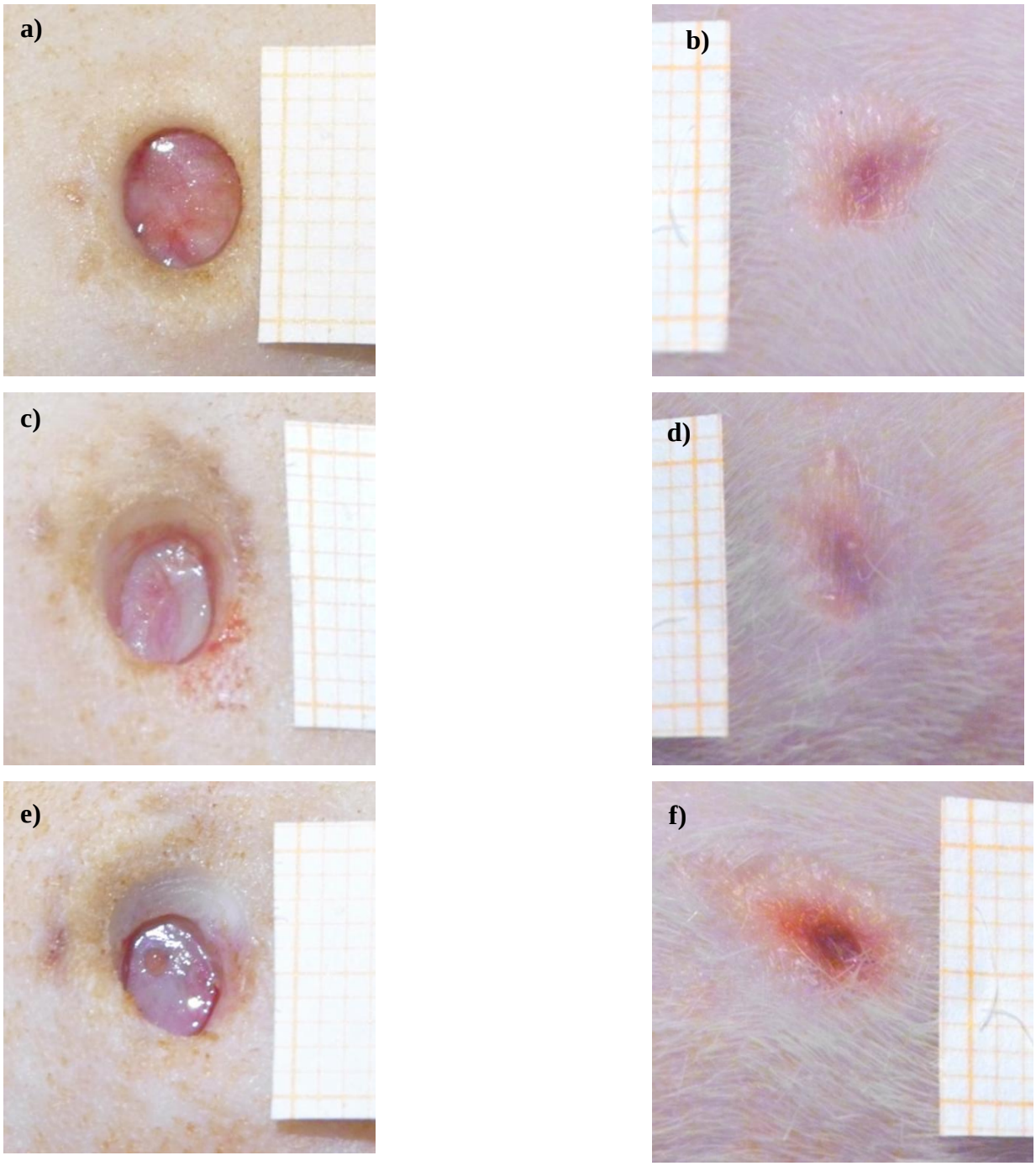

Figure 10 - Third grade excisional wounds 24 h after thermal injury (a, c, e) and 18 days after treatment with particles loaded with PL (b), particles loaded with Fr1 (d) or with saline solution as reference (f). One square of the reference grid corresponds to 1 mm^2.

It should be stressed that these are classified as third degree lesions since they were full-thickness injuries that deeply affected both epidermis and dermis. Furthermore, the capillary network of the dermis was completely destroyed, leaving the underlying structures unaffected. At the beginning of the experiment, each lesion presented a mean area of 23.46 ± 0.8 mm^2 (n=9) for a total injured area

(3 lesions) equal to 70.38 ±1.7 mm^2, accounting for less than 2% of the total body area of each animal.

At the end of the evaluation period (18 days) wound recovery equal to 73.20 ± 2.2% and 70.75 ± 3.8% was observed for PL-loaded and Fr1-loaded particles, respectively. After treatment of the lesions with physiological solution, a recovery of only 42.8 ± 9.2% was observed (Figure 10).

It is reported in literature that chronic ulcers can be characterized by an exudate excess that can slow down healing. In fact, an excessive production of exudates can cause maceration of healthy skin tissue around the wound, inhibiting tissue regeneration (Boateng et al., 2008). For this reason, all three lesions (not only the one used as control) were wetted with physiological solution

The time course of the wound healing process is reported in Figure 11. A faster wound healing was detected for particles loaded with both PL and Fr1. In particular, a significant ($p<0.05$) improvement in the wound healing rate was reported at the final stages of the treatment, i.e. 14 and 18 days after treatment with both loaded particles compared to physiological solution. These results were conceivably due to the slow and continuous release of the active substances, resulting from hydration and gelation of polymeric particles.

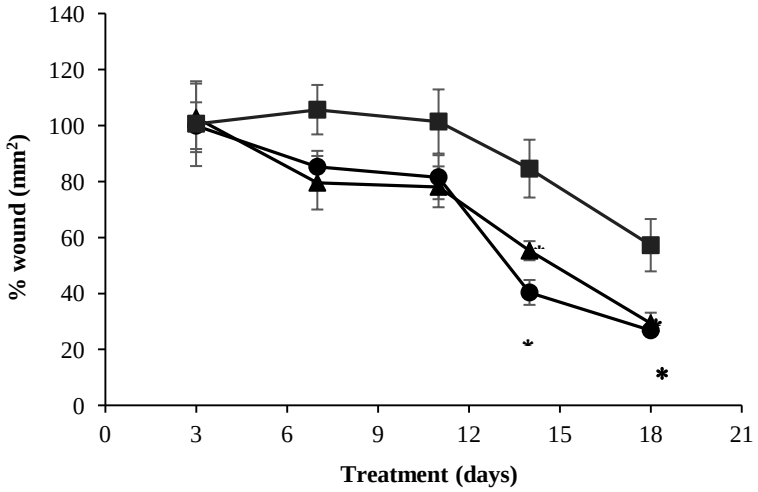

Figure 11 - Time course of wound healing. Percentage of wound area *vs* days after treatment (filled circle = PL-loaded particles, n=3; filled triangle = MH Fr1 loaded particles, n=3; filled square = saline solution, NaCl 0.9% w/v, n=3). * $p<0.05$ *vs* saline solution.

PL- and Fr1-loaded particles significantly increased wound healing to the same extent, in fact, no statistical difference was found between the two treatments (Figure 11). Since PL is known to strongly enhance wound healing, such a result indicates the very good properties of Fr1 as a healing

promoter. It should be stressed that for the first time, the *in vivo* results reported in the present study strongly suggest that Fr1 is the fraction responsible for the wound healing properties of MH.

Likewise, histological examination of skin sections reveals a more advanced stage of wound healing for samples treated with PL- and Fr1-loaded particles in comparison with the control samples. In Figure 12a, light microphotographs of skin sections taken 18 days after treatment with particles loaded with PL is reported. The epidermis was thin, but complete and well organized in several cell layers, showing a fair degree of keratinization (cornification). The underlying connective tissue contained a moderate inflammatory infiltrate and numerous blood vessels, some of which appear slightly dilated. Collagen fibers were dispersed and not yet organized in the large bundles typical of the reticular layer of the dermis. A similar picture was detected in the skin specimen of rats treated with Fr1-loaded particles after 18 days (Figure 12b): complete and well organized epidermis and moderate inflammatory infiltrate were visible as well, while large vacuoles were present in the dermis. The wall, made of a single layer of flattened cells, suggests that they were probably very dilated vessels; the collagen, in small parallel bundles, appeared more organized.

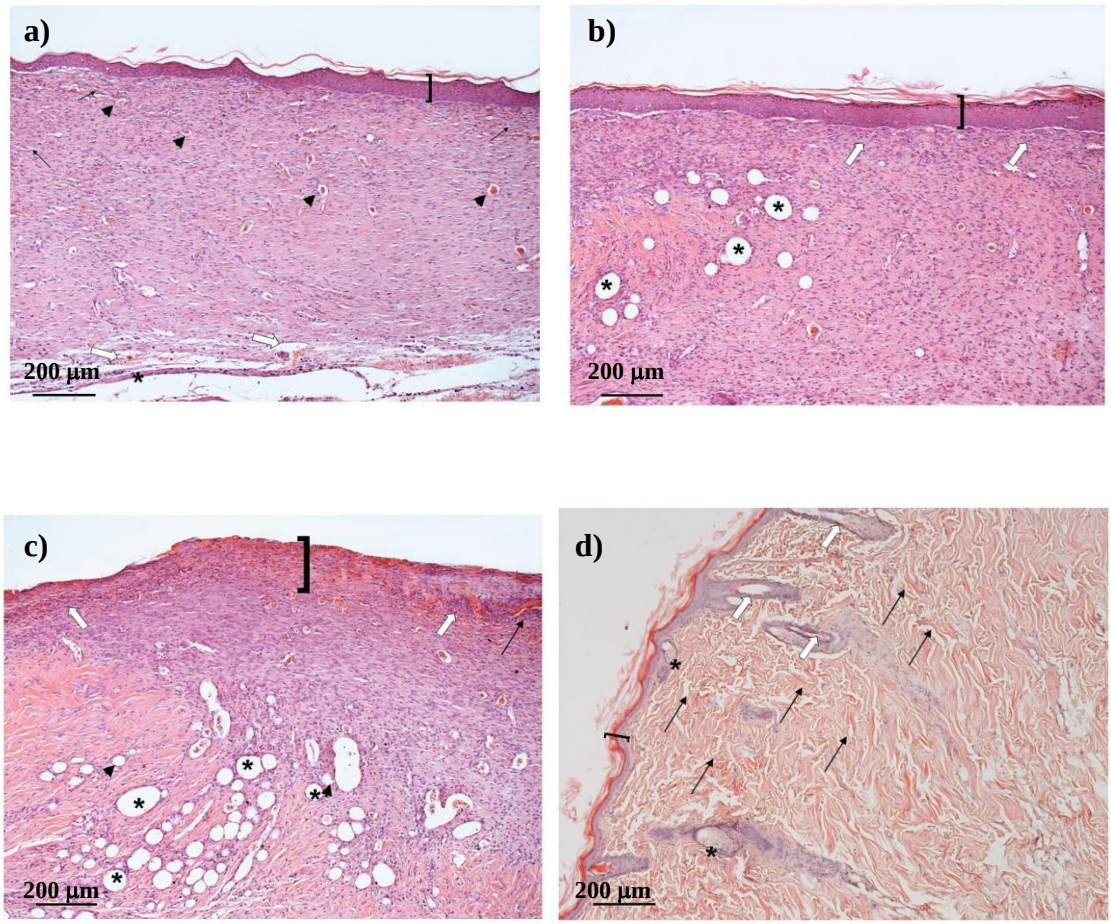

Figure 12 - Haematoxylin and eosin staining section of skin specimens. Light microphotographs (5X) of skin section 18 days after treatment (a) with PL-loaded particles, (b) with MH-Fr1-loaded particles, (c) with saline solution (NaCl 0.9%). Light microphotograph (5X) of intact tissue is illustrated in panel d). Skin structures labelled as follows: a) epidermis = bracket; vessel = arrowheads; great vessel of hypodermis = empty arrows; muscle tissue = asterisk; b) epidermis = bracket; connective tissue = empty arrows; dermis vacuole = asterisk; c) epidermis = bracket; epithelial cell = arrow; dermal connective tissue= empty arrows; adipocytes =arrowheads, vacuole = asterisk; d) epidermis = bracket; collagen fibers =arrows, hair follicles = empty arrows, glands = asterisks.

On the contrary, in the control tissue after 18 days of treatment with physiological solution (Figure 12c), the epidermis was not yet complete and replaced by a markedly eosinophilic necrotic tissue. In the peripheral regions of the lesion, epithelial cell division was detectable, which would enable the reorganization of the epidermal tissue. The underlying dermal connective was affected by an abundant granulation tissue; collagen fibers were dispersed and not yet organized, while there were numerous very dilated vessels. The aspects described above, especially the complete re-

epithelialization and the reduced granulation tissue in the treated samples, suggest that lesions treated with PL- and Fr1-loaded particles already showed features of early remodeling stage after 18 days, that is, the last phase of wound healing, whereas the control was still naturally in the former process of proliferation and repair with neovascularization / angiogenesis (Reinke and Sorg, 2012).

1.5 CONCLUSIONS

Particles prepared by ionotropic gelation from aqueous PEC solution (3% w/w) and 0.5% (w/w) $CaCl_2$ solution with and without CS (1% w/w) were characterized by 800 μm particle size, good mechanical resistance, capacity to hydrate and gelify when placed in contact with PBS (medium mimicking wound exudates). These particles were able to load and release active substances presented into Fr1 and PL.

The loading of PL into particles caused an increase in particle size, while particle size did not change in presence of Fr1. The loading of both PL and Fr1 produced a decrease of particle mechanical resistance, that is, however, suitable for their administration.

The presence of CS in unloaded and Fr1-loaded particles produced an improvement in fibroblast proliferation. Both the two formulations (with and without CS) loaded with PL were characterized by % proliferation values comparable with that obtained for fresh PL. These results demonstrate that loading PL into particles did not affect the biological activity of the hemoderivative. The *in vivo* results on a rat model proved that PL- and Fr1-loaded particles based on CS and PEC were able to promote wound healing to the same extent, showing that a specific fraction of MH, i.e. Fr1, is equally effective as PL and mainly responsible for the healing properties of MH. Additional experimental and clinical studies are necessary to further understand the mechanisms underlying the action and the efficacy of Fr1 and its clinical role.

A powder constituted by a mixture of these particles could therefore represent a promising candidate for the treatment of skin ulcers.

Given its easy preparation method, this formulation can be prepared in a hospital pharmacy service and promptly administered to patients. Moreover, it is easier and less painful to administer with respect to gauzes and semisolid preparations and makes the co-administration of active substances of different nature possible, avoiding any incompatibility problems. It also allows for a long interval between consecutive administrations, as evidenced by *in vivo* results upon treatment of ulcers; only once in an 18-day period.

1.6 REFERENCES

Anitua, E., Sanchez, M., Orive, G., Andia, I., 2007. The potential impact of the preparation rich in growth factors (PRGF) in different medical fields. Biomaterials 28, 4551–4560.

Boateng J.S., Catanzano O., 2015. Advanced therapeutic dressings for effective wound healing. J. Pharm. Sci. 104, 3653-3680.

Boateng, J.S., Matthews, K.H., Howard, N.E.S., Eccleston, G.M., 2008. Wound healing dressing and drug delivery system: a review. J. Pharm. Sci. 97, 2892–2923.

Caramella, C., Bonferoni, M.C., Rossi, S., Sandri, G., Ferrari, F., Perotti, G., Del Fante, C., 2011. Platelet lysate and bioadhesive compositions thereof for the treatment of mucositis. US2011/0280952.

Crovetti, G., Martinelli, G., Issi, M., Barone, M., Guizzardi, M., Campanati, B., Moroni, M., Carabelli, A., 2004. Platelet gel for healing cutaneous chronic wounds. Transfus. Apher. Sci. 30, 145-151.

Daglia, M., Ferrari, D., Collina, S., Curti, V., 2013. Influence of *in vitro* simulated gastroduodenal digestion on methylglyoxal concentration of manuka (Lectospermum scoparium) honey. J. Agr. Food Chem. 61, 2140-2145

Del Fante, C., Perotti, C., Bonferoni, M.C., Rossi, S., Sandri, G., Ferrari, F., Scudeller, L., Caramella, C., 2011. Platelet lysate mucoadhesive formulation to treat oral mucositis in graft versus host disease patients: a new therapeutic approach. AAPS PharmSciTech 12, 893-899.

Dellera, E., Bonferoni, M.C., Sandri, G., Rossi, S., Ferrari, F., Del Fante, C., Perotti, C., Grisoli, P., Caramella, C. 2014. Development of chitosan oleate ionic micelles loaded with silver sulfadiazine to be associated with platelet lysate for application in wound healing. Eur. J. Pharm. Biopharm. 83, 643- 650.

Mavric, E., Wittmann, S., Barth, G., Henle, T., 2008. Identification and quantification of methylglyoxal as the dominant antibacterial constituent of Manuka (*Leptospermum scoparium*) honeys from New Zealand. Mol. Nutr. Food Res. 52, 483−489.

Mazzucco, L., Borzini, P., Gope, R., 2010. Platelet-derived factors involved in tissue repair—from signal to function. Transfus Med Rev. 24, 218–234.

Molan, P., Rhodes, T., 2015. Honey: A Biologic Wound Dressing. Wounds 27, 141-51.

Mori, M., Rossi, S., Bonferoni, M.C., Ferrari, F., Sandri, G., Riva, F., Del Fante, C., Perotti, C., Caramella, C. 2014. Calcium alginate particles for the combined delivery of platelet lysate and vancomycin hydrochloride in chronic skin ulcers. Int. J. Pharmaceut. 461, 505-513.

Mori, M., Rossi, S., Ferrari, F., Bonferoni M.C., Sandri, G., Chlapanidas, T., Torre, M. L., Caramella, C., 2016a. Sponge-like dressings based on the association of chitosan and sericin for the

treatment of chronic skin ulcers. I. Design of experiments assisted development. J. Pharm. Sci. 105, 1180- 1187.

Mori, M., Rossi, S., Ferrari, F., Bonferoni, M. C., Sandri, G., Riva, F., Tenci, M., Del Fante, C., Nicoletti, G., Caramella, C., 2016b. Sponge-like dressings based on the association of chitosan and sericin for the treatment of chronic skin ulcers. II. Loading of the hemoderivative platelet lysate. J. Pharm. Sci. 105, 1188- 1195.

Munarin, F., Tanzi, M.C., Petrini, P., 2012. Advances in biomedical applications of pectin gels. Int. J. Biol. Macromol. 51, 681–689.

Muzzarelli, R.A.A, 2009. Chitins and chitosans for the repair of wounded skin, nerve, cartilage and bone. Carbohyd. Polym. 76, 167- 182.

Oelschlaegel, S., Gruner, M., Wang, P.N., Boettcher, A., Koelling-Speer, I., Speer, K., 2012. Classification and characterization of manuka honeys based on phenolic compounds and methylglyoxal. J. Agr. Food Chem. 60 (29), 7229-7237.

Rabea, E.I., Badaway, M.E.-T., Stevens, CV., Smagghe, G., Steurbaut, W., 2003. Chitosan as antimicrobial agent: applications and mode of action. Biomacronolecules 4, 1457–1465.

Ranzato, E., Patrone, M., Mazzucco, L., Burlando, B., 2008. Platelet lysate stimulates wound repair of HaCaT keratinocytes. British J. Dermatol. 159, 537–545.

Reinke, J.M., Sorg. H., 2012. Wound repair and regeneration. Eur. Surg. Res. 49, 35-43.

Rossi, S., Faccendini, A., Bonferoni, M.C., Ferrari, F., Sandri, G., Del Fante, C., Perotti, C., Caramella, C., 2013. "Sponge-like" dressings based on biopolymers for the delivery of platelet lysate to skin chronic wounds. Int. J. Pharmaceut. 440, 207-215.

Rossi, S., Ferrari, F., Sandri, G., Bonferoni, M.C., Del Fante, C., Perotti, C., Caramella, C., 2015. Wound Healing: Biopolymers and Hemoderivatives in: Mishra, M., (Ed.), Encyclopedia of Biomedical Polymers and Polymeric Biomaterials, 1st Ed., Vol. 11. Taylor & Francis, New York, pp. 8280-8298.

Rossi, S., Marciello, M., Bonferoni, M.C., Ferrari, F., Sandri, G., Caramella, C., Dacarro, C., Grisoli, P., 2010. Thermally sensitive gels based on chitosan derivatives for the treatment of oral mucositis. Eur. J. Pharm. Biopharm. 74, 248–254.

Rossi, S., Marciello, M., Sandri, G., Ferrari, F., Bonferoni, M.C., Papetti, A., Caramella, C., 2007. Wound dressings based on chitosans and hyaluronic acid for the release of chlorhexidine diacetate in skin ulcer therapy. Pharm. Dev. Technol. 12, 415–422.

Sandri, G., Bonferoni, M.C., Ferrari, F., Rossi, S., Del Fante, C., Perotti, C., Gallanti, A., Caramella, C., 2011b. An *in situ* gelling buccal spray containing platelet lysate for the treatment of oral mucositis. Curr. Drug Discov. Technol. 8, 277- 285.

Sandri, G., Bonferoni, M.C., Rossi, S., Ferrari, F., Mori, M., Cervio, M., Riva, F., Liakos, I., Athanassiou, A., Saporito, F., Marini, L., Caramella, C., 2015. Platelet lysate embedded scaffolds for skin regeneration. Expert Opin. Drug Deliv. 12, 525-545.

Sandri, G., Bonferoni, M.C., Rossi, S., Ferrari, F., Mori, M., Del Fante, C., Perotti, C., Caramella, C., 2012. Thermosensitive eyedrops containing platelet lysate for the treatment of corneal ulcers. Int. J. Pharmaceut. 426, 1- 6.

Sandri, G., Bonferoni, M.C., Rossi, S., Ferrari, F., Mori, M., Del Fante, C., Perotti, C., Scudeller, L., Caramella, C., 2011a. Platelet lysate formulations based on mucoadhesive polymers for the treatment of corneal lesions. J. Pharm. Pharmacol. 63, 189-198.

Werner, S., Grose, R., 2003. Regulation of Wound Healing by Growth Factors and Cytokines. Physiol. Rev. 83, 835 – 870.

Zheng, L.Y., Zhu, J.F., 2003. Study on antimicrobial activity of chitosan with different molecular weights. Carbohyd. Polym. 54, 527–530.

This work was object of 1 published paper (see page 29) and 3 conference presentations:

1. Tenci M., Rossi S., Ferrari F., Daglia M., Di Lorenzo A., Bonferoni M.C., Sandri G., Mori M., Caramella C.M., Platelet lysate and manuka honey loaded-pectin particles to promote healing of skin chronic ulcers. 2014 AAPS Annual Meeting and Exposition, San Diego November 2nd-6th 2014 (poster presentation);
2. Tenci M., Rossi S., Ferrari F., Daglia M., Di Lorenzo A., Bonferoni M.C., Sandri G., Mori M., Boselli C., Caramella C.M., Pectin beads for the combined delivery of platelet lysate and manuka honey to promote wound healing. CRS workshop "Nanomedicine: pharmacokinetic challenges, targeting and clinical outcomes", Florence November 6th-8th 2014 (poster presentation);
3. Tenci M., Rossi S., Bonferoni M.C., Ferrari F., Daglia M., Di Lorenzo A., Sandri G., Boselli C., Invernizzi A., Caramella C. Particulate systems based on pectin-chitosan association for the delivery of Manuka honey components effective in wound healing. 55° Simposio AFI "Innovazione e prospettive del settore farmaceutico: ricerca e sviluppo, produzione, distribuzione e regolamenti", Rimini June 10-12th 2015 (oral presentation).

Chapter 2

Application of DoE approach in the development of mini-capsules, based on biopolymers and manuka honey polar fraction, as powder formulation for the treatment of skin ulcers

International Journal of Pharmaceutics (2017) 516, 266-277.

Tenci, M., Rossi, S., Bonferoni, M.C., Sandri, G., Mentori, I., Boselli, C., Icaro Cornaglia, A., Daglia, M., Marchese, A., Caramella, C., Ferrari, F.

Corresponding author: Silvia Rossi

2.1 ABSTRACT

The aim of the present work was the development of a powder formulation for the delivery of manuka honey (MH) bioactive components in the treatment of chronic skin ulcers. In particular pectin (PEC) / chitosan glutamate (CS) / hyaluronic acid (HA) mini-capsules were obtained by inverse ionotropic gelation in presence of calcium chloride and subsequently freeze-dried. Optimization of unloaded (blank) formulation was performed using DoE approach. In a screening phase, the following three factors were investigated at two levels: CS (0.5% - 1% w/w), PEC (0.5% - 1% w/w) and HA (0.3% - 0.5% w/w) concentrations. For the optimization phase a "central composite design" was used. The response variables considered were: particle size, buffer (PBS) absorption and mechanical resistance. In a previously work two different MH fractions were investigated, in particular MH fraction 1 (Fr1), rich in polar substances (sugars, methylglyoxal (MGO), dicarbonyl compounds, ...), was able to enhance human fibroblasts *in vitro* proliferation. In the present work, the loading of MH Fr1 into mini-capsules of optimized composition determined a significant increase in cell proliferation in comparison with the unloaded ones. Loaded particles showed antimicrobial activity against *Staphylococcus aureus* and *Streptococcus pyogenes*; they were also able to improve wound healing *in vivo* on a rat wound model.

2.2 INTRODUCTION

Wounds are tissue injuries, that can be classified as acute or chronic on the basis of the nature of the repair process. Acute wounds are tissue injuries that heal completely, usually in 8–12 weeks; chronic wounds, i.e. diabetic and leg ulcers, on the contrary, do not heal within 12 weeks and often reoccur (Boateng and Catanzano, 2015). Chronic wounds fail to heal due to repeated trauma of the injured area or to underlying pathological conditions. Such wounds could involve a significant tissue loss and, in presence of neutropenia, lead to severe, even life-threatening, systemic infections (Boateng and Catanzano, 2015).

Wound healing is a complex process involving inter-related biological and molecular activities. The main physiological events are generally classified into five phases: hemostasis, inflammation, proliferation, migration and remodeling (Boateng et al., 2008; Enoch and Leaper, 2008)

Wound dressings are traditionally used to protect the area of the lesion from external contaminations, but they can also be useful to deliver active molecules into wound sites. Unlike traditional dressings, such as gauzes and cotton wool, the modern ones, based on bioactive polymers, take active part in wound healing process, to achieve rapid and complete recovery of chronic wounds (Rossi et al., 2015). Among bioactive polymers, chitosan and hyaluronic acid are known for bioadhesive and biocompatible properties and represent ideal candidates for the preparations of modern dressings (Muzzarelli, 2009; Rossi et al., 2013).

Chitosan (CS), a polysaccharide constituted by β(1-4)-linked N-acetyl-D-glucosamine residues and obtained by chitin deacetylation, shows antimicrobial activity and is used in the biomedical, i.e. tissue engineering, and biotechnological fields (Muzzarelli et al., 2015; Rossi et al., 2010; Zheng and Zhu, 2003). Several chitosan based dressings and bandages are commercially available (Muzzarelli, 2009). Various mechanisms are reported in literature for chitosan activity on wound healing. It acts as a chemo-attractant for neutrophils and stimulates granulation tissue formation or re-epithelization. Chitosan promotes dermal regeneration, possesses a stimulatory effect on macrophages and inhibits metalloproteinases (Muzzarelli, 2009).

Hyaluronic acid, a glycosaminoglycan, is one of the main components of the human connective tissues and is involved in different phases of the wound healing process (Rossi et al., 2015; Frenkel, 2012). The day after injury, hyaluronic acid binds to fibrinogen to form a temporary matrix that supports fibroblasts and endothelial cells. During the early inflammatory phase, hyaluronic acid stimulates the production of pro-inflammatory cytokines and facilitates adhesion of cytokine-activated lymphocytes to endothelium (Chen et al., 1999). During the proliferative phase of wound healing, hyaluronic acid stimulates the migration and proliferation of endothelial cells and the

production of collagen (type 1 and 8) (Slevin et al., 2002). Moreover, it promotes re-epithelisation by directly enhancing the migration of keratinocytes (Rossi et al., 2015).

Hyaluronic acid is included in topical formulations for its high capability to retain water and creates a moist environment useful to protect the lesion area and enhance wound healing (Catanzano et al., 2015; Humbert et al., 2013; Frenkel, 2012).

Honey is known for its biomedical activity in the treatment of various types of wounds, including burns, diabetic ulcers, pressure ulcers and leg ulcers (Molan, 2001). Thanks to its antimicrobial and anti-inflammatory properties, honey is able to enhance the rate of wound healing (Seckam and Cooper, 2013). In particular, in the literature it is reported that manuka honey (MH) is used in wound dressings. MH is a monofloral honey, obtained from the nectar of *Leptospermum scoparium*, a native plant in New Zealand and Australia (Kamaratos et al., 2014). MH exhibits activity against bacteria, including *Staphylococcus aureus* and *Pseudomonas aeruginosa* (Mavric et al., 2008; Kamaratos et al., 2014). Medihoney® dressing, indicated for the management of light to moderately exuding wounds, is the first wound dressing, based on MH, approved by FDA for clinical use (Boateng and Catanzano, 2015). In a previously work of ours, two different MH fractions, one (Fr1) rich in methylglyoxal and the other (Fr2) rich in polyphenols, were investigated for their capability to enhance fibroblast proliferation. Fr1 was able to improve cell proliferation and, when loaded in chitosan-pectin based matrices, to enhance wound healing in a rat model (Tenci et al., 2016).

Given these premises, aim of the present work was to develop mini-capsule formulations able to load Fr1 and to improve its efficacy in wound healing, thanks to its association, in addition to chitosan glutamate (CS), with hyaluronic acid sodium salt (HA).

Mini-capsules constituted by pectin (PEC), HA, CS and calcium ions were obtained by ionotropic inverse gelation, that implies the addition of Ca^{++} solution to an anionic polymer solution (Blandino et al., 2001; Leong et al., 2016). In this paper, the cationic solution was constituted by $CaCl_2$ and CS, the anionic one by PEC and HA.

Optimization of capsule composition was supported by a Design of experiments (DoE) approach.

In particular, in a screening phase, a “two level full factorial design” was used to investigate the effect of each factor (PEC, CS and HA concentrations) on the response variables such as particle size, capability to absorb wound exudate and mechanical resistance. The screening design was subsequently expanded to a “central composite design” (CDD) to determine the formulation of optimized composition. In order to confirm the predictive power of the model, the optimized formulation was subjected to the same characterization of the formulations of the CDD and the results obtained were compared with those predicted by the model. Mini-capsules of optimized composition were loaded with Fr1 and subsequently their cell proliferation properties were studied

on human fibroblasts. Antimicrobial activity of CS solution with and without Fr1 employed for mini-capsule preparation was investigated against *Staphylococcus aureus* and *Streptococcus pyogenes.* Finally *in vivo* efficacy of unloaded and loaded mini-capsules was evaluated on a rat wound model.

2.3 MATERIALS AND METHODS

2.3.1 Materials

The following materials were used: antibiotic antimycotic solution (100×), stabilized with 10,000 units penicillin, 10 mg streptomycin and 25 µg amphotericin B per ml (Sigma Aldrich, Milan, I); calcium chloride (Sigma Aldrich, Milan, I); chitosan low MW (CS) (DD: 80%) (Sigma Aldrich, Milan, I); Dulbecco's Modified Eagles Medium (DMEM, Lonza, BioWhittaker, B); Dulbecco's Phosphate Buffer Solution (Sigma Aldrich, Milan, I); Genu® Pectin type LM-18 CG (Giusto Faravelli, Milan, I); formic acid 1M (Sigma Aldrich, Milan, I); glutamic acid (Sigma Aldrich, Milan, I); Hank's balance salt solution (HBSS) (Sigma Aldrich, Milan, I); hyaluronic acid low MW (HA) (Bioiberica, Barcelona, E); inactivated foetal calf bovine serum (Euroclone, Pero, I); manuka honey (Marica Natura, Trezzano Rosa, I); methanol HiPerSolv CHRONANORM, HPLC-grade (VWR International, Milan, I); MTT (3-(4,5-dimethylthiazol-2-yl)-2,5-diphenyltetrazolium bromide) (Sigma Aldrich, Milan, I); $NaH_2PO_4 \cdot H_2O$ (Carlo Erba, Milan I); $Na_2HPO_4 \cdot H_2O$ (Carlo Erba, Milan, I); NaCl (Carlo Erba, Milan, I); PTA-blocking solution (PBS/Tween20/Albumin) (Sigma Aldrich, Milan, I); trypan blue solution (Biological Industries, Beit-Haemek, IL); trypsin–EDTA solution (Sigma Aldrich, Milan, I).

2.3.2 Experimental design

2.3.2.1 “Full factorial design” (FFD)

A “full factorial design” containing all possible combinations between the factors and their levels was chosen (Figure 1). Three factors (corresponding to the polymers CS, PEC and HA) at two different levels, corresponding to two different concentrations, were investigated (Figure 1).

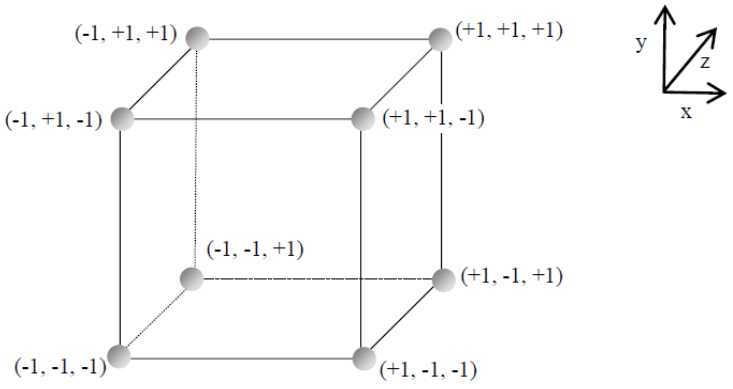

Figure 1 - Factor space and experimenting points of a “full factorial design”.

The polymer concentrations considered were: 0.5%, 1% w/w for CS and PEC; 0.3%, 0.5% w/w for HA. Eight capsule formulations were prepared. Polymer concentrations employed for their preparation are reported in Table 1: for each polymer the upper level is indicated as +1 and the lower level as -1.

Table 1 - Experimenting points of the "full factorial design".

	Chitosan (CS)	**Pectin (PEC)**	**Hyaluronic acid (HA)**
1	+1	-1	+1
2	+1	-1	-1
3	+1	+1	+1
4	+1	+1	-1
5	-1	+1	-1
6	-1	+1	+1
7	-1	-1	+1
8	-1	-1	-1

CS: level -1 (0.5%); level +1 (1%);

PEC: level -1 (0.5%); level +1 (1%);

HA: level -1 (0.3%); level +1 (0.5%).

The response variables considered were: particle size, hydration properties and mechanical resistance to compression. The statistical analysis of the data was carried out with a statistical software package (Statgraphics 5.0 Statistical Graphics Co., Rockvillle, MD, USA).

2.3.2.2 "Central composite design" (CDD)

As explained in the Introduction section, the 2^3 "full factorial design" was expanded to a "central composite design" (CDD), adding a "star design" and a "central point" to find the formulation of optimized composition.

CDD is a symmetrical response surface design, that cover a symmetrical experimental domain, and is useful to determine the optimal conditions for each factor. A CDD contains a two-level "full factorial design" (2^f experiments), a "star design" ($2*f$ experiments) and a "central point"; the model requires N experiments ($N = 2^f + (2*f) + 1$) to examine f factors (Figure 2).

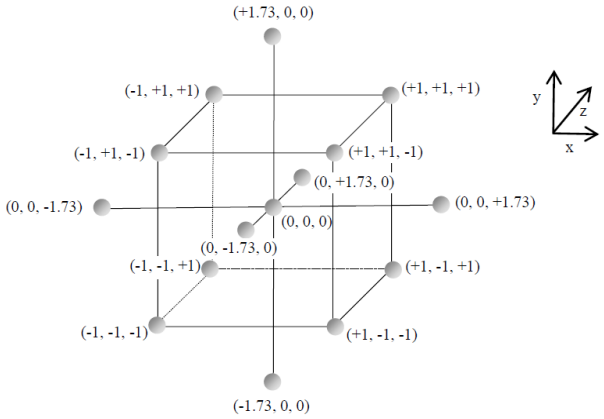

Figure 2 - Factor space and experimenting points of a "central composite design".

For three variables, the total number of formulations to be tested is 15. The points of the 2^3 "full factorial design" are situated at the levels -1 and +1, those of the star design at the levels 0, -α and +α (α=1.73), and the central point at the level 0 as indicated in Figure 2 (Dejagher and Vander Heyden, 2011). The factors and the response variables considered in the CDD were the same of the screening phase. Five levels for each factor were considered and seven additional capsule formulations were investigated with respect to the "full factorial design" (Table 2).

Table 2 – Additional experimenting points investigated to expand "full factorial" to "central composite" design.

	Chitosan (CS)	**Pectin (PEC)**	**Hyaluronic acid (HA)**
9	+1.73	0	0
10	0	0	+1.73
11	0	+1.73	0
12	0	-1.73	0
13	0	0	-1.73
14	-1.73	0	0
15	0	0	0

CS: level -1.73 (0.32%); level (+1.73) 1.18%; level 0 (0.75%).

PEC: level -1.73 (0.32%); level (+1.73) 1.18%; level 0 (0.75%).

HA: level -1.73 (0.227%); level (+1.73) 0.573%; level 0 (0.4%).

A polynomial model (Equation 1), describing the relation between each response variable and the considered factors, was build using the experimental results.

$$y = \beta_0 + \sum_{i=1}^{f} \beta_i x_i + \sum_{i=1}^{f} \beta_{ij} x_i x_j + \sum_{i=1}^{f} \beta_{ii} x_i^2$$

Equation 1 - Polynomial model, describing the relation between each response variable and the considered factors.

where y is the response, β_0 the intercept, β_i the main coefficients, β_{ij} the two-factor interaction coefficients, and β_{ii} the quadratic coefficients (Dejaegher and Vander Heyden, 2011). This polynomial model is useful to predict the response variables of any combination of factors within the experimental region (Vandervoort and Ludwig, 2002).

The model was interpreted graphically and visualized by drawing 2D contour plots and 3D response surface plots. 2D contour plots showed the iso-response lines as a function of the levels of two factors, while 3D response surface plots represented the response in a third dimension. From such plots, it was possible to derive the optimal polymer concentrations. When three or more factors are considered, 2D and 3D contours plots represent only a part of the entire response surface in the experimental domain (Dejaegher and Vander Heyden, 2011).

The statistical analysis of the data was performed by means of Statgraphics 5.0 (Statistical Graphics Co., Rockvillle, MD, USA) and pointed out that the best fit model for each response variable was the quadratic one (Equation 2).

$$y_i = \beta_0 + \beta_1 x_1 + \beta_2 x_2 + \beta_3 x_1 x_2 + \beta_4 x_1^2 + \beta_5 x_2^2$$

Equation 2 - Quadratic model, describing the relation between each response variable and the considered factors.

2.3.3 Preparation of unloaded mini-capsules

Mini-capsules were prepared by ionic gelation. In particular 500 μl of a $CaCl_2$ (0.75% w/w) / CS aqueous mixture was dropped with a syringe needle (32 G: 0.26 mm Ø x 4 mm) in 50 ml of an aqueous PEC/HA mixture. To prepare CS solution, an exact amount of glutamic acid (to obtain a 1:1 molar ratio with chitosan deacetylated amino groups) was added to distilled water before chitosan dispersion. Mini-capsules were immediately separated by vacuum filtration, freeze-dried overnight (Heto DRY WINNER®, Analitica De Mori, Milan, I) and then characterized.

2.3.4 Characterization of unloaded mini-capsules

Mini-capsules were characterized for particle size, hydration properties and mechanical resistance to compression as hereafter described.

2.3.4.1 Particle size

Particle size was evaluated by means of an optical microscope (Leica DMI 3000B), equipped with internal camera and PC Leica Application Suite EZ V1.8.1 program (Leica Microequipments, Milan, I).

2.3.4.2 Hydration properties

Mini-capsules were subjected to hydration measurements at 32 °C as described in (Tenci et al., 2016). Briefly, the hydration properties of mini-capsules were evaluated by means of Franz cells, using PBS (phosphate buffer saline, $NaH_2PO_4 \cdot H_2O$ 0.036%, w/w, $Na_2HPO_4 \cdot H_2O$ 0.137%, w/w, NaCl 0.85%, w/w), as medium mimicking wound exudate. The donor and receptor chambers of Franz cells were separated by a previously hydrated dialysis membrane (cut-off 12000-14000 Da). 5 mg of particles were layered on a paper disc and, in turn, placed on the dialysis membrane. After 6 h the increase in weight of hydrated with respect to dry mini-capsules was measured. The normalized parameter amount of PBS absorbed by unit weight (gPBS/g) was then calculated.

2.3.4.3 Mechanical resistance

The mechanical resistance of the mini-capsules was investigated by means of penetrometry measurement. TA.XT plus apparatus (ENCO, Spinea, I), equipped with a cone probe (P/10C), was used. The probe was lowered on mini-capsules at a rate of 0.1 mm/s up to 0.5 mm. The work of penetration ($mN \cdot mm$), calculated as the area under the penetration force *vs* distance curve, was recorded. The work of penetration was normalized for capsule volume to obtain penetration area / capsule volume parameter (mN/mm^2).

2.3.5 Optimization procedure

Each response variable of the experimental design (particle size (μm), PBS amount absorbed / unit weight (g/g), penetration area / capsule volume (mN/mm^2)) can be related to capsule composition by means of a suitable mathematical model. Experimental data were therefore subjected to multiple linear regression analysis, testing a series of models including linear, quadratic and special cubic (Draper and Smith, 1981). When the experimental conditions did not produce mini-capsules, the following response variable values were considered for the optimization procedure: particle size

5000 μm, PBS amount absorbed/unit weight 0 g/g; area/capsule volume 0 mN/mm^2. Model selection was effected by means of a statistical software package (Statgraphics 5.0, Statistical Graphics, Rocknille, MD), employing the Analysis of Variance (ANOVA) (Dejagher and Vander Heyden, 2009; 2011).

2.3.6 Characterization of the optimized capsule formulation

Mini-capsules of optimized composition, chosen on the basis of the results obtained, were prepared by ionic gelation, freeze-dried (as described in section 2.3.3) and subjected to the same characterization previously effected on the formulations of the "central composite design" (section 2.3.4). The experimental results obtained for the optimized mini-capsules were compared with those provided by the model, in order to confirm its predictive power.

2.3.7 Preparation of mini-capsules loaded with fraction 1 (Fr1) of MH

2.3.7.1 Extraction (SPE) of MH Fr1

Native MH was subjected to SPE as previously described (Tenci et al., 2016). In brief, a tC18 Sep-Pak Vac 6cc cartridge (Waters, Milford, Ma, USA) containing 1 g of stationary phase was conditioned with methanol (10 ml) and formic acid 0.1% (% v/v, 10 ml). Two grams of MH were dissolved in 3 ml of 0.1% formic acid and then poured into the cartridge at a flow rate of 1 ml/min. After loading the honey solution, the polar substances (sugars, methylglyoxal (MGO), dicarbonyl compounds, . .) were recovered with 1 ml formic acid 0.1% v/v (Fraction 1, Fr1), while the non-polar substances were eluted with a 1 ml mixture of methanol/0.1% v/v formic acid (75/25, % v/v). Fr1, after removal of methanol under a nitrogen stream and reconstitution of the initial volume with HPLC-grade water, were freeze-dried at 8 x 10^{-1} mbar and -50 °C (Modulyo1 Edwards Freeze-Drier, Kingston, NY).

2.3.7.2 Preparation of loaded mini-capsules

Mini-capsules of optimized composition were loaded with Fr1 of MH. For their preparation the same method used for unloaded mini-capsules was used (section 2.3.3), with the only exception that r1 was added to $CaCl_2$ / CS mixture to obtain a final Fr1 concentration of 50 mg/ml.

2.3.8 Characterization of mini-capsules loaded with fraction 1 (Fr1) of MH

Fr1 loaded mini-capsules were characterized for particle size, hydration properties and mechanical resistance as described for the unloaded formulations (section 2.3.4). Moreover, they were

characterized for loading capacity, *in vitro* cell proliferation properties, *in vitro* antimicrobial properties and *in vivo* efficacy on rat model as hereafter described.

2.3.8.1 Assessment of % Fr1 loaded into mini-capsules

The amount of Fr1 loaded into mini-capsules was indirectly measured, by means of an RP-HPLC-DAD method, previously developed and validated by Daglia et al. (2013). Breefly, an Agilent 1200 HPLC system (Agilent, Waldbronn, Germany), equipped with a quaternary pump and diode array detector, was used. The separation was performed on a Zorbax Eclipse XDB-C18 column (150 x 4.6 mm i.d., 5 μm particle size), equipped with the corresponding guard column, both maintained at 25°C. The mobile phase consisted of water acidified with 0.1% v/v formic acid (eluent A) and acetonitrile (eluent B), eluted with the following gradient at a flow rate of 0.3 ml/min: 0 min, 10% B; 0−5 min, 15% B; 5−30 min, 15% B; 30−45 min, 30% B; 45−50 min, 50% B; 50−60 min, 100% B; 60−65 min, 100% B; 65−70 min, 10% B; 70−80 min, 10% B. The injection volume was 5 μl. Spectral data were collected within the range of 200-800 nm for all peaks and chromatograms were processed at 314 nm.

The amount of Fr1 loaded was expressed as % of loaded MGO and calculated on the basis of the unloaded MGO into the aqueous PEC/HA mixture employed for capsule preparation. Upon vacuum filtration, in order to separate mini-capsules, the solution was concentrated five times by freeze-drying (Modulyo® Edwards Freeze-Dryer, Kingston, NY) and subsequent refilling with HPLC-grade water. Before HPLC analysis, MGO, contained in the filtrated solutions, was derivatized with 6 mg of o-phenylenediamine (OPD) and kept at 37°C for 1 h under constant stirring, to obtain the corresponding and UV-detectable quinoxaline. 1 h later, the samples were centrifuged at 8000 rpm for 10 min at room temperature. The supernatant was collected and submitted to HPLC analysis.

2.3.8.2 Assessment of cell proliferation properties

Mini-capsules of optimized composition, unloaded and loaded with Fr1, were characterized by cell proliferation properties using NHDF fibroblasts (Promocell GmbH, Heidelberg, Germany) from 6^{th} to 16^{th} passage.

5 x 10^4 cells/cm^2 were seeded in the basolateral chamber of Transwell® Permeable Supports System (Corning Costar, NY, USA) in presence of medium without fetal bovine serum (M w/s). 30 mg of mini-capsules was placed into the filter of the apical chamber, hydrated with 100 μl of M w/s and left in contact with cells for 24 h.

The Transwell® Permeable Supports System was used, since it avoids the direct contact of formulation with cells, thus impeding cell sufferance consequent to the formation of a viscous gel

after mini-capsules hydration. Such system allows to test mini-capsules as such, without any dilution in cell medium (Mori et al., 2016). After 24 h, Transwell® Supports containing the hydrated mini-capsules were removed; 500 µl of 7.5 µM MTT (3-(4,5-dimethylthiazol-2-yl)-2,5-diphenyltetrazolium bromide) solution in 1 ml of HBSS (pH 7.4) was added to each well and incubated for 3 h. After shaking for 60 s, absorbance was determined at a wavelength of 570 nm, with a 690 nm reference wavelength, by means of an IMark® Microplate reader (Bio-Rad Laboratories S.r.l., Segrate (MI), I). Results were expressed as % proliferation by normalizing the absorbance measured in presence of dressings with that measured in presence of M w/s.

2.3.8.3 Assessment of antimicrobial activity

CS and CS/Fr1 aqueous solutions employed for the preparation of unloaded and loaded mini-capsules of optimized composition and Fr1 aqueous solution (50 mg/ml) were freeze-dried overnight (Modulyo® Edwards Freeze-Dryer, Kingston, NY) and subsequently subjected to susceptibility test as hereafter described.

2.3.8.3.1 Susceptibility tests

The bacteria were isolated from skin and soft tissue infections and stored at the Institute of Microbiology, University of Genoa, Italy. They comprised of (i) ten *Staphylococcus aureus* strains, including five methicillin-resistant (MRSA) and five methicillin-susceptible (MSSA), furthermore, the MRSA isolates were multi-resistant (resistant at least three classes of antibiotics); (ii) five group A streptococci (*Streptococcus pyogenes*) strains, which remain universally susceptible to penicillin, and also were susceptible to macrolides.

All isolates were identified to the species level by using API STAPH and API STREP system (bioMèrieux, Marcy l'Etoile, F) for *S. aureus* and *S. pyogenes*, respectively.

The antibiotype was determined using the disk diffusion test suggested by the latest Clinical and Laboratory Standards Institute (CLSI) guidelines (Performance standards for antimicrobial disk susceptibility tests; approved standard. 12Th ed., Document M2-A12, Wayne, PA: CLSI, 2015). *S. aureus* ATCC 29213 and *S. pneumoniae* ATCC 49619 were used control strains.

Minimum Inhibitory concentrations (MICs) values of the sample against *S. aureus* and *S. pyogenes* isolates were determined by the broth microdilution method suggested by the CLSI guidelines (Methods for dilution antimicrobial susceptibility test for bacteria that grow aerobically, approved standard, 10th ed. Document M7-A10, Wayne, PA: CLSI, 2015).

In brief, exponentially growing bacteria ($5x10^5$ cells/ml, final inoculum) were added to various sample concentrations, 2-fold serially diluted in 96-well microtitre plates with Mueller-Hinton broth

(for *S. aureus*) or with cation-adjusted Mueller-Hinton broth containing 5% v/v lysed horse blood (*S. pyogenes*). After 18-24 h of incubation at 37°C, the concentrations at which sample prevented visible bacterial growth were recorded as the MIC. All tests were performed in triplicate. *S. aureus* ATCC 29213 and *S. pneumoniae* ATCC 49619 were added as control strains.

2.3.8.4 *In vivo* efficacy on rat wound model

All animal experiments were carried as previously described (Tenci et al., 2016). They were carried out in full compliance with the standard international ethical guidelines (European Communities Council Directive 86/609/EEC) approved by Italian Health Ministry (D.L. 116/92). The study protocol was approved by the Local Institutional Ethics Committee of the University of Pavia for the use of animals. Briefly, 6 male rats (Wistar 200-250 g) were anesthetized with equitensine (3 ml/kg) and shaved to remove all hair from the site of injury. Three full thickness burns, having a circular diameter of 4 mm, were produced on the backs of the animals by contact with a brass rod (105 °C for 40 s). The day after, three 6-mm full-thickness excisional wounds were outlined using a punch biopsy tool on each animal back and photographed with a digital camera (Sigma SD 14). Then, each wound was treated using a different sample: Fr1-loaded mini-capsules (25 mg) wetted with saline solution (NaCl 0.9% w/v) (25 μl), unloaded mini-capsules (blank) (25 mg) wetted with saline solution (25 μl), and physiological solution (25 μl) (reference). Wounds were covered with a sterile gauze and the rat back was wrapped with a surgery stretch (Safety, Monza, I), to keep particles or physiological solution into lesions. At prefixed times after treatment (3, 7, 10, 14 and 18 days) the three lesions were photographed with a digital camera (Sigma SD 14) and wetted with 25 μl of saline solution. The analysis of the photographs was carried out using UTHSCSA Image Tool v. 3.0 software. 18 days after the treatment full thickness biopsies were obtained and immuno-histochemical analysis of the excised tissues was carried out. A wound healing > 70% was considered the endpoint.

2.3.8.4.1 Microscopic analysis

A histological examination of the wounds was performed 18 days after the treatment as described in (Tenci et al., 2016). The animals were sacrificed and tissue samples were bisected along the widest line of the wound, then fixed in 4% w/v neutral buffered paraformaldehyde for 48 h, dehydrated with gradient alcohol series, cleared in xylene and embedded in paraffin. Sections (8 μm) were obtained using a Leitz microtome (Wetzlar, G) and stained with haematoxylin and eosin (H&E). The slices were examined at the magnification of 5X under a light microscope Axiophot Zeiss (Oberkochen, G) equipped with a digital camera.

2.3.9 Statistical analysis

Whenever possible, experimental values of the various types of measures were subjected to statistical analysis. In particular Anova one way-multiple range test was used (Statgraphics 5.0, Statistical Graphics Corporation, Rockvillle, MD, USA).

2.4 RESULTS AND DISCUSSION

2.4.1 "Full factorial design" (FFD)

Screening designs, such as "full factorial design", are used to study the influence of each factor (X) on the response variables (Y) and to indicate the most important factors (Dejagher and Vander Heyden, 2011). The effect of each X and that of their interactions on each Y is estimated by means of Pareto charts. These graphical representations are useful to determine which factors and relevant interactions have a significant effect, negative or positive, on each response variable of the experimental design. Table 3 reports the experimental results obtained for the 8 formulations (points 1- 8).

Table 3 - Particle size (μm), buffer (PBS) amount absorbed (g/g) and mechanical resistance (penetration area/volume of capsules; mN/mm^2) of the various capsule preparations of the "full factorial design" (points 1-8) and of the "central composite design" (points 1-15) (mean values ± s.d.; n=3).

Point of the design	Particle size (μm)	PBS amount absorbed (g/g)	Area/Volume (mN/mm^2)
1	2380 ± 115^{a}	9.2 ± 0.2 $^{a'}$	14.5 ± 3.4 $^{a''}$
2	2278 ± 212 ^{b}	3 ± 1 $^{b'}$	6.6 ± 1.7 $^{b''}$
3	2078 ± 125 ^{c}	6.1 ± 1.6 $^{c'}$	9.2 ± 1.3 $^{c''}$
4	2411 ± 29 ^{d}	9.5 ± 1.5 $^{d'}$	39.3 ± 6.7 $^{d''}$
5	2954 ± 192 ^{e}	21.0 ± 1.5 $^{e'}$	1.8 ± 0.3 $^{e''}$
6	3254 ± 42 ^{f}	11.2 ± 2.8 $^{f'}$	2.8 ± 0.5 $^{f''}$
7	n. d.	n. d.	n. d.
8	n. d.	n. d.	n. d.
9	1944 ± 200 ^{I}	12.0 ± 3.2 $^{I'}$	74.5 ± 10.5 $^{I''}$
10	2397 ± 43 ^{l}	7.6 ± 2.3 $^{l'}$	32.0 ± 6.9 $^{l''}$
11	2212 ± 54 ^{m}	10.0 ± 3.1 $^{m'}$	36.8 ± 10.7 $^{m''}$
12	n. d.	n. d.	n. d.
13	n. d.	n. d.	n. d.
14	n. d.	n. d.	n. d.
15	2204± 170 ^{q}	7.0 ± 2.3 $^{q'}$	23.2 ± 1.2 $^{q''}$

n.d.: not detectable, capsules did not form

t-test ($p<0.05$): *′*

a vs c/e/f/I; b vs e/f; c vs d/e/f; d vs e/f/I/m; e vs I/l/m/q; f vs I/l/m/q; I vs l; l vs m;

a′ vs b′/c′/e′; b′ vs d′/e′/f′/I′/m′; c′ vs e′/f′/I′; d′ vs e′; e′ vs f′/I′/l′/m′/q′; f′ vs m′;

a″ vs d″/e″/f″/I″/l″/m″/q″; b″ vs d″/e″/f″/I″/l″/m″/q″; c″ vs d″/e″/f″/I″/l″/m″/q″; d″ vs e″/ f″/I″; e″ vs f″/I″/l″/m″/q″; f″ vs I″/l″/m″/q″; I″ vs l″/m″ /q″.

It can be observed that mini-capsules prepared with the highest concentrations of CS, PEC and HA (formulation 3) was characterized by the smallest particle size, while the greatest value of hydration parameter was shown by the formulation 5 prepared with the highest PEC concentration and lowest CS and HA concentrations. As for mechanical resistance, formulation 4, characterized by the highest CS and PEC concentrations and by the lowest HA concentration, presented the best performance. The polymer concentrations employed for formulations 7 and 8 did not produce mini-capsules.

In Figure 3, the Pareto chart and the interaction plot of the response variable particle size are reported.

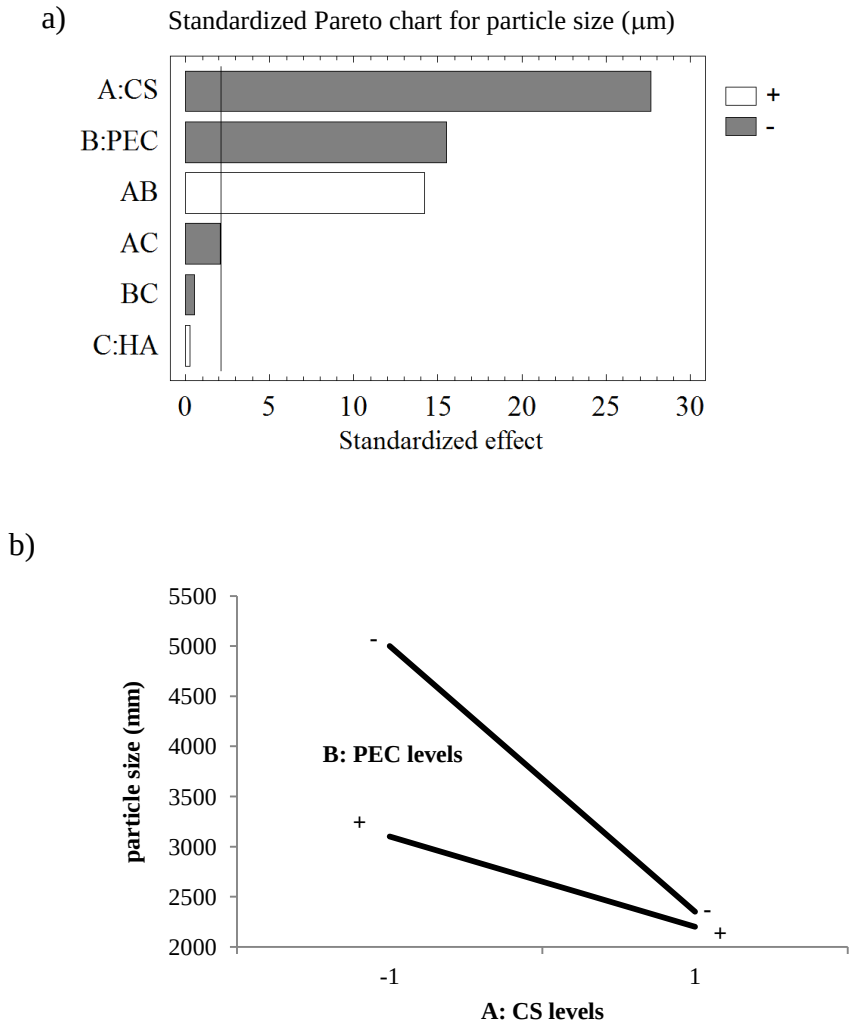

Figure 3 - Standardized Pareto chart and interaction plot of the response variable particle size (μm) of the "full factorial design".

It can be observed that chitosan (CS) and pectin (PEC) had a significant negative effect, meaning that an increase in CS or PEC concentrations caused a decrease of particle dimensions (Figure 3a). A possible explanation of this is that a high polymer concentration could be responsible for a faster and more important ionic interaction between CS and PEC. Such an effect was greater for CS than for PEC. On the contrary, hyaluronic acid (HA) concentration did not affect particle size. Beside the effect of each factor (CS, PEC and HA concentrations), it is important to check their interaction. The only interaction with a significant effect on particle size was that of CS and PEC. In Figure 3b the relevant interaction plot is reported; a positive sign indicates a synergistic effect. An increase in PEC concentration, independently of CS concentration, produces a decrease of particle size. This is more evident for the lowest CS level. Moreover, the highest PEC concentration produced a lower dependence of particle size on CS concentration. The results concerning particle size suggest the use of the highest concentrations of PEC and CS to obtain the lowest particle size.

In Figure 4 the relevant Pareto chart and interaction plots of hydration properties are reported.

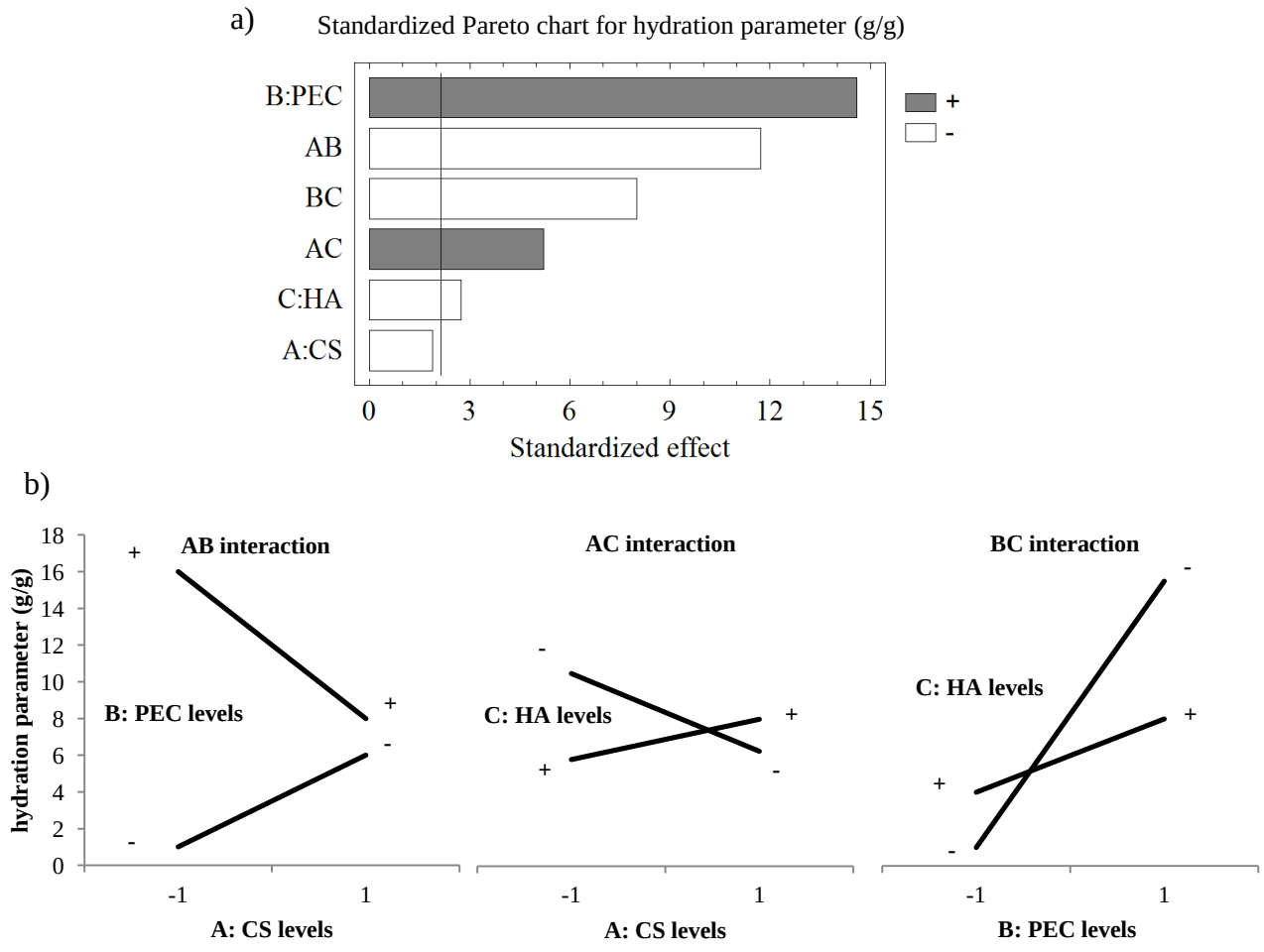

Figure 4 - Standardized Pareto chart and interaction plots of the response variable PBS amount

As illustrated in Figure 4a, the strongest effect on hydration properties was played by PEC: on increasing its concentration an improvement in capsule capability to absorb buffer was observed. Such an effect is attributable to the decrease of capsule size and to PEC high solubility in the hydration medium. All interactions showed significant effects, an antagonistic effect for CS-PEC and PEC- HA interactions and a synergic one for CS-HA interaction (Figure 4b). As for PEC/CS interaction, for both CS levels, an increase in PEC concentration produces an increase in hydration properties. Such an effect is greater for the lowest level of CS; this is in accordance with the decrease of capsule size (Figure 4b). At the highest PEC concentration, an increase in CS determines a decrease of hydration properties, probably due to the occurrence of a greater interaction between CS and PEC on capsule surface. A packed shell structure that hampers particle hydration forms. On the contrary, when the lowest PEC level is considered, an increase in CS level is responsible for an increase in hydration properties. As for PEC-HA interaction, when HA concentration is high, the effect of PEC is less marked. This is probably due to the competition of the two anionic polymers for the interaction with the cationic CS. As for CS-HA interaction, the highest hydration properties are observed for the low levels of both polymers.

Both CS and PEC concentrations showed a significant effect on capsule mechanical resistance (Figure 5).

As expected, an increase in CS or PEC concentration determined an increase in the parameter penetration work normalized for particle volume parameter. Between the two polymers, CS affects mainly capsule mechanical resistance. HA showed the same effect of CS and PEC, even though to lower extent. No polymer interaction showed a significant effect on mechanical resistance.

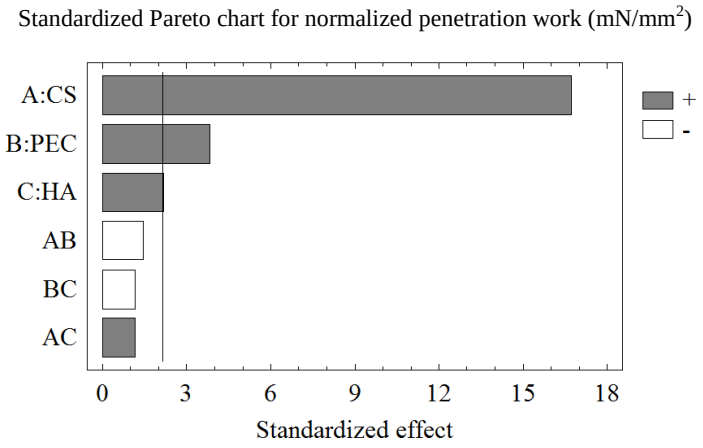

Figure 5 - Standardized Pareto chart for the response variable normalized penetration work for capsule volume (mN/mm^2) of the "full factorial design"

2.4.2 "Central composite design" (CDD)

In Table 3 the experimental results obtained for the 15 formulations are reported.

Figure 6 shows the Pareto charts of the three response variables.

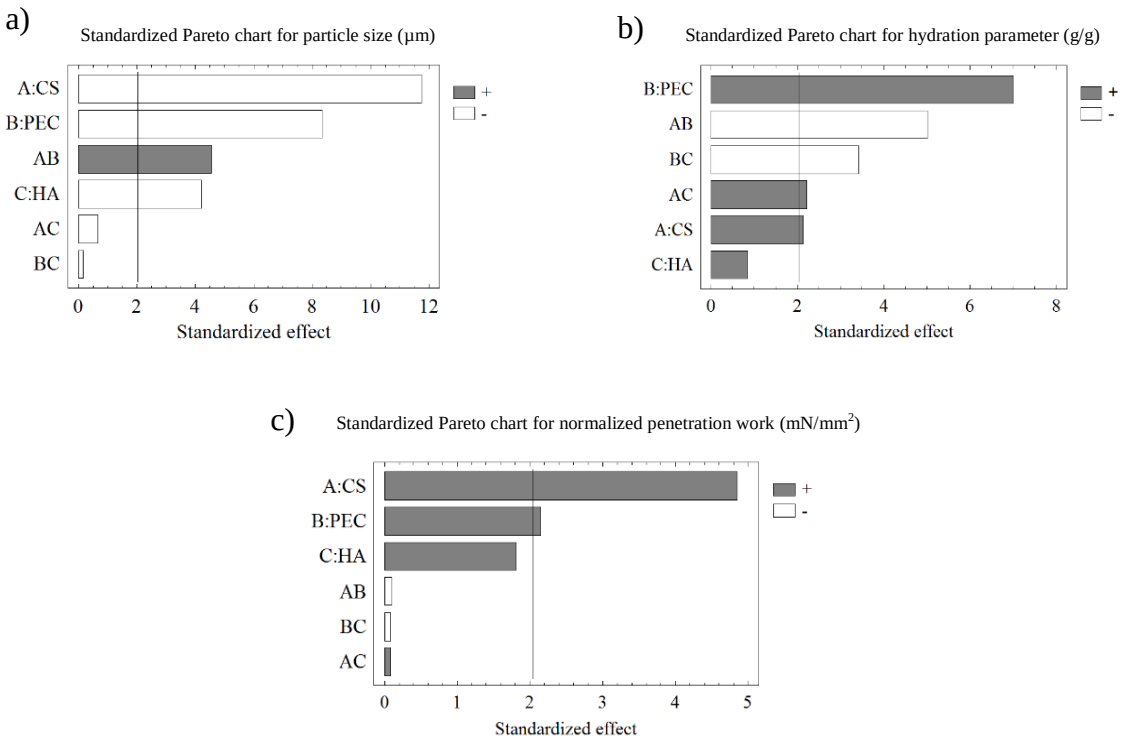

Figure 6 - Standardized Pareto chart (referring to main effects and their interactions) for the response variables particle size (µm), PBS amount absorbed/ unit weight (g/g) and penetration work normalized for capsule volume (mN/mm^2) of the "central composite design".

As for particle size, all the polymers possessed a negative effect. The extension of "full factorial" to "central composite design" has evidenced the significant effect on particle size not only of CS and PEC but also of HA. The interactions were not influent, except for CS-PEC interaction that, analogously to what observed in the *full factorial design*, had a significant effect on such parameter (Figure 6a). For both hydration and mechanical resistance properties, no changes on the effects of each polymer and of polymer-polymer interactions was determined by the extension of "full factorial" to "central composite design" (Figure 6b,c), with the exception of HA concentration that did not significantly affect capsule hydration properties. The results demonstrated that, among the factors considered, HA was the less influent on the response variables: while both CS and PEC significantly affects all the three response variables, HA significantly influences only particle size.

For such reason, it was decided to fix HA concentration for the optimization procedure. In table 4 the minimum values of particle size and the maximum values of hydration and mechanical resistance parameters predicted by the model for different levels of HA are reported.

Table 4 – Minimum values of particle size (μm) and maximum values of buffer (PBS) amount absorbed (g/g) and mechanical resistance (penetration area/volume of capsules; mN/mm^2) predicted by the model for different levels of HA.

HA level (HA conc. w/w)	**Particle size (μm)**	**PBS amount absorbed (g/g)**	**Area/Volume (mN/mm^2)**
-1.73 (0.23% w/w)	4000	20	180
-1 (0.30% w/w)	2000	20	140
0 (0.40% w/w)	1000	15	140
+1 (0.50% w/w)	1000	12.5	160
+1.73 (0.86% w/w)	2500	12	200

It must be underlined that PBS amount absorbed values higher than 10 (g/g) (corresponding to the capability of the sample to absorb buffer more than 10 times its weight) are indexes of good hydration properties. In this perspective, between the two levels (0, +1) for which the lowest value of particle size was predicted, +1 (0.50 w/w HA) has been chosen, since characterized by a higher value of mechanical resistance.

In Figures 7-9, contour plots (in bi- and tri- dimensional projections) drawn according to quadratic model for each response variable are reported. The model predicts that the lowest value of particle size is obtained for CS and PEC concentrations ranging, respectively, into the intervals 0.7% w/w (-0.18) – 1% w/w (+1.07) and 0.65% w/w (-0.39) – 0.94% w/w (+0.79) (Figure 7).

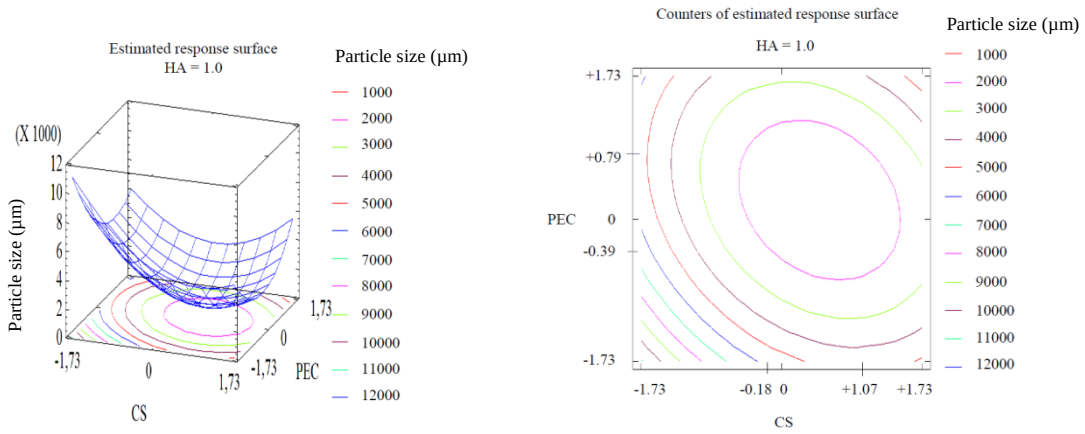

Figure 7 - Contour plots (in bi- and tri- dimensional projections) drawn according to quadratic model for the response variable particle size (µm) of the "central composite design"

As evidenced in Figure 8, the model predicts that the highest PBS amount is absorbed by mini-capsules characterized by high CS concentration (≥ 0.75% w/w) and by a PEC concentration in the range 0.32% w/w (-1.73) – 0.86% w/w (+ 0.47).

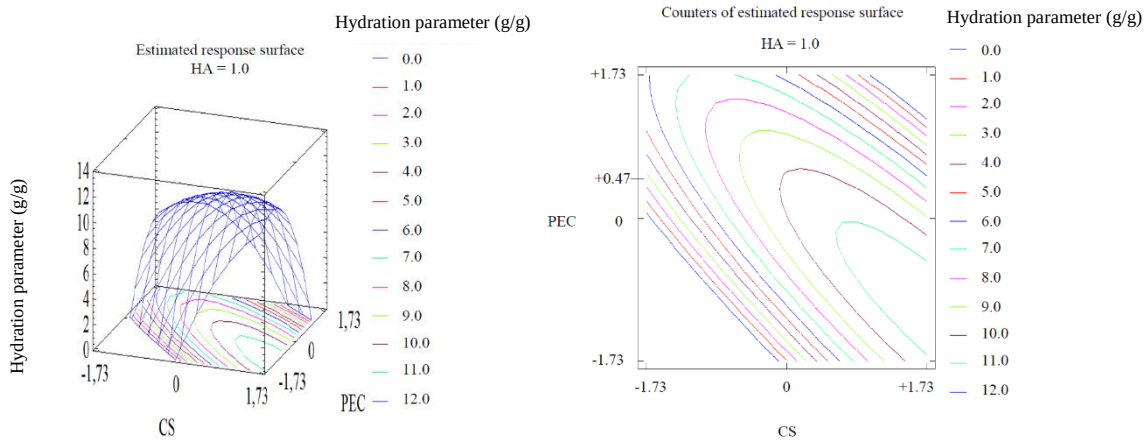

Figure 8 - Contour plots (in bi- and tri- dimensional projections) drawn according to quadratic model for the response variable amount of PBS absorbed/ unit weight (g/g) of the "central composite design"

As for mechanical resistance (Figure 9), the contour plots indicate that an increase in CS concentration above 1% w/w (+ 1.45) determines an increase in mechanical resistance, independently of PEC concentration. High normalized penetration work values (> 100 mN/mm^2) were obtained also for a low CS concentration (0.32% w/w: -1.73) and a high PEC concentration 1.18 w/w (+1.73). The highest mechanical resistance was observed for CS and PEC at a concentration equal to 1.18% w/w.

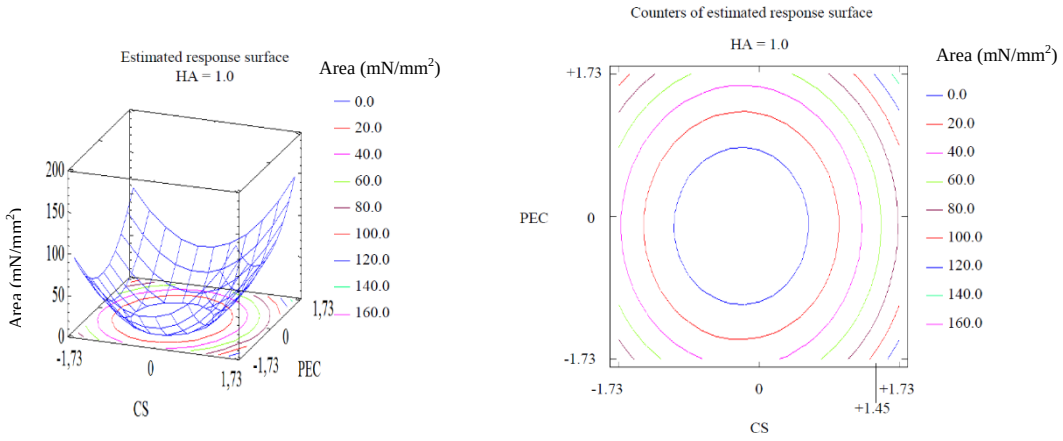

Figure 9 - Contour plots (in bi- and tri- dimensional projections) drawn according to quadratic model for the response variable penetration area normalized respect the volume of formulation (mN/mm^2) of "central composite design*"*.

The individual 2D contour plots were superimposed to identify the region of the experimental domain (Figure 10), satisfying the following constraints: particle size ≤ 2500 mm; amount (g) of PBS absorbed by unit weight of dressing ≥ 10 g/g; penetration work normalized by mini-capsules volume ≥ 60 mN/mm^2.

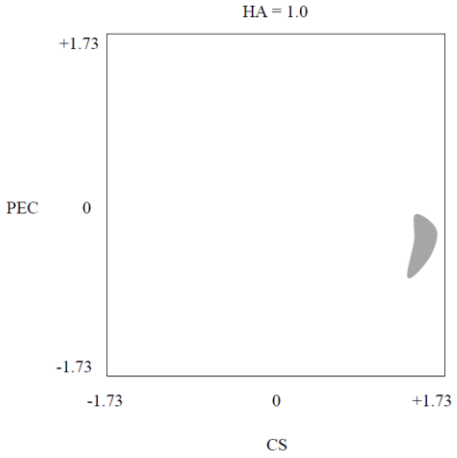

Figure 10 - Combined contour plot showing the region of optimal mini-capsules composition which satisfies all the constraints of the response variables.

The choice of the constrains was based on the following considerations: a low particle size facilitates administration, a good mechanical resistance is required to avoid problems during packaging and storage and a good capability to absorb the excess of wound exudate improves wound healing. It is in fact reported in literature, that, in the case of chronic wounds, an excess of exudate, that produces the maceration of the surrounding tissue, is present. Such an exudate is

characterized by higher concentrations of tissue destructive proteinase enzymes (such as metalloproteinases and polymorphonuclear elastase) with respect to that of acute wounds. For this reason, chronic wound exudate is more "corrosive" than that of acute wounds. Therefore, an important characteristic of modern wound dressings is the capability to absorb the excess of exudate to maintain a skin moisture functional to healing (Rossi et al., 2015; Boateng et al., 2008).

The formulation of optimized composition, chosen inside the area evidenced in Figure 10, was: CS 1.15% w/w - $CaCl_2$ 0.75% w/w / PEC 0.64% w/w - HA 0.5% w/w.
The optimized formulation was subjected to the same characterization previously effected on the design formulations. The experimental results obtained were the following (mean values ± s.d.; n=3): particle size= 1849 ± 109 μm, PBS amount absorbed by unit weight = 12 ± 2 g/g, penetration area normalized by capsule volume = 63 ± 2 mN/mm^2. Since such results lie inside the confidence interval of the relevant values predicted by the model, the model is predictive.

2.4.3 Characterization of Fr1-loaded mini-capsules

Fr1 loading into mini-capsules did not produce any statistically significant changes in particle size, hydration and mechanical properties with respect to unloaded mini-capsules. The experimental results (mean values ± s.d.; n=3) obtained for the loaded mini-capsules were: particle size = 1996 ± 72 μm, PBS amount absorbed by unit weight = 14 ± 3 g/g, penetration area normalized by capsule volume = 61 ± 2 mN/mm^2. Mini-capsules were characterized by % Fr1 values equal to the theoretical ones (100 ± 3.3 %). No significantly different results were obtained when particles were tested after 15 days storage at ambient temperature in hermetically sealed containers.

2.4.3.1 Cell proliferation properties

In Figure 11 % fibroblasts proliferation values after treatment with Fr1-loaded mini-capsules and unloaded mini-capsules are shown. It can be observed that loaded mini-capsules were characterized by % proliferation values significantly higher than the reference medium (M w/s) and unloaded formulations. These results indicate that loaded mini-capsules were able to enhance human fibroblast proliferation. Such an effect is attributable to the activity of Fr1 that is released from hydrated mini-capsules.

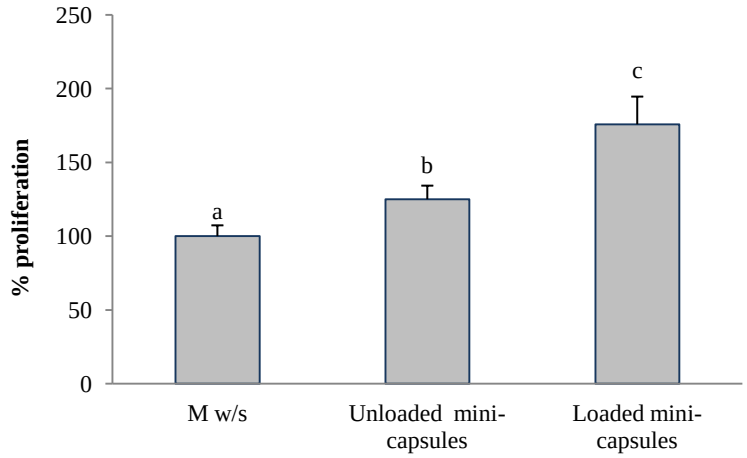

Figure 11 - % proliferation values of unloaded and Fr1-loaded mini-capsules. M w/s were used as references (mean values ± s.e.; n=8). Anova one way- MRT ($p < 0.05$): a *vs* c, b *vs* c.

2.4.3.2 Antibacterial activity

As for Fr1, even at the maximum concentration tested (50mg/ml), microbial growth was observed for all the clinical isolates (MICs >50 mg/ml). CS solutions with and without Fr1 showed antibacterial activity against all the tested *S. aureus* (MIC range 0.09-0.39 mg/ml and MIC range 0.09-0.78, respectively) and *S. pyogenes* (MIC range 0.09-0.39 mg/ml and MIC range 0.09-0.78, respectively).

MIC mode for each group of microorganisms tested are reported in Table 5.

Table 5 - MIC (mg/ml) of polymer aqueous solution with and without Fr1 against ten *S. aureus* and ten *S. pyogenes*. Frequencies (%) of the different bacterial species within MIC classes are shown.

Sample	Bacterial species	Number of isolates	MIC mg/ml 0.09	MIC mg/ml 0.19	MIC mg/ml 0.39	MIC mg/ml 0.78
Polymer solution (blank)	*S. aureus*	10	10%	60%	30%	0%
	S. pyogenes	10	20%	60%	20%	0%
Polymer solution + Fr1	*S. aureus*	10	10%	50%	30%	10%
	S. pyogenes	10	30%	40%	20%	10%

All the clinical isolates species exhibit equal values of MIC mode for the two solutions (with and without Fr1) that was 0.19 mg/ml. This result is indeed justified by the fact that CS is a polymer characterized by well-known antimicrobial properties (Muzzarelli et al., 2015; Rossi et al., 2010; Zheng and Zhu, 2003). Furthermore, no significant differences were observed between *S. aureus* carrying well-known mechanism of resistance and susceptible ones.

2.4.3.3 *In vivo* efficacy on a rat wound model

2.4.3.3.1 In vivo rat wound model

The wounds consisted of a full-thickness injury affecting either epidermis and dermis but leaving intact the underlying muscular structures. At the beginning of the experiments (t_0), the mean area of one lesion was 21.83 ± 0.59 mm^2 (n=18), for a total mean injured area (3 lesions for each animal) of 65.50 ± 2.21 mm^2 (n=6), accounting for less than 2% of the total body area of each animal. 18 days after treatment a wound recovery equal to 77.8 ± 2.8 % (n=6), 54.0 ± 8.2 % (n=6) and 46.6 ± 6.7 % (n=6) was observed for Fr1-loaded mini-capsules, unloaded mini-capsules and saline solution, respectively. No significant differences were found between the wound recovery of unloaded formulation and saline solution, while a significant ($p<0.05$) improvement in wound recovery was detected for Fr1-loaded formulation, with respect to saline solution. It must be pointed out that all the three lesions, not only the control one, were wetted with saline solution to mimic the *in vivo* conditions. As already mentioned, it is reported in the literature that the exudate excess present in chronic ulcers could delay healing process (Boateng et al., 2008). Recently Ousey et al. (2016) suggested that an appropriate moist environment actively supports the healing process, confirming previously published data in a full-thickness porcine wound model (Svensjö et al., 2000).

The time course of the wound healing process is reported in Figure 12. It must be underlined that the values 116% and 109%, observed after 3 days for the physiological solution and unloaded mini-capsules, respectively, are not significantly different from 100%.

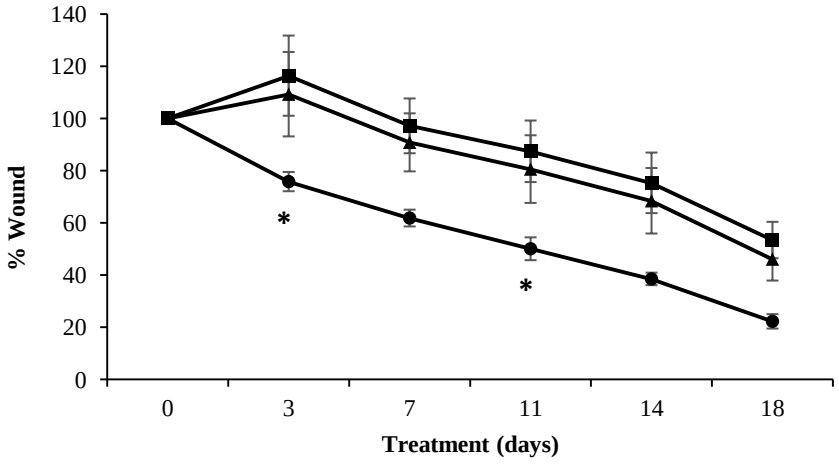

Figure 12 - Time course of wound healing. Percentage of wound area vs days after treatment (filled circle = MH Fr1 loaded particles, n=6; filled triangle = unloaded particles, n=6; filled square = saline solution, NaCl 0.9% w/v, n=6). * $p<0.05$ *vs* saline solution/unloaded particles; ○ no significantly different from 100%.

For all the time points considered, rats treated with Fr1-loaded mini-capsules showed a lesion area significantly ($p<0.05$) lower than that of those treated with unloaded mini-capsules and saline solution. This is conceivably due to the slow and continuous release of bioactive substances from Fr1-loaded mini-capsules, resulting in a positive and faster wound healing outcome.
No differences were observed between unloaded mini-capsules and saline solution. The *in vivo* data are in agreement with our previous results (Tenci et al, 2016), and proved that Fr1 loaded mini-capsules are able to accelerate wound healing.

2.4.3.3.2 Histological examination

The *in vivo* data reported above were supported by the histological examination of the tissue samples (or full thickness biopsies) taken 18 days after treatments.
In detail, 18-days after treatment with Fr1-loaded mini-capsules (Figure 13A) the epidermal layer, though not yet fully restored in some samples, appeared thick and well organized in several cell layers, and showed a fair degree of keratinization (cornification). Even in not fully healed samples, the overlying necrotic tissue was almost completely detached from the repaired tissue and granulation tissue as well as dilated vessels were present in a limited area, just beneath the not yet re-epithelized part, while hereinafter collagen fibers were organized in large bundles typical of the reticular layer of the dermis. Furthermore, skin appendages such as hair follicles and glands were reforming.

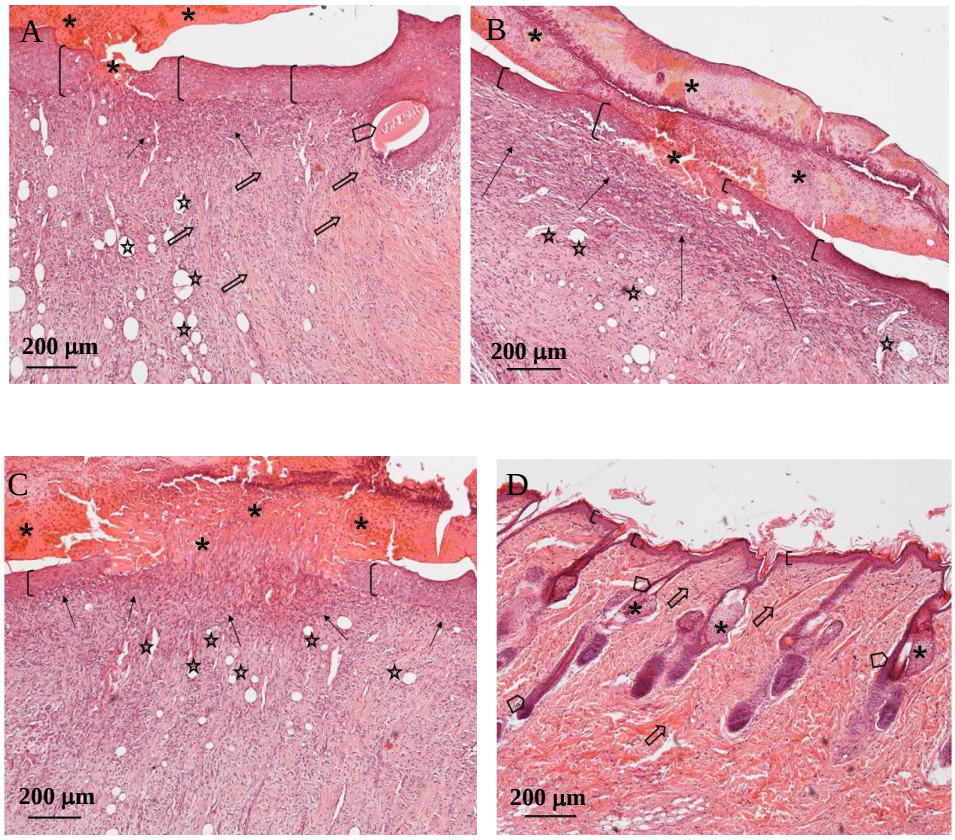

Figure 13 - Haematoxylin and eosin staining section of skin specimens. Light photomicroaphs of skin section 18 days after treatment (A) with MH-Fr1-loaded mini-capsules, (B) with unloaded mini-capsules, (C) with saline solution (NaCl 0.9%). Light microphotograph of intact tissue is illustrated in panel D. Skin structures labelled as follows: a) epidermis = bracket; necrotic tissue = asterisk; granulation tissue = arrow; vessel = star; dermal reticular layer = empty arrow; hair follicle = pentagon; b) epidermis = bracket; necrotic tissue = asterisk; granulation tissue = arrow; vacuole = star c) epidermis = bracket; necrotic tissue = asterisk; granulation tissue = arrow; vacuole = star; d) epidermis = bracket; collagen fibres = empty arrow, hair follicles = pentagon, glands = asterisk.

On the contrary, a deeply different picture has been detected for tissue samples treated with unloaded mini-capsules and saline solution (Figure 13B,C). In the first case (blank formulation) the epidermis was not yet completely restored and a large amount of necrotic material was detectable over the lesion. The underlying connective tissue was yet affected by an abundant granulation tissue; collagen fibers were dispersed and not yet organized in large bundles typical of the reticular layer of the dermis. In spite of what seen with Fr1-loaded mini-capsules, the tissue treated with unloaded formulation showed no evidence of skin appendage (hair follicles and glands) growth. In the dermis large vacuoles were present: the wall made of a single layer of flattened cells suggested that they were probably very dilated vessels. In the control tissue (saline solution) (Figure 13C) a

large part of epidermis was replaced by a markedly eosinophilic necrotic tissue. The underlying dermal connective was affected by an abundant granulation tissue; collagen fibers were dispersed and not yet organized in large bundles typical of the reticular layer of the dermis. No evidence of skin appendages (hair follicles and glands) could be detected, while there were numerous vacuoles of different size, delimited by a wall consisting of a monolayer of flattened cells (endothelium), that were probably very dilated vessels. In intact skin (Fig 13D) the epidermis was well organized in several cell layers and showed a high degree of keratinization (cornification). The underlying connective tissue displayed large bundles of collagen fibers; typical of the reticular layer of the dermis as expected in physiological conditions. In fact, skin appendages such as hair follicles and glands were detectable and well defined. The above described aspects, especially the occurrence of skin appendages and the reduced granulation tissue extension, as well as the arrangement of the collagen bundles suggested that lesions treated with Fr1-loaded mini-capsules showed an advanced stage of healing compared to those treated with unloaded formulations.

2.5 CONCLUSIONS

The optimization of capsule composition was performed by using a Design of experiments (DoE) approach. In particular, a "two level full factorial design" was used to investigate the effect of each factor (PEC, CS and HA concentrations) on the response variables (particle size, capability to absorb wound exudate and mechanical resistance). The expansion to a "central composite design" (CDD) permitted to determine the formulation of optimized composition. The ensuing mathematical model rightly predicted the functional properties of the formulation. The experimental values agreed with the predicted results; this implicates that the optimization using a DoE approach have saved the time and effort by the estimation of the optimum concentrations to obtain mini-capsules characterized by the best functional properties.

The results obtained prove that Fr1 fraction is the responsible for wound healing promotion, whereas the antimicrobial properties of the formulation are attributable to the presence of chitosan.

In a previous work of ours (Tenci et al., 2016), it has been shown that Fr1 possesses a wound healing effect comparable to platelet lysate (PL), a hemoderivative well-known for its wound repairing activity (Mazzucco et al., 2010; Del Fante et al., 2011; Mori et al., 2014; 2016).

In the present paper it has been proved that Fr1 loading into mini-capsules containing, beside pectin and chitosan, hyaluronic acid promotes wound healing in an *in vivo* animal model, stimulating tissue growth, enhancing epithelization and minimizing scar formation.

Fr1 is more easily recovered and manipulated than PL and its use does not determine problems related to a heterologous administration of hemoderivatives. Moreover, separation of Fr1 from other honey components is not expensive, thus resulting in an affordable therapy in terms of costs.

Finally, the simple method employed for capsule production makes such formulation easily obtainable in a hospital pharmacy service and promptly administrable to patients.

2.6 REFERENCES

Blandino, A., Macías, M., Cantero, D., 2001. Immobilization of glucose oxidase within calcium alginate gel capsules. Process Biochemistry 36, 601–606.

Boateng, J., Matthews, K.H., Stevens, H.N., Eccleston, G.M., 2008. Wound healing dressings and drug delivery systems: a review. J. Pharm. Sci. 97, 2892-2923.

Boateng, J., Catanzano, O., 2015. Advanced therapeutic dressings for effective wound healing- a review. J. Pharm. Sci. 104, 3653-80.

Catanzano, O., D'Esposito, V., Acierno, S., De Caro, C., Avagliano, C., Ambrosio, M., Russo, P., Russo, R., Miro, A., Ungaro, F., Calignano, A., Formisano, P., Quaglia, F., 2015. Alginate-hyaluronan composite hydrogels accelerate wound healing process. Carbohydr. Polym. 131, 407-414.

Chen, W., Abatangelo, G., 1999. Functions of hyaluronan in wound repair. Wound Repair Regen. 7, 79-89.

Daglia, M., Ferrari, D., Collina, S., Curti, V., 2013. Influence of *in vitro* simulated gastroduodenal digestion on methylglyoxal concentration of manuka (*Lectospermum scoparium*) honey. J. Agric. Food Chem. 61, 2140–2145.

Del Fante, C., Perotti, C., Bonferoni, M.C., Rossi, S., Sandri, G., Ferrari, F., Scudeller, L., Caramella, C., 2011. Platelet lysate mucoadhesive formulation to treat oral mucositis in graft versus host disease patients: a new therapeutic approach. AAPS PharmSciTech 12, 893–899.

Dejagher, B., Vander Heyden, Y., 2009. The use of experimental design in separation science. Acta Chromatogr. 21, 161- 201.

Dejagher, B., Vander Heyden, Y., 2011. Experimental designs and their recent advances in set-up, data interpretation, and analytical applications. J. Pharm. Biomed. Anal. 56, 141-158.

Draper, N.R., Smith, H., 1981. Applied regression analysis, New York: Wiley & sons, pp 412- 19

Enoch, S., Leaper, D.J., 2008. Basic science of wound healing. Surgery 26, 31- 37.

Frenkel, J.S., 2012. The role of hyaluronan in wound healing. Int. Wound J. 11, 159-163.

Humbert, P., Mikosinki, J., Benchikhi, H., Allaert, F.A, 2013. Efficacy and safety of a gauze pad containing hyaluronic acid in treatment of leg ulcers of venous or mixed origin: A double-blind, randomised, controlled trial. Int. Wound J. 10, 159- 166.

Kamaratos, A.V., Tzirogiannis, K.N., Iraklianou, S.A., Panoutsopoulos, G,I., Kanellos, I.E., Melidonis, A.I., 2014. Manuka honey-impregnated dressings in the treatment of neuropathic diabetic foot ulcers. Int. Wound J. 11, 259–263.

Leong, J.-Y., Lam, W.-H., Ho K.-W., Voo W.-P., Lee, M. F.-X., Lim H.-P., Lia, S.-L., Tey, B.-T., Poncelet, D., Chan, E.-S., 2016. Advances in fabricating spherical alginate hydrogels with controlled particle designs by ionotropic gelation as encapsulation systems. Particuology 24, 44-60.

Mavric, E., Wittmann, S., Barth, G., Henle, T., 2008. Identification and quantification of methylglyoxal as the dominant antibacterial constituent of Manuka (*Leptospermum scoparium*) honeys from New Zealand. Mol. Nutr. Food Res. 52, 483–489.

Mazzucco, L., Borzini, P., Gope, R., 2010. Platelet-derived factors involved in tissue repair—from signal to function. Transfus. Med. Rev. 24, 218–234.

Molan, P, 2001. Honey as a topical antibacterial agent for treatment of infected wounds. Am. J. Clin. Dermatol. 2, 13–19.

Mori, M., Rossi, S., Bonferoni, M.C., Ferrari, F., Sandri, G., Riva, F., Del Fante, C., Perotti, C., Caramella, C., 2014. Calcium alginate particles for the combined delivery of platelet lysate and vancomycin hydrochloride in chronic skin ulcers. Int. J. Pharm. 461, 505–513.

Mori, M., Rossi, S., Ferrari, F., Bonferoni, M.C., Sandri, G., Riva, F., Tenci, M., Del Fante, C., Nicoletti, G., Caramella, C., 2016. Sponge-like dressings based on the association of chitosan and sericin for the treatment of chronic skin ulcers. II. Loading of the hemoderivative platelet lysate. J. Pharm. Sci. 105, 1188–1195

Muzzarelli, R.A.A., 2009. Chitins and chitosans for the repair of wounded skin nerve, cartilage and bone. Carbohydr. Polym. 76, 167–182.

Muzzarelli, R.A.A., Mehtedi, M.E., Bottegoni, C., Aquili, A., Gigante, A., 2015. Genipin-crosslinked chitosan gels and scaffolds for tissue engineering and regeneration of cartilage and bone. Mar. Drugs 13, 7314–7338.

Ousey, K., Cutting, K.F., Rogers, A.A., Rippon, M.G., 2016. The importance of hydration in wound healing: reinvigorating the clinical perspective. J. Wound Care 25, 122-30

Rossi, S., Marciello, M., Bonferoni, M.C., Ferrari, F., Sandri, G., Caramella, C., Dacarro, C., Grisoli, P., 2010. Thermally sensitive gels based on chitosan derivatives for the treatment of oral mucositis. Eur. J. Pharm. Biopharm. 74, 248–254.

Rossi, S., Faccendini, A., Bonferoni, M.C., Ferrari, F., Sandri, G., Del Fante, C., Perotti, C., Caramella, C., 2013. Sponge-like dressings based on biopolymers for the delivery of platelet lysate to skin chronic wounds. Int. J. Pharm. 440, 207–215.

Rossi, S., Ferrari, F., Sandri, G., Bonferoni, M.C., Del Fante, C., Perotti, C., Caramella, C., 2015. Wound healing: biopolymers and hemoderivatives, In: Mishra, M. (Ed.), Encyclopedia of Biomedical Polymers and Polymeric Biomaterials 1st ed., vol. 11. Taylor & Francis, New York, pp. 8280–8298.

Seckam, A., Cooper, R., 2013. Understanding how honey impacts on wounds: An update on recent research findings. Wounds Int. 4, 20–24.

Slevin, M., Kumar, S., Gaffney, J. 2002. Angiogenic oligosaccharides of hyaluronan induce multiple signalling pathways affecting vascular endothelial cell mitogenic and wound healing responses. J. Biol. Chem. 277, 41046-41059.

Svensjö, T., Pomahac, B., Yao, F., Slama, J., Eriksson, E, 2000. Accelerated healing of full-thickness skin wounds in a wet environment. Plast. Reconstr. Surg. 106, 602-12.

Tenci, M., Rossi, S., Bonferoni, M.C., Sandri, G., Boselli, C., Di Lorenzo, A., Daglia, M., Icaro Cornaglia, A., Gioglio, L., Perotti, C., Caramella, C., Ferrari, F., 2016. Pectin/chitosan particles for the delivery of platelet lysate and manuka honey in chronic skin ulcers. Int. J. Pharm. 509, 59- 70.

Vandervoort, J., Ludwig, A., 2002. Biocompatible stabilizers in the preparation of PLGA nanoparticles: a factorial design study. Int. J. Pharm. 15, 238, 77-92.

Zheng, L.Y., Zhu, J.F., 2003. Study on antimicrobial activity of chitosan with different molecular weights. Carbohydr. Polym. 54, 527–530.

This work was object of 1 published paper (see page 60) and 5 conference presentations:

1. Tenci M., Rossi S., Bonferoni M.C., Ferrari F., Daglia M., Di Lorenzo A., Sandri G., Caramella C.M., Capsules based on pectin, chitosan and hyaluronic acid for the delivery of manuka honey into skin ulcers. 9th A.It.U.N. Annual Meeting "From food to pharma: the polyhedral nature of polymers", Milan, May 25-26th 2015 (poster presentation);
2. Tenci M., Rossi S., Bonferoni M.C., Ferrari F., Daglia M., Di Lorenzo A., Sandri G., Boselli C., Invernizzi A., Caramella C. Particulate systems based on pectin-chitosan association for the delivery of Manuka honey components effective in wound healing. 55° Simposio AFI "Innovazione e prospettive del settore farmaceutico: ricerca e sviluppo, produzione, distribuzione e regolamenti", Rimini, June 10-12th 2015 (oral presentation);
3. Tenci M., Rossi S., Ferrari F., Bonferoni M.C., Daglia M., Di Lorenzo A., Sandri G., Caramella C.M., Loading of manuka honey components into capsules based on chitosan, pectin and hyaluronic acid for the treatment of skin ulcers. ICC/EUCHIS 2015 12th International Conference of the European Chitin Society, 13th International Conference on Chitin and Chitosan, Münster, August 30th to September 2nd 2015 (poster presentation);
4. Tenci M., Rossi S., Ferrari F., Bonferoni M.C., Daglia M., Di Lorenzo A., Sandri G., Caramella C. Loading of manuka honey components into capsules based on chitosan, pectin and hyaluronic acid for the treatment of skin ulcers. COST Workshop on Electrospinning of Chitosan, Münster, September 2nd-4th 2015 (oral presentation);
5. Tenci M., Rossi S., Ferrari F., Bonferoni M.C., Sandri G., Di Lorenzo A., Mentori I., Boselli C., Caramella C., DoE assisted development of capsules based on biopolymers for the delivery of Manuka honey components into skin ulcers. 10th World Meeting on Pharmaceutics, Biopharmaceutics and Pharmaceutical Technology, Glasgow, United Kingdom, April 4-7th 2016 (poster presentation).

Chapter 3

In situ gelling system for the local treatment of inflammatory bowel disease (IBD). loading of maqui (*Aristotelis chilensis*) berry extract as antioxidant agent

3.1 ABSTRACT

The aim of the present work was the development of an innovative *in situ* gelifying system, to be applied on the mucosa of the distal colon via rectal route. The system consisted of three polymers having different functions: gellan (GG) able to gelify in presence of ions, methyl cellulose (MC), a thermosensitive polymer with a gelation temperature (Tg) close to 50°C, and hydroxypropyl cellulose (HPC), a mucoadhesive polymer. The three polymers were able to act sinergically, increasing the permanence of the vehicle on the mucosa and forming a protective gel layer on it. Surprisingly, the addition of GG to MC produced a lowering of MC Tg in the physiological range. A DoE approach, "simplex centroid design", was used to identify the optimal quantitative composition of the vehicle. The response variables considered were: vehicle viscosity at room temperature; increase in vehicle viscosity resulting from an increase in temperature (from room to the physiological value) and from the dilution with simulated colonic fluid (SCF); viscoelastic behavior, tixotropic area and mucoadhesion properties of the gel formed at 37°C upon dilution in SCF.

The optimized vehicle was loaded with maqui berry extract (MBE), known for its antioxidant and anti-inflammatory properties. MBE loading (0.5% w/w) into the vehicle improved rheological and mucoadhesive properties, functional to a better spreading and a longer permanence of the formulation onto mucosa. Both MBE and the optimized vehicle were not cytotoxic towards human fibroblasts and Caco-2 cells. Moreover, the optimized vehicle did not disturb MBE antioxidant properties.

3.2 INTRODUCTION

The inflammatory bowel disease (IBD), characterized by a chronic inflammation of the gastrointestinal tract, includes ulcerative colitis (UC) and Crohn's disease (CD). Such disease has a high prevalence in the Western industrialized countries, especially in young people (Lautenschläger et al., 2014). In particular, UC is an inflammation disease of mucosa and submucosa, locating in the large intestine. Even though the etiology is unknown, it has been recognized the role of genetic, immunoregulatory and environmental factors on the onset of UC. Among environmental factors there are: oral contraceptive use, breast-feeding, infections, microorganisms, smoking, appendectomy, sanitation and stress (Hanauer, 2006; Lichtenstein and Rutgeerts, 2010; Lautenschläger et al., 2014). The clinical picture of UC can include: several intestinal manifestations, like abdominal pain, bloody stool and diarrhoea; and extra-intestinal ones, affecting joints, skin, eyes and bile ducts (Lautenschläger et al., 2014).

The treatment of UC is dependent on the severity of disease and on patient-related factors, such as pre-existing illnesses, adherence and acceptability of the therapy (Taylor and Irving, 2011). Actually, the mainstay of UC treatment still consists of the so-called conventional therapies, including aminosalicylates (i.e. mesalazine and olsalazine), corticosteroids (i.e. prednislone) and immunomodulatory agents (i.e. azathioprine) (Taylor and Irving, 2011; Lautenschläger et al., 2014). Surgery is considered a therapeutic strategy for UC only when patients fail to adequately respond to the pharmacologic therapies, such as in case of refractory and fulminate diseases, or when disease complications occur (Irvine, 2008; Neurath and Travis, 2012). .

Many of the drugs mentioned above show from mild to severe adverse drug reactions, including mortality (Lautenschläger et al., 2014). The development of innovative therapeutic systems with a suitable balance between therapeutic efficacy and adverse drug reactions represents a stimulating challenge for pharmaceutical technology scientists (Lautenschläger et al., 2014).

In the last decade, *in situ* gelling systems to be applied locally have been recently proposed as alternative to conventional dosage forms (Pásztor et al., 2011; Yuan et al. 2012). Such systems, based on stimuli-responsive polymers, also called "smart" materials, do not require organic solvents or copolymerization agents (Ward and Georgiou, 2011). They are liquid aqueous solutions before administration and under physiological conditions they are able to gelify. In fact, *in situ* sol-gel transition occurs as a response of the contact with biological fluids, rich in ions, or of a change in pH or temperature (Ruel-Gariépy and Leroux, 2004; Schmaljohann, 2006).

Among thermoresponsive polymers, some cellulose derivatives, like methylcellulose (MC) and hydroxylpropylmethylcellulose (HPMC), have been investigated (Jeong et al., 2002; Klouda, 2015). In particular, for MC a gelling temperature (Tg) higher than 50°C has been reported in literature. In

the past, many attempts have been made to lower MC Tg into the physiological range. Some authors demonstrated the influence of various water-soluble polymers, such as polyvinylpyrrolidone, on MC Tg (Shimokawa et al., 2009). In another research paper the effects of pH and additives on MC Tg has been investigated (Makó et al. 2009). Other interesting "smart" materials are ion-sensitive polymers, including gellan gum and k-carageenan, which may undergo a sol-gel transition in presence of specific ions (Van Tomme et al., 2008; Parekh et al., 2012).

In literature, there are strong evidences of the beneficial effects of a dietary rich in polyphenols on health. Recently, some authors demonstrated that polyphenols, like anthocyanins, exhibit protective and therapeutic effects on IBD. In particular, they do not only show antioxidant activities, but also exert a down regulation of inflammatory mediators, such as cytochines, and suppression of inflammatory pathways (Yoshioka et al., 2008; Piberger et al., 2011; Biedermann et al., 2013; Farzei at al. 2015). Maqui fruits (*Aristotelia chilensis*), grown in Chile and Argentina, represent a rich source of polyphenolic compounds (Suwalsky et al. 2008). The increasing interest in maqui fruits has been attributed to the phytochemical profile of berry extracts (MBE) and their biological properties, like antioxidant activity, which are strongly correlated to anthocyanin content (Rubilar et al. 2011). Many studies on *in vitro* and *in vivo* biological activities of MBE demonstrated its efficacy as antioxidant (Céspedes et al., 2008; Ruiz et al., 2010), antimicrobial (Mølgaard et al., 2011) and anti-inflammatory (Schreckinger et al., 2010) agent.

Given these premises, the aim of the present work was the development of an innovative *in situ* gelifying system, to be applied on the mucosa of the distal colon via rectal route.

The system consisted of three polymers having different functions: two of them able to gelify with different mechanisms (presence of ions and increase in temperature) and the third one characterized by mucoadhesive properties. The three polymers should act sinergically to increase the contact time of the formulation with the mucosa, forming a protective gel layer on it.

The research was articulated in two phases. The first one was devoted to the choice of the three polymers, components of the vehicle, and of their concentrations. Gellan (GG) and k-carrageenan (K CARR) were investigated as ion-sensitive polymers, whereas methyl cellulose (MC) and hydroxypropylmethyl cellulose (HPMC) were studied as thermosensitive gelling agents. Hydroxypropyl cellulose was employed as mucoadhesive polymer. A DoE approach, "simplex centroid design", was used to identify the optimal quantitative composition of the vehicle. The response variables considered were: vehicle viscosity at room temperature; increase in vehicle viscosity resulting from an increase in temperature (from room to the physiological value) and the dilution with simulated colonic fluid (SCF); viscoelastic behavior; tixotropic area and mucoadhesion properties of the gel formed at 37°C upon dilution in simulated colonic fluid (SCF).

In the second phase of the research, the vehicle developed was loaded with maqui berry extract (MBE), known for antioxidant properties. MBE was obtained from the fruits of maqui (Aristotelia chilensis) (Tanaka et al., 2013). Antioxidant activity of the loaded vehicle was tested *in vitro* on both human fibroblast (NHDF) and human colorectal adenocarcinoma (Caco-2) cell lines.

3.3 MATERIALS AND METHODS

3.3.1 Materials

The following materials were used: acetonitrile HPLC-grade (Chromasolv, Sigma Aldrich, Milan, I); antibiotic antimycotic solution (100×), stabilized with 10,000 units penicillin, 10 mg streptomycin and 25 μg amphotericin B per ml (Sigma Aldrich, Milan, I); calcium chloride (Sigma Aldrich, Milan, I); cyanidin 3 glucoside (PhytoLab GmbH & Co. KG, Vestenbergsgreuth, Germany); Dulbecco's Modified Eagles Medium (DMEM, Lonza, BioWhittaker, B); Dulbecco's Phosphate Buffer Solution (Sigma Aldrich, Milan, I); formic acid 1M (Bioultra, Sigma Aldrich, Milan, I); gellan gum with low acetilation degree (GG; Kelcogel®; Giusto Faravelli, Milan, I); Hank's balance salt solution (HBSS) (Sigma Aldrich, Milan, I); HCl 1M (Carlo Erba, Milan, I); inactivated foetal calf bovine serum (Euroclone, Pero, I); k-carrageen (K CARR; Fluka BioChemika, Buchs, CH); KCl (Carlo Erba, Milan, I); $KHPO_4$ (Carlo Erba, Milan, I); maqui powder from dehydrated berries (Cibo Crudo, Milan, I); methanol HPLC-grade (Chromasolv, Sigma Aldrich, Milan, I); Methocel A4M (viscosity 3000-5500 mPa.s; Colorcon Ltd, Dartford, Kent, UK); Metolose 60SH-400 (Inpharzam Limited, Bresso, Milan, I); MTT (3-(4,5-dimethylthiazol-2-yl)-2,5-diphenyltetrazolium bromide) (Sigma Aldrich, Milan, I); mucin from porcine gastric source (Sigma Aldrich, Milan; I); NaCl (Panreac, Milan, I); Na_2PO_4 (Carlo Erba, Milan, I); trypan blue solution (Biological Industries, Beit-Haemek, IL); trypsin–EDTA solution (Sigma Aldrich, Milan, I).

3.3.2 Choice of the ion-sensitive gelling agent

The capability of gellan (GG) and k-carrageenan (K CARR) to gelify as response of ions present in the colonic fluid was investigated. GG and K CARR aqueous solutions (1.4% w/w) upon dilution in simulated colonic fluid (SCF) according to 5:2 weight ratio were subjected to viscosity measurements by means of a rotational rheometer (Rheostress 600, Haake, I), equipped with a cone plate (C60/1: Ø 60 mm; angle=1°) combination as measuring system. SCF was prepared according to Marques et al. (2011): KCl 0.2 g/l, NaCl 8 g/l, KH_2PO_2 0.24 g/l and Na_2PO_4 g/l. pH was adjusted to 6.3 by adding HCl 1 M.

Viscosity was measured at increasing shear rate (ranging from 10 up to 300 s^{-1}) at a constant temperature (37°C). In order to evaluate the ion-sensitive gelling properties of the two polymers, viscosity profiles of the polymer solutions diluted in SCF were compared with those obtained for the same solutions diluted in distilled water. The results were expressed as *normalized Δ viscosity* (Δ%), calculated, at each shear rate considered, as follows:

$$\Delta\% = ((\eta_{SCF} - \eta_{DW})/\eta_{DW})*100 \quad \text{Eq. 1}$$

where η_{SCF} is the viscosity (Pa.s) of the polymer solution diluted 5: 2 w/w in SCF and η_{DW} is the viscosity (Pa.s) of the polymer solution diluted in distilled water, according to the same weight ratio.

3.3.3 Choice of the thermo-sensitive gelling agent

Methyl cellulose (MC) and hydroxypropylmethyl cellulose (HPMC) were considered. MC and HPMC aqueous solutions (1% w/w) were diluted according to a weight ratio 5:2 in SCF and subsequently subjected to viscosity measurements by means of a rotational rheometer equipped with C60/1 cone plate measuring system. In particular, viscosity was measured at a constant shear rate (35 s^{-1}) and different temperatures (ranging from 20 to 60°C) (Van Vlierberghe et al. 2011).

To evaluate the effect of GG on MC rheological properties, a mixture 1:1 w/w of MC (2% w/w) and GG (2% w/w) aqueous solutions was subjected to oscillation measurements in comparison with a MC solution prepared at the same concentration present in the mixture. Before the analysis, both GG/MC mixture and MC solution were diluted in SCF (5:2 w/w). Oscillation measurements were performed by means of a rotational rheometer (cone C20/1). A constant shear stress, chosen in the linear viscoelastic region previously investigated, was applied at a fixed frequency (1 Hz) and at increasing temperature values (ranging from 20 up to 42°C). G' (storage elastic modulus), index of sample elasticity, was recorded as a function of temperature.

3.3.4 DoE approach: simplex centroid mixture design

Mixture designs are response surface designs, studying factors as mixture components. Such approach is applied to optimize the composition of mixtures, e.g. excipients in pharmaceutical products manufacturing (Dejagher and Vander Heyden, 2011). To examine a three-components mixture the experimental space becomes a triangular plane and three different experimental designs with three, six, seven or ten points can be selected (Dejagher and Vander Heyden, 2011; Hibbert, 2012). The goal of a mixture design is to determine an optimum blend of components (factors) throughout the experimental region, providing the desired or optimal values of each response variable considered (Furlanetto et al., 2011).

In this work a "simplex centroid mixture design" with 7 points was applied. When 3 factors (k) are considered, 7 ($n=2^k-1$) experiments are to be performed. Such a mixture design includes: three single mixture components, corresponding to the triangle corners; three binary combinations, graphically represented as points along the triangle edges; and one ternary combination, that overlaps with the centre of the triangle (Brereton, 2003). Three aqueous stock solutions: GG 0.8%

w/w, MC 1% w/w, and HPC 1% w/w were considered. The 3 stock solutions were used as such or mixed in predetermined weight ratios to obtain the significant points of the simplex centroid design, corresponding to the characteristic points of a Sheffè triangle (Figure 1 and Table 1).

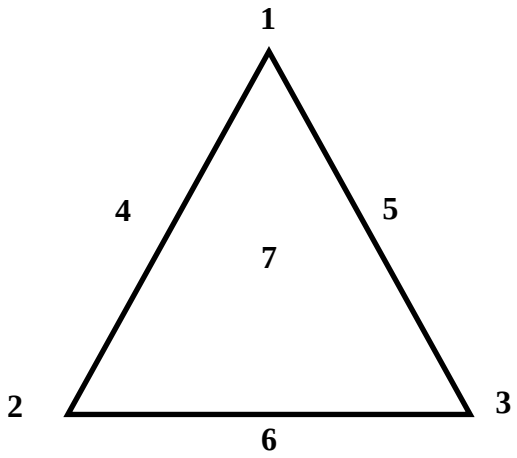

Figure 1 - Factor space and experimenting points of a simplex centroid design

Table 1 - Fractional mixture composition corresponding to the characteristic points of a Sheffè triangle

Points of Scheffè triangle	GG % w/w	MC % w/w	HPC % w/w
Vehicle 1	0.8	0	0
Vehicle 2	0	1	0
Vehicle 3	0	0	1
Vehicle 4	0.4	0.5	0
Vehicle 5	0.4	0	0.5
Vehicle 6	0	0.5	0.5
Vehicle 7	0.27	0.33	0.33

3.3.5 Vehicles characterization

The vehicles corresponding to the 7 experimental points of the "simplex centroid mixture design" were characterized for rheological (viscosity, viscoelasticity and thixotropic area) and mucoadhesive properties as hereafter described.

3.3.5.1 Rheological properties

Rheological properties were evaluated by means of a rotational rheometer (Rheostress 600, Haake, I), equipped with a cone plate measuring system (C20/1or C60/1). Vehicles were subjected to viscosity measurements at 25°C applying $10s^{-1}$ shear rate. Moreover each vehicle was diluted according to 5:2 w/w ratio with distilled water or SCF and subjected to viscosity measurements as above described. Viscosity measurements were performed at 25°C for the vehicles diluted in water

and at 37°C for the vehicles diluted in SCF. The results were expressed as: i) *viscosity* of undiluted vehicles *at 25°C* and $10s^{-1}$ shear rate; ii) *normalized Δη.* The interaction parameter *normalized Δη* has been calculated by subtracting the viscosity at 25°C of the vehicle diluted in water from the viscosity at 37°C of the same vehicle diluted in FCS. The value obtained has been normalized for the viscosity at 25°C of the vehicle diluted in water (see Eq. 2).

$$\text{normalized } \Delta\eta = (\eta_{SCF,\ 37°C} - \eta_{DW,\ 25°C})/\eta_{DW,\ 25°C} \quad \text{Eq. 2}$$

where $\eta_{SCF,\ 37°C}$ = viscosity at 37°C of the vehicle diluted in FCS and $\eta_{DW,\ 25°C}$ = viscosity at 25°C of the vehicle diluted in distilled water.

Vehicles upon dilution (5:2 w/w) with water or SCF were also subjected to dynamic viscoelastic analysis (oscillation test) at 37°C. It provides to apply a fixed shear stress chosen in the linear viscoelastic region, at 1 Hz frequency and to record the loss (G″) and storage (G′) moduli. The results were expressed as *loss tangent at 37°C and 1Hz,* calculated as the ratio between G" and G'.

Vehicle previously diluted (5:2 w/w) in SCF were subjected to thixotropy measurements: increasing and decreasing shear rates (range 10 - 300 s^{-1}) were applied at a constant temperature (37°C). The results were expressed as *thixotropic area (TA),* also called hysteresis area, calculated by the following equation:

$$TA=(A_{up} - A_{down})/A_{app} \quad \text{Eq. 3}$$

where A_{up} and A_{down} are the area under the flow up- and down-curve, respectively.

3.3.5.2 Mucoadhesive properties

The mucoadhesive properties of the vehicles were assessed at 37°C by means of a TA-XT plus Texture Analyzer (ENCO, Spinea, Venice, I) equipped with 1 kg load cell and with a cylindrical movable probe (P/10C). Gastric porcine mucin (Sigma, Milan, I) was used as biological substrates. A mucin dispersion at 8% (w/w) concentration in SCF was prepared. Before testing, vehicles were diluted (5:2 w/w) with SCF. Each sample (40 mg) was layered on a filter paper disc (area=2 cm^2) and fixed on the movable probe. 40 µl of gastric mucin dispersion were fixed, faced to the formulation, on the sample holder. The probe was lowered to put in contact mucin dispersion and diluted vehicle. A preload of 2500 mN for 180s was applied (Sandri et al., 2004). Then, the probe

was raised at a constant speed (2.5 mm/s) up to the complete separation of the two surfaces. Blank measurements were also carried out using 40 µl of SCF instead of mucin dispersion.

The normalized work of adhesion (ΔAUC/AUC) was calculated according to the following equation (Ferrari et al. 1997):

$$\Delta AUC/AUC = (AUC_m - AUC_b)/AUC_b \quad \text{Eq. 4}$$

where AUC_m is the adhesion work obtained in presence of gastric mucin dispersion; while AUC_b is the adhesion work obtained from blank measurements.

3.3.6 Optimization procedure

For each vehicle, the following response variables were considered: *viscosity of undiluted vehicles at 25°C, normalized Δ viscosity, loss tangent of vehicles diluted in SCF at 37°C, thixotropy area of vehicles diluted in SCF at 37°C and work of adhesion of vehicles diluted in SCF at 37°C*.

Each response variable can be related to mixture composition by means of a suitable mathematical model. Experimental data were subjected to multiple linear regression analysis, testing a series of models, like linear, quadratic and special cubic model (Draper and Smith, 1981). To determine the best fitting model for each response variable, a statistical analysis (ANOVA) was performed by means of a statistical software package (Statgraphics 5.0, Statistical Graphics, Rocknille, MD). The best fit model was chosen on the basis of statistical parameter such as F-ratio for significance of regression and adjusted correlation coefficient for the goodness of fit of the model (Draper and Smith, 1981).

Vehicle of optimized composition, chosen on the basis of the results of the experimental design, were prepared and subjected to the same characterization previously effected on the 7 vehicles of the Sheffè triangle, as described in paragraph 3.3.5.

3.3.7 Maqui berry extract (MBE) preparation

Maqui powder, from dehydrated berries, was submitted to solid-liquid extraction to obtain an extract rich in anthocyanins. In brief, one portion (1 g) was extracted with 20 ml of an hydroalcoholic mixture (H_2O:MeOH/10:90, with 0.1 % of formic acid 1 M) for 30 min, under constant stirring, in an ice bath and protected from light, under nitrogen atmosphere. After 30 min, the extract was centrifuged at 8000 rpm for 10 min at room temperature. The extraction procedure was repeated 3 times. The three extracts were gathered, filtered under vacuum on a 0.45 µm cellulose membrane filter (Sartorius Stedim Biotech GmbH, Gottingen, Germany) and freeze-dried at 8 x 10^{-1} mbar and -50 °C (Modulyo® Edwards Freeze-Drier, Kingston, NY).

3.3.8 Preparation and characterization of MBE-loaded optimized vehicle (MBE-VH)

MBE was solubilized under stirring in GG/MC/HPC solution. The final polymer concentrations in MBE-VH were equal to those of the optimized vehicle. MBE concentration in the vehicle was 0.5% w/w.

MBE-VH was characterized for rheological and mucoadhesive properties as described in the paragraphs 3.3.5.1 and 3.3.5.2.

3.3.9 Anthocyanin assay in MBE and MBE-loaded optimized vehicle (MBE-VH)

RP-HPLC-PDA analysis was performed using a Thermo Finnigan Surveyor Plus HPLC, equipped with a quaternary pump and a Surveyor UV−Vis diode array detector (Thermo Fisher Scientific, Waltham, MA, USA). A Synergi Fusion RP-18 column (150 x 4.6 mm, 5 μm), equipped with a Hypersil Gold C18 precolumn (10 x 2.1 mm, 5 μm), both from Phenomenex (Torrance, USA), was used. The mobile phase consisted of water acidified with 2% w/v formic acid (eluent A) and acetonitrile acidified with 0.8% w/v formic acid (eluent B) and was eluted in gradient as follow: 0-5 min 2% B, from 2 to 25% B in 65 min, from 25 to 100% B in 10 min, followed by a 5 min isocratic run of 100% B. Total run time was 92 min, including column reconditioning. The flow rate was maintained at 0.5 ml/min, the autosampler and column temperatures were maintained at 4 and 25 °C, respectively. The injection volume was set at 5 μl. The chromatograms were registered at 254, 280, and 520 nm; spectral data were collected within the range of 200−800 nm for all peaks.

The analytical method was validated following ICH procedures to demonstrate its suitability to quantify anthocyanins in MBE and in the developed formulation as cyanidin-3-glucoside (C3G) equivalents (*ICH Harmonised Tripartite guideline. Validation of analytical procedures: Text and methodology (Q2 (R1).http://www.ich.org/fileadmin/Public_Web_Site/ICH_Products/Guidelines/ Quality/ Q2_R1/Step4/Q2_R1__Guideline.pdf (2012 ICH)*). The linearity of the method was studied by testing in triplicate C3G solutions at different concentrations. A calibration curve was generated to confirm the linear relationship between the analyte peak areas *versus* the analyte concentrations. Calibration curves (slope and intercept) and correlation coefficient (R^2) were calculated as regression parameters by linear regression. The accuracy of the method was measured analyzing in triplicate three concentrations of C3G solutions, different from those tested for the linearity range. The accuracy is expressed as a percentage of the amount recovered, compared the experimental peak areas with those obtained from the calibration curve. The precision was evaluated both intraday (repeatability) and interday (intermediate precision). The repeatability was investigated analyzing in triplicate C3G solutions at three different concentrations included in the linearity range. The intermediate precision was determined using freshly prepared solutions at the same

concentrations used for the repeatability study after two consecutive days. The results are expressed as the relative standard deviation percentage of the measurements (RSD%). Method sensibility was determined as limit of quantification (LOQ) and limit of detection (LOD). The LOD and LOQ were estimated as signal to noise (S/N) ratio.

The validated RP-HPLC-PDA method was applied both to quantify anthocyanins content in MBE and to estimate the percentage of MBE incorporation in the vehicle, expressed as % of loaded C3G. The formulation was properly diluted with Milli-Q grade water to reduce its viscosity before the analysis. The results were expressed as % of loaded C3G as mean of 4 different samples, each one analyzed in triplicate, ± standard deviation.

3.3.10 *In vitro* evaluation of biocompatibility and antioxidant properties of MBE-VH

3.3.10.1 Cell cultures: normal human dermal fibroblasts and Caco-2 cells

Normal human dermal fibroblasts (NHDF; Promocell GmbH, Heidelberg, Germany) from 6th to 16th passage and human colorectal adenocarcinoma cell lines (Caco-2), obtained from the American Type Culture Collection (ATCC, USA), were used.

Human fibroblasts and Caco-2 cells were cultured in polystyrene flasks (Greiner bio-one, PBI International, Milan, I) with 13-15 ml of Dulbecco's Modified Eagle's Medium (DMEM) containing 4.5 g/l glucose and l-glutamine and supplemented with 1% (v/v) antibiotic antimycotic solution (100×), stabilized with 10,000 units penicillin, 10 mg streptomycin and 25 µg amphotericin B per ml, 10% (v/v) inactivated foetal calf bovine serum and 1% (v/v) non essential aminoacids.

Cells were maintained in incubator (Shellab® Sheldon® Manufacturing Inc., Oregon, USA) at 37°C with 95% air and 5% CO_2 atmosphere. All the operations required for cell culture were carried out in a vertical laminar air flow hood (Ergosafe Space 2, PBI International, Milan, I). When cells had reach 80-90% of confluence in the flask, a trypsinization was performed as described by Tenci et al. (2016). The amount of viable cells in the suspension recorded after trypsinization, was determined in a counting chamber (Hycor Biomedical, Garden Grove, California, USA), using 0.5% (w/v) trypan blue solution.

3.3.10.2 Assessment of cell viability properties

To assess the biocompatibility of MBE and of unloaded (VH) and MBE-loaded optimized vehicle (MBE-VH) towards human fibroblasts and Caco-2 cells, cell viability tests were performed. Such tests were used to estimate the number of viable cells after contact for a prefixed time with the samples considered.

$3.5 \cdot 10^4$ cell/well (0.35 cm^2 area) were seeded in 96-well plate (Greiner bio-one, VWR International, Milan, I) with culture medium (CM) and let to grow to reach confluence. When the medium was removed, cells were put in contact with 200 µl of each sample.

Dependently on cell line, different experimental conditions have been considered: dilution medium (complete medium (CM) or pH 7.4 HBSS) and contact time of cells with samples (24 or 2 h).

As for fibroblasts, samples were previously diluted in CM and then put in contact for 24 h with cells. In the case of Caco-2, samples were prepared in pH 7.4 HBSS and 2 h was the contact time. MBE (0.5% w/w) solution in CM or HBSS was prepared and then diluted in according to different v/v ratios (1:2, 1:5, 1:10, 1:20, 1:40 v/v) with CM or HBSS. Biocompatibility of undiluted 0.5% w/w MBE was also investigated. VH and MBE-VH were diluted in CM or HBSS in according to different v/v ratios (1:2, 1:5, 1:10, 1:20, 1:40 v/v).

After 24 h for fibroblasts and 2 h for Caco-2, cells were washed with 100 µl of HBSS (pH 7.4) and a MTT test was performed (Tenci et al., 2016). Results were expressed as% viability, calculated by normalizing the absorbance measured after contact with samples with that measured after contact with CM or HBSS, representing the positive references.

3.3.10.3 Assessment of antioxidant properties of MBE and MBE-VH

The capability of MBE and MBE-VH to protect NHDF fibroblasts and Caco-2 cells against oxidative damage was investigated.

To asses antioxidant activity on human fibroblasts, cells were pre-incubated with sample (200 µl) for 24 h and subsequently treated with H_2O_2 (1 mM; Carlo Erba, Milan, I) for 24 h (Mori et al., 2016). As for Caco-2 cells, 2 h of pre-incubation time and 6 h of H_2O_2-cells contact were considered (Peng et al., 2016). Finally, cell substrates were washed with HBSS pH 7.4 (100 µl) and a MTT test was performed as described in 3.3.10.2 paragraph.

3.3.11 Statistical analysis

Whenever possible, experimental values of the various types of measures were subjected to statistical analysis. In particular Anova one way-multiple range test and t-test were used (Statgraphics 5.0, Statistical Graphics Corporation, Rockvillle, MD, USA).

3.4 RESULTS AND DISCUSSION

3.4.1 Choice of the gelling agents

In Figure 2 Δ% values obtained for GG and K CARR aqueous solution (1.4% w/w) upon dilution in SCF (5: 2 w/w) are reported. It can be observed that between the two polymers, GG shows a greater capability to interact with SCF ions: dilution produces a higher increase in viscosity of GG solution with respect to K CARR solution. For this reason GG was chosen as ion sensible gelling agent.

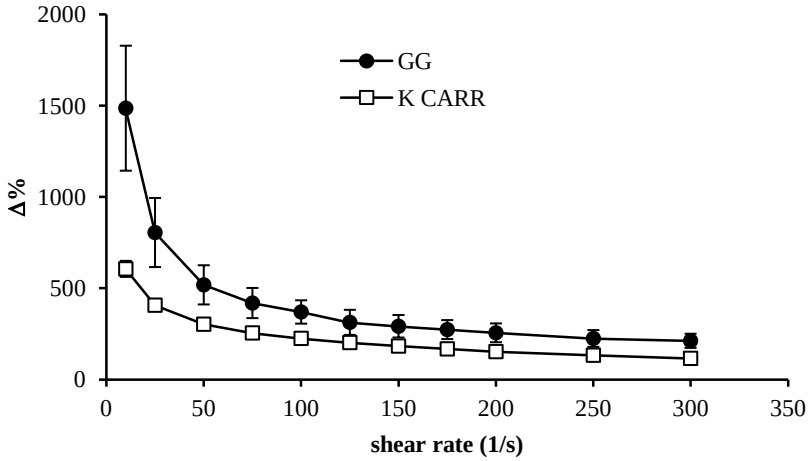

Figure 2 - Δ% values obtained for GG an K CARR aqueous solution (1.4% w/w) upon dilution in SCF (5:2 w/w) (mean values ± d.s.; n=3)

In Figure 3 viscosity vs temperature curves obtained for MC and HPMC 1% w/w aqueous solutions upon dilution in SCF (5: 2 w/w) are reported. Both MC and HPMC are well-known as temperature sensible polymers (Jeong et al., 2002; Klouda, 2015). For both polymers a gelling temperature (Tg) $\geq$ 50°C, is reported in literature. Upon dilution with SCF, MC solution is characterized by a Tg lower than that of HPMC solution: the increase in viscosity is observed in the temperature range 48-55°C for MC solution, while HPMC shows no sign of gelation in the range considered 20-60°C (Figure 3). For this reason between the two cellulose derivatives, MC was chosen for the continuation of the work.

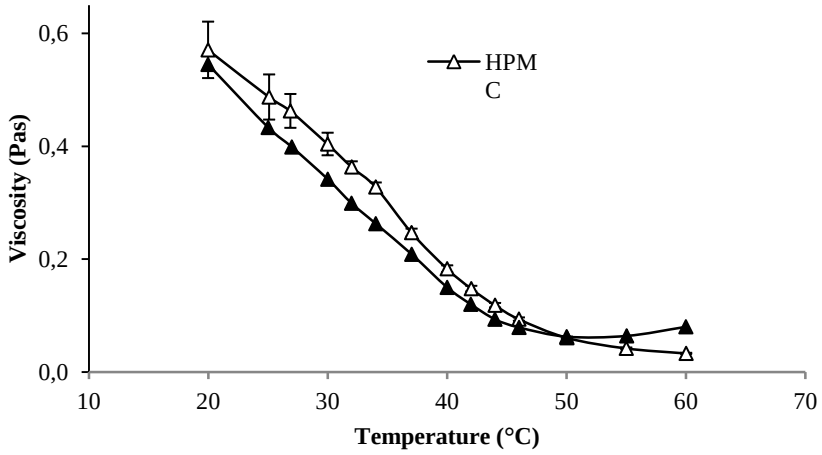

Figure 3 - Viscosity values (measured at 35 s^{-1}) obtained for HPMC and MC aqueous solutions (1.0% w/w) upon dilution in SCF (5: 2 w/w) (mean values ± d.s.; n=3)

In the past, many attempts have been made to lower MC Tg temperature. In particular, some authors investigated the influence of various water-soluble polymers on Tg of MC. They observed a decrease of Tg upon addition of polyvinylpyrrolidone (PVP). Such a decrease depended on PVP concentration (Shimokawa et al., 2009).

In the present work, it seemed interesting to investigate if the addition of GG to MC could produce a decrease of MC Tg. At this aim, a mixture 1:1 w/w of MC and GG was subjected to oscillation measurements in comparison with MC solution prepared at the same concentration present in the mixture. Viscoelastic (oscillatory) measurements were chosen instead of viscosity ones since they provide a more accurate characterization of sample structure by subjecting it to very low and not destructive shear stresses (Tadros, 2004).

In Figure 4 G′ vs temperature profiles of 0.5% w/w MC/0.5% w/w GG mixture and of 0.5% MC solution upon dilution in SCF are compared. As suggested in literature, Tg is indicated by a step increase in G′ (Aka-Any-Grah et al., 2010; Rossi et al., 2014; Caramella et al., 2015).

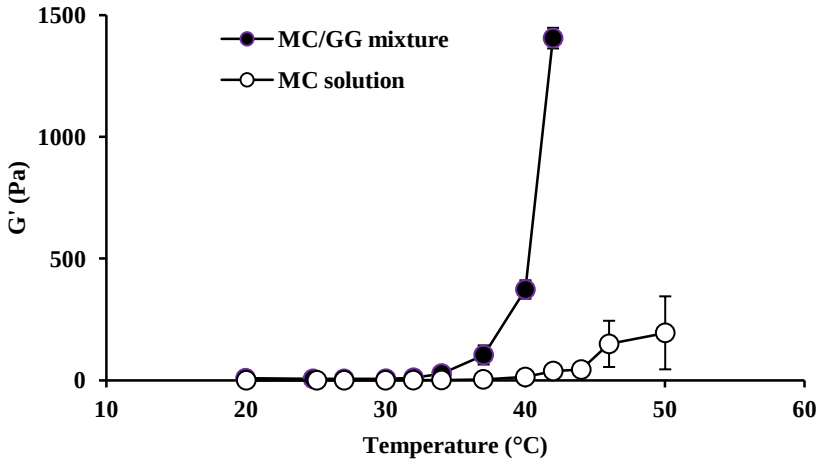

Figure 4 – G′ values (measured at1 Hz frequency) as a function of temperature obtained for GG 0.5% w/w /MC 0.5% w/w mixture and MC 0.5% w/w aqueous solutions (mean values ± d.s.; n=3)

Surprisingly, the presence of GG produces a lowering of MC Tg, that falls in the physiological range. In fact, while for pure MC solution a marked increase in G' is observed for temperature higher than 47°C, MC/GG mixture shows a step increase in G' in the temperature range 36-40°C. The results obtained strengthen the choice of GG as ion-sensitive gelling agent.

3.4.2 Experimental design

The best fit model for all the response variables (*viscosity at 25°C, normalized Δ viscosity, loss tangent at 37°C, thixotropy area at 37°C, work of adhesion at 37°C*) of the experimental design vehicles was found to be the special cubic, except for the thixotropy area. For such response variable, the quadratic was the best model.

In Table 2 the mean experimental values of all response variables considered for the seven vehicles of experimental design are reported.

Table 2 – Response variables of the vehicles of the simplex centroid design (mean values ± s.e.; n= 3- 5)

	Response variables				
Vehicles	Viscosity (Pa.s) at 25°C	Δ viscosity normalized	Loss tangent (tg Δ) at 37°C	Thixotropy area ($Pa.s^{-1}$)	Δ adhesion work (mN.mm)
1	0.639 ± 0.005^{a}	$6.96 \pm 0.13^{a'}$	$0.23 \pm 0.16^{a''}$	$290 \pm 8^{a*}$	$73 \pm 22^{a**}$
2	0.258 ± 0.005^{b}	$- 0.47 \pm 0.05^{b'}$	$0.28 \pm 0.11^{b''}$	$- 163 \pm 29^{b*}$	$18 \pm 4^{b**}$
3	0.378 ± 0.012^{c}	$- 0.28 \pm 0.06^{c'}$	$3.92 \pm 0.35^{c''}$	$- 14 \pm 6^{c*}$	$126 \pm 18^{c**}$
4	0.1914 ± 0.0006^{d}	$7.15 \pm 0.40^{d'}$	$0.09 \pm 0.02^{d''}$	$- 82 \pm 12^{d*}$	$32 \pm 6^{d**}$
5	0.1842 ± 0.0006^{e}	$1.08 \pm 0.14^{e'}$	$0.215 \pm 0.005^{e''}$	$65 \pm 5^{e*}$	$79 \pm 9^{e**}$
6	0.238 ± 0.001^{f}	$- 0.78 \pm 0.03^{f'}$	$3.53 \pm 0.14^{f''}$	$23 \pm 7^{f*}$	$59 \pm 19^{f**}$
7	0.179 ± 0.027^{g}	$- 0.940 \pm 0.001^{g'}$	$1.42 \pm 0.45^{g''}$	$26 \pm 3^{g*}$	$95 \pm 32^{g**}$

Anova one way, Multiple range test, $p<0.05$:

a *vs* b/c/d/e/f/g; b *vs* c/d/e/g; c *vs* d/e/f/g; d *vs* f; e *vs* f; f *vs* g

a′ *vs* b′/c′/e′/f′/g′; b′ *vs* d′/e′; c′ *vs* d′/e′/g′; d′ *vs* e′/f/′g′; e′ *vs* f′/g′

a″ *vs* b″/c″/d″/e″/f″/g″; b″ *vs* f″/g″; c″ *vs* f″/g″

a^{*} *vs* $b^{*}/c^{*}/d^{*}/e^{*}/f^{*}/g^{*}$; b^{*} *vs* $c^{*}/d^{*}/e^{*}/f^{*}/g^{*}$; c^{*} *vs* d^{*}/e^{*}; d^{*} *vs* $e^{*}/f^{*}/g^{*}$; e^{*} *vs* f^{*}

b^{**} *vs* $c^{**}/ e^{**}/g^{**}$; c^{**} *vs* d^{**}/f^{**}; d^{**} *vs* g^{**}

The vehicle 1, based on only GG (0.8% w/w), is characterized by the highest value of viscosity at 25°C, while vehicles 4 – 7, prepared with GG concentrations ≤ 0.4 w/w, show the lowest viscosity values. Since such response variable is an index of sample consistency before administration, low viscosity values are preferable in order to permit an easier administration.

The interaction parameter *normalized Δ viscosity* was used to point out the contribution of both GG (sensible to ions) and MC (sensible to temperature) to the increase of viscosity upon administration. As explained in the experimental part, it has been calculated by subtracting the viscosity at 25°C of the vehicle diluted in water from the viscosity at 37°C of the same vehicle diluted in FCS. The value obtained has been normalized for the viscosity at 25°C of the vehicle diluted in water. In the calculation of this parameter, viscosity at 25°C has been employed instead of that at 37°C to bring out the eventual sensibility of the vehicle to temperature (due to the presence of MC in mixture with GG), whereas the vehicle dilution in FCS has been effected to point out GG contribution. The vehicles 4, based on a mixture of GG (0.4% w/w) and MC (0.5%), is characterized by the highest value of *normalized Δ viscosity.* A high value is also observed for vehicle 1 containing only GG at 0.8% w/w concentration. At 0.8 w/w concentration the interaction of GG with FCS is very strong and able to increase vehicle viscosity by 7 times with respect to that measured at 25°C for the vehicle diluted in water.

The viscoelastic parameter *loss tangent* and *thixotropy area* measured at 37°C upon vehicle dilution in FCS were considered as indexes of the structuration degree of the gel formed upon

administration. Vehicles 1, 2, 4 and 5 are characterized by loss tangent values lower than 1. Since such a parameter is calculated by the ratio between the loss (G″) and the storage (G′) moduli, values lower than 1 indicate a prevalence of the elastic behavior on the viscous one (Mori et al, 2016b). On the contrary, vehicles 3, 6 and 7 are characterized by a prevailing viscous behavior, showing loss tangent values higher than 1. After administration it is desirable that vehicle possesses higher elastic than viscous behavior. This should be functional to the protection action of the vehicle towards mucosa. The results indicate that HPC 1% w/w alone (vehicle 3) does not possess a marked elastic behavior, on the contrary MC 1% w/w (vehicle 2) and GG 0.8% w/w (vehicle 1) alone are characterized by optimal viscoelastic properties. It seems necessary to associate HPC with GG at concentration higher than 0.27% w/w to obtain the desirable properties.

Also *thixotropy area (TA)* is a parameter correlated to sample structure. Positive values of TA indicate a time effect on flow. At any given shear rate or shear stress, sample viscosity continues to decrease with increasing the time of shear. When shear is stopped, viscosity recovers to its initial value (Tadros, 2004). This behavior can be explained by the break of sample structure on applying shear force and by its building up on reducing the shear force to zero. The presence of a *TA* should assure a reduction in sample consistency, useful to facilitate administration, and a sample "structuration" with consequent increase in consistency upon administration, functional to a protective action towards mucosa. All the vehicles containing GG, with the exception of vehicle 4, are characterized by positive values of *TA*. The highest value of such parameter is observed for vehicle 1 containing GG at 0.8% w/w.

The response variable *Δ adhesion work* is an index of vehicle muchoadhesive properties. As expected, vehicle 3 containing the highest concentration of the mucoadhesive polymer HPC is characterized by the highest mucoadhesive potential. Also GG at 0.8% w/w (vehicle 1) shows good mucoadhesive properties. The lowest values of Δ adhesion work are observed for vehicle 2 and 4, lacking in HPC.

For each response variable, contour plots (in bidimensional and tridimensional projection) were drawn according to the best fit model. As an example in Figure 5 contour plots of *Δ adhesion work* are reported.

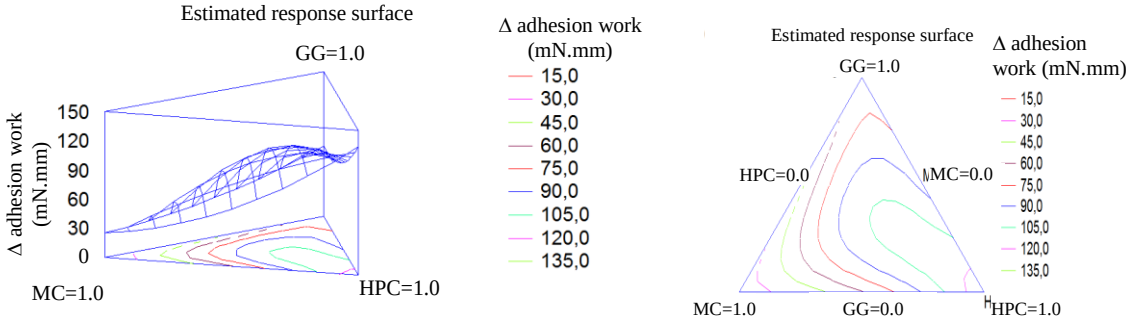

Figure 5 – Contour plots (in bidimensional and tridimensional projections) drawn according to the best fit model for the response variables Δ adhesion work.

The lines in each plot represent the dressing compositions for which a same response value is predicted by the model. The individual contour plots have been subsequently superimposed to identify the region of the factor space fulfilling the following constraints: *viscosity* at *25°C* $\leq$ 0.25 Pa.s; *normalized Δ viscosity* $\geq$ 0.6, (corresponding to an increase of 60% with respect to viscosity at room temperature of the vehicle diluted in water); *loss tangent at 37°C* $\leq$1.2; *thixotropy area at 37°C* $\geq$ 20 Pa/s; *Δ adhesion work at 37°C* $\geq$ 50 mN.mm. These constraints were chosen bearing in mind that vehicle should possess, as already discussed, rheological properties suitable, at room temperature, for an easy administration and, at 37°C, for the formation of a mucoadhesive gel layer. Figure 6 shows the region of optimal composition (coloured area) that satisfies all the constraints.

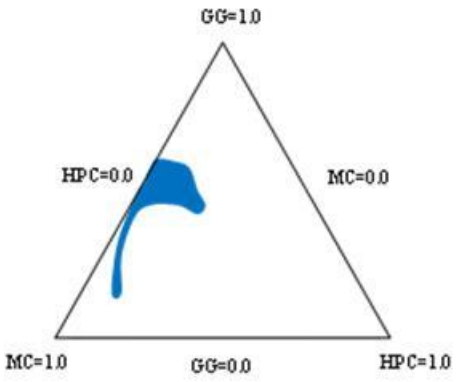

Figure 6 – Combined contour plot showing the region of optimal mixture composition that satisfies all the constraints of the response variables.

The composition of the optimized vehicle (VH) (GG 0.38% p/p, MC 0.31% p/p e HPC 0.22% p/p) was chosen in this area. The results obtained from the characterization of VH are the following (mean values ± es; n= 3-5): *viscosity* at 25°C= 0.109 ± 0.003 Pa.s; *normalized Δ viscosity* = 0.7 ± 0.2; *loss tangentat 37°C* = 0.11 ± 0.01; *thixotropy area at 37°C* = 98 ± 33 Pa/s; *Δ adhesion work at 37°C* = 50 ± 10 mN.mm. In all cases, the experimental results fall inside the confidence interval of the relevant values predicted by the model, to indicate its predictive power.

3.4.3 Characterization of MBE loaded optimized vehicle (MBE-VH)

MBE-VH was characterized by the following rheological and mucoadhesive properties (mean values ± es; n= 3-5): *viscosity at 25°C* = 0.22 ± 0.02 Pa.s; *normalized Δ viscosity* = 0.92 ± 0.06; *loss tangent at 37°C* = 0.13 ± 0.02; *thixotropy area* at 37°C = 297 ± 62 Pa/s. *Δ adhesion work at 37°C*= 70 ± 6 mN.mm. It can be observed that, even though the addition of MBE into the optimized vehicle produces a significant ($p<0.05$) increase in *viscosity at 25°C* with respect to the vehicle as such, MBE-VH gelation properties are improved as demonstrated by a significant increase in *normalized Δ viscosity* parameter. Also *thysotropy area* and *Δ adhesion work* parameters increase upon MBE addition. This should result, as already explained, in an easier spreading and in a longer permanence of the formulation on the mucosa. Moreover, it must be underlined that the observed increase in viscosity at 25°C still satisfies the constraints fixed for the optimization procedure.

3.4.3.1 Anthocyanins assay in MBE and MBE loaded optimized vehicle (MBE-VH)

Anthocyanins in MBE were expressed as μg (C3G)/mg of dried extract, considering all the area under the curve of peaks at 520 nm (Figure 7a). Before quantification, the developed RP-HPLC-PDA method was validated according to ICH guidelines. The method was linear within the range from 10 to 500 μg/ml and the correlation coefficient was higher than 0.99. To evaluate the accuracy and precision of the method, different concentrations of C3G standard solutions were analysed in triplicate. The obtained results indicate that the developed method was accurate, providing recoveries ranging from 97% to 118%; and precise, since the intraday and interday variation were lower than 1% for all the concentration levels. As far as sensibility is concerned, LOQ and LOD values determined for C3G were 10 and 3.3 μg/ml, respectively.

MBE resulted to contain 13.51 ± 0.02 μg of C3G/mg of dried weight: this content is within the range already reported in the literature for MBE (Fredes et al., 2014; Brauch et al., 2016). Before evaluating the percentage of incorporation of MBE, the formulation itself was analysed, after dilution with MilliQ-grade water, to determine if some interfering peaks are present at 520 nm.

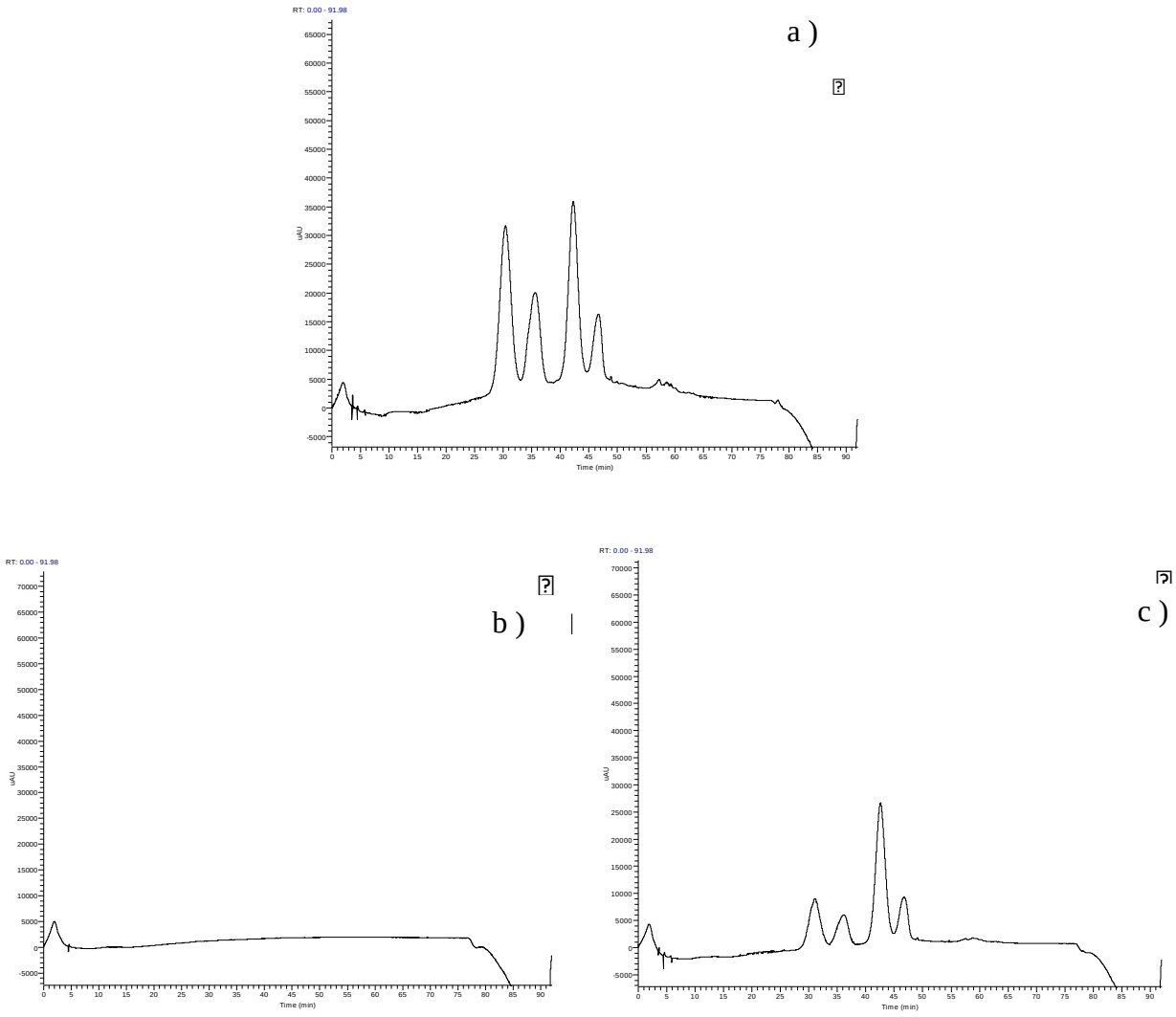

Figure 7 – Chromatographic profiles, acquired at 520 nm, of a) of MBE at 20 mg/ml, b) unloaded vehicle (1:5 w/w diluted with MilliQ-grade water); c) MBE loaded vehicle (1:5 w/w diluted with MilliQ-grade water)

As shown in Figures 7b, c, the method resulted to be specific for the determination of % of MBE incorporated in the formulation. The percentage of incorporation resulted to be 86 ± 10 % (mean value ± s.d.; n=4) with respect to the theoretical value.

3.4.3.2 *In vitro* evaluation of biocompatibility and antioxidant properties of MBE-VH

3.4.3.2.1 Assessment of fibroblast and Caco-2 cells viability properties

In Figure 8a % fibroblast viability values observed for MBE solution (0.5% w/w) diluted according to different ratios (1:40, 1:20, 1:10, 1:5 and 1:2 v/v) with complete medium (CM) are reported. It can be observed that all the samples showed % viability comparable to that obtained for CM (reference), with the exception of undiluted MBE (0.5% w/w) solution, which was characterized by % viability value significantly ($p < 0.05$) lower than CM.

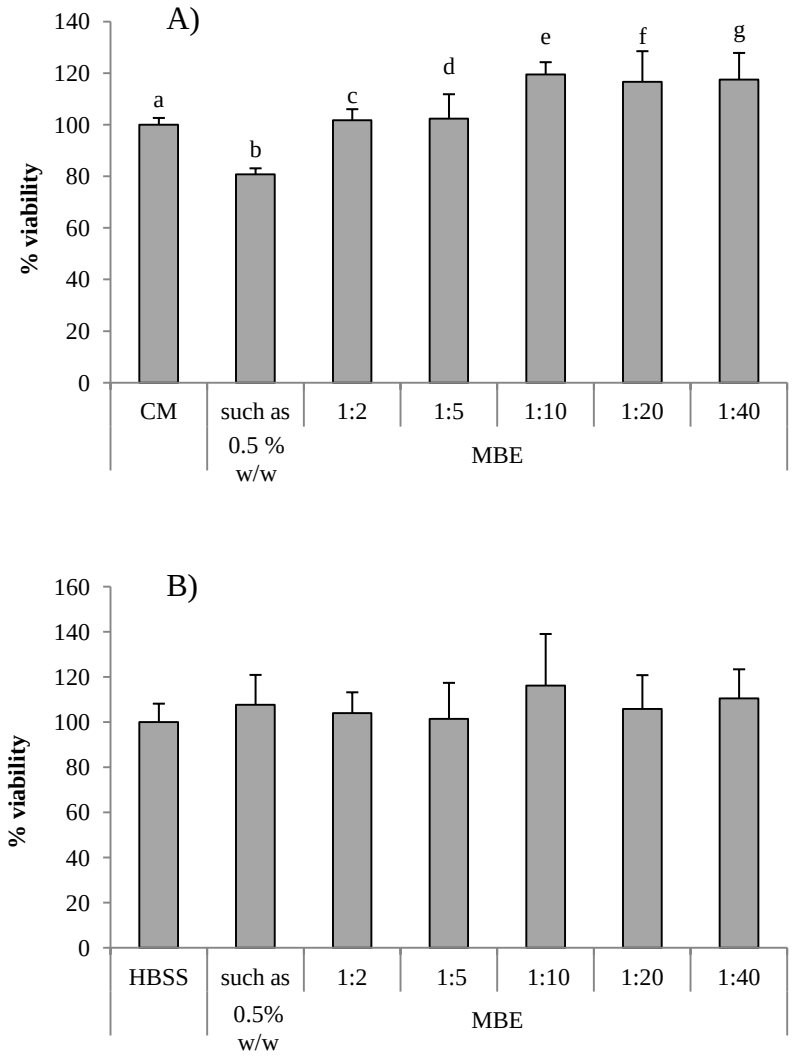

Figure 8 - % viability values of MBE upon contact with: A) NHDF fibroblasts; B) human colorectal adenocarcinoma cells (Caco-2). MBE 0.5% w/w solution was diluted according to different ratios (1:2, 1:5, 1:10, 1:20, and 1:40 v/v) with CM or HBSS. CM and HBSS were used as references (mean values ± s.e.; n=8).

T-test ($p<0.05$): A) a *vs* b/e; b *vs* c/e/f/g.

Figure 8b reports the viability results for MBE solution (0.5% w/w), diluted according to different ratios (1:40, 1:20, 1:10, 1:5 and 1:2 v/v) with Hank's buffer solution pH 7.4 (HBSS), upon contact with Caco-2 cells. No significant ($p < 0.05$) differences between MBE solution/dilutions and the reference (HBSS) could be observed.

On the basis of the results obtained, MBE 1:5 and 1:2 v/v dilutions were chosen for the assessment of MBE antioxidant properties with both the two cell lines, as discussed in 3.3.10.3 paragraph.

Figure 9 shows % cell viability values after contact (24h for fibroblasts, 2h for Caco-2 cells) with VH and MB-VH. Different dilutions in CM or HBSS were considered: 1:2, 1:5, 1:10, 1:20, 1:40 v/v.

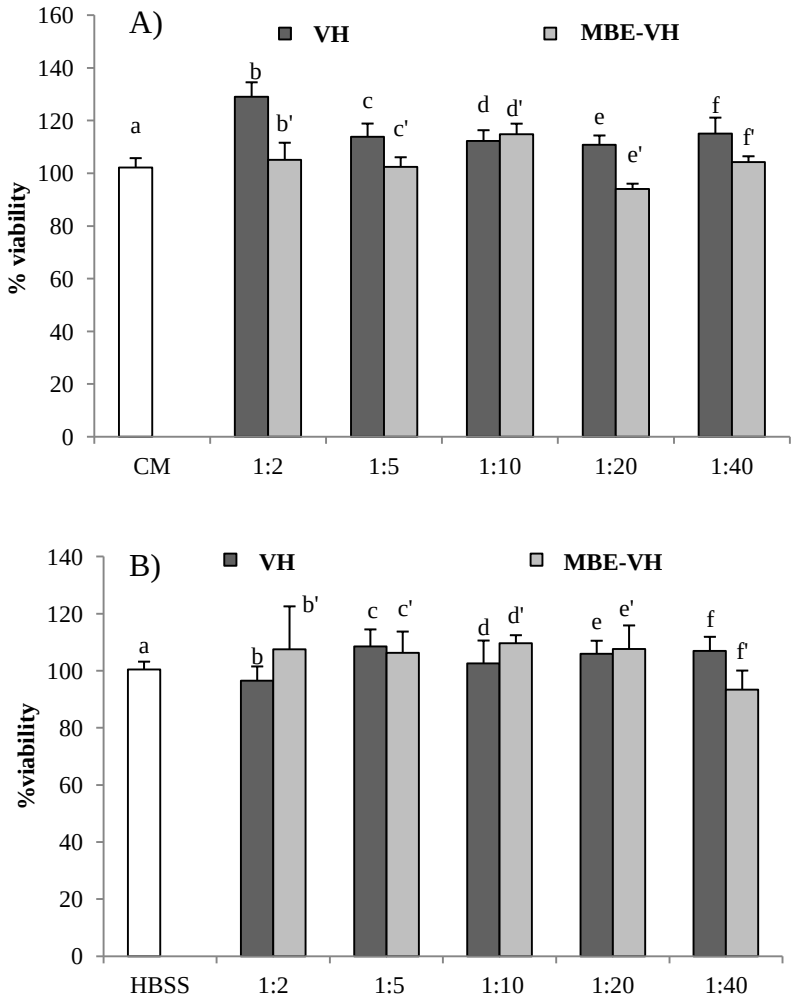

Figure 9 - % viability values of unloaded (VH) and loaded (MBE-VH) vehicles of optimized composition observed after contact with A) NHDF fibroblasts; B) human colorectal adenocarcinoma cells (Caco-2). Different dilutions (1:2, 1:5, 1:10, 1:20, and 1:40 v/v) in CM or HBSS were considered. CM and HBSS were used as references (mean values ± s.e.; n=8).

T-test ($p<0.05$): A) e *vs* e′.

VH does not present any cytotoxic effect towards both the two cell lines. In particular, in the case of fibroblasts, 1:2 v/v dilution is able to improve fibroblast proliferation in comparison to the reference (CM). As for MBE-VH, all the samples possess % viability values similar to that of the reference CM or HBSS. Such results indicate that VH and MBE-VH at the concentration/dilution investigated do not disturb cell vitality. The gelation of unloaded and loaded formulations, induced by both temperature and ions effects, does not impair nutrient exchange between cells and the medium.

3.4.3.2.2 Assessment of MBE antioxidant activity

Figure 10 (A, B) reports the results of *in vitro* evaluation of MBE antioxidant properties on NHDF fibroblasts (A) and Caco-2 cells (B) for MBE.

Both cell lines upon contact with H_2O_2 show % viability values significantly ($p < 0.05$) lower than reference (CM or HBSS); these results prove the suitability of the experimental conditions (H_2O_2 concentration and contact time) to produce an oxidative damage.

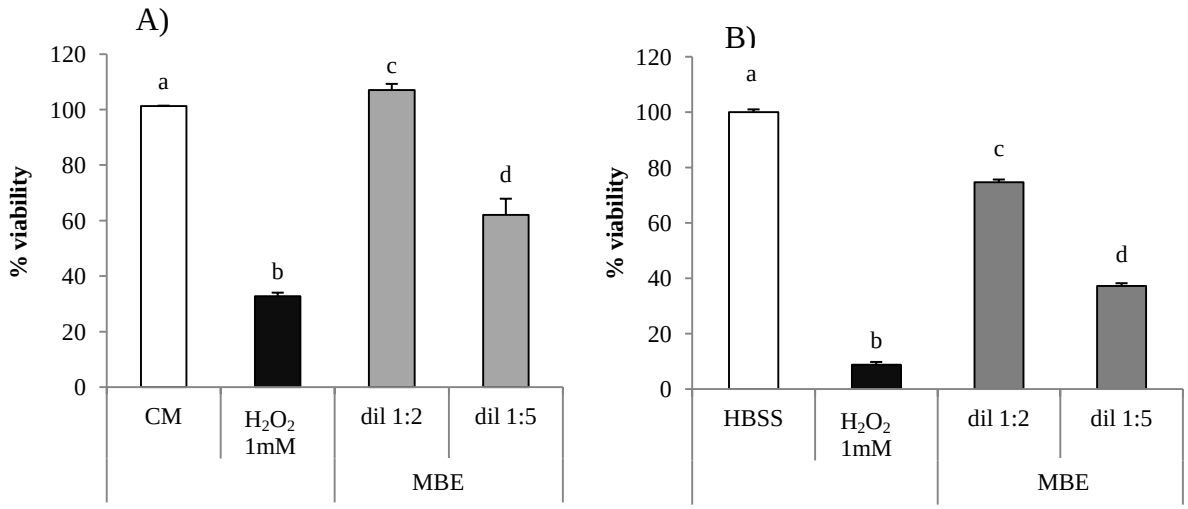

Figure 10 - Antioxidant activity of MBE on A) NHDF fibroblasts; B) human colorectal adenocarcinoma cells (Caco-2). CM/HBSS and H_2O_2 were used as references. Anova one way – MRT ($p < 0.05$): A) a *vs* b/d; b *vs* c/d; c *vs* d; B) a *vs* b/c/d; b *vs* c/d; c *vs* d.

MBE is able to protect fibroblasts against oxidative stress, as indicated by % viability values higher in presence of MBE than in absence of the extract (Figure 10A). Such an effect is higher for 1:2 v/v dilution, which is characterized by % viability values comparable to that observed for untreated cells (CM). A greater dilution (1:5 v/v) corresponds to a decrease of the effect.

Also for Caco-2 cells, a significant ($p < 0.05$) decrease of cell viability (5%) is observed in comparison with untreated cells (HBSS). MBE exerts a protective effect in a concentration-dependent manner against oxidative H_2O_2-induced damage: cell viability values for 1:2 and 1:5 dilutions are around 75% and 35%, respectively. The comparison of the results obtained for the two cell lines points out that Caco-2 cells are more sensible to oxidative damage than NHDF fibroblasts.

3.4.3.2.3 Assessment of MBE-VH antioxidant properties

Figure 11 (A, B) compares the results of *in vitro* evaluation of MBE and MBE-VH antioxidant properties on NHDF fibroblasts (A) and Caco-2 cells (B). MBE-VH exercises a protective effect against oxidative damage for both cell lines considered. No statistical differences are observed

between % viability values obtained for the extract as such and after loading into vehicle. This result indicates that the vehicle does not disturb MBE activity.

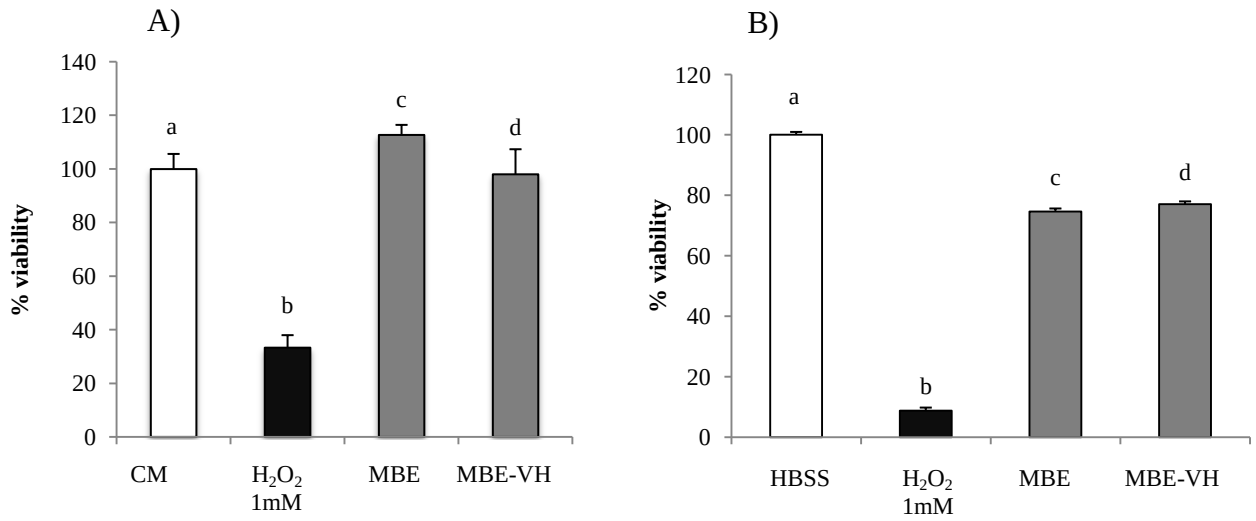

Figure 11 - Antioxidant activity of MBE and MBE-VH on A) NHDF fibroblasts; B) human colorectal adenocarcinoma cells (Caco-2). CM/HBSS and H_2O_2 were used as references. Anova one way – MRT ($p < 0.05$): A) a *vs* b; b *vs* c/d.; B) a *vs* b/c/d; b *vs* c/d.

3.5 CONCLUSIONS

DoE approach permitted to optimize the quantitative composition of a vehicle intended for colonic application via rectal route. The vehicle was able to gelify in the colon in response to the increase in temperature at 37°C and to the presence of colonic fluid ions. MBE loading (0.5% w/w) into the vehicle enhanced rheological and mucoadhesive properties, functional to a better spreading and a longer permanence of the formulation on the mucosa. Loading capacity of anthocyanins, responsible for MBE antioxidant properties, was about 90% w/w with respect to the theoretical value. Both MBE and the optimized vehicle were not cytotoxic towards both fibroblasts and Caco-2 cells. Moreover, the optimized vehicle did not disturb MBE antioxidant properties.

The overall results indicate that the optimized vehicle is a promising candidate for the local treatment of inflammatory bowel disease.

3.6 REFERENCES

Aka-Any-Grah, A., Bouchemal, K., Koffi, A., Zhang, M., Djabourov, M., Ponchel, G., 2010. Formulation of mucoadhesive vaginal hidrogels insensitive to dilution with vaginal fluids, Eur. J. Pharm. Biopharm. 76, 293- 303.

Biedermann, L., Mwinyia, J., Scharla, M.., Freia, P., Zeitzc, J., Kullak-Ublickb, G.A., Vavrickaa, S.R., Frieda, M., Webere, A., Humpff, H.U., Peschkeh, S., Jetterb, A., Krammerh, G., Rogler, G., 2013. Bilberry ingestion improves disease activity in mild to moderate ulcerative colitis - An open pilot study. J. Crohns Colitis. 7, 271-279.

Brauch, J.E., Buchweitz, M., Schweiggert, R.M., Carle, R., 2016. Detailed analyses of fresh and dried maqui (*Aristotelia chilensis* (Mol.) Stuntz) berries and juice. Food Chem., 190, 308-316.

Brereton, R.G., Chemometrics: data analysis for the laboratory and chemical plant. Wiley, Chichester, 2003.

Caramella, C., Rossi, S., Ferrari, F., Bonferoni, M.C., Sandri, G., 2015. Mucoadhesive and thermogelling systems for vaginal drug delivery, Advanced Drug Delivery Reviews 92, 39- 52

Céspedes, C.L., El-Hafidi, M., Pavon, N., Alarcon, J., 2008. Antioxidant and cardioprotective activities of phenolic extracts from fruits of Chilean blackberry *Aristotelia chilensis* (Elaeocarpaceae), Maqui. Food. Che. 107, 820-829.

Dejagher, B., Vander Heyden, Y., 2009. The use of experimental design in separation science. Acta Chromatogr. 21, 161-201.

Dejagher, B., Vander Heyden, Y., 2011. Experimental designs and their recent advances in set-up, data interpretation, and analytical applications. J. Pharm. Biomed. Anal. 56, 141-158.

Draper, N.R., Smith, H., 1981. Applied regression analysis, New York: Wiley & sons, 412-419.

Farzaei, H.M., Rahimi, R., Abdollahi, M., 2015. The role of dietary polyphenols in the management of inflammatory bowel disease. Curr. Pharm. Biotechnol. 16, 196-210.

Ferrari, F., Rossi, S., Martini, A., Muggetti, L., De Ponti, R., Caramella, C., 1997. Technological induction of mucoadhesive properties on waxy starches by grinding. Eur. J. Pharm. Sci. 5, 277–285.

Fredes, C., Yousef, G.G., Robert, P., Grace, M.H, Lila, M.A., Gómez, M., Gómez, M., Montenegro, G., 2014. Anthocyanin profiling of wild maqui berries (*Aristotelia chilensis* [Mol.] Stuntz) from different geographical regions in Chile. J. Sci. Food Agric. 94, 2639-2648.

Furlanetto, S., Cirri, M., Piepel, G., Mennini, N., Mura, P., 2011. Mixture experiment methods in the development and optimization of microemulsion formulations. J. Pharm. Biomed. Anal. 55, 610–617.

Hanauer, S.B., 2006. Inflammatory bowel disease: epidemiology, pathogenesis, and therapeutic opportunities. Inflamm. Bowel. Dis. 12, S3-S9.

Hibbert, D.B., 2012. Experimental design in chromatography: A tutorial review. J. Chromatogr. B. 910, 2– 13.

Irvine, E.J., 2008. Quality of life of patients with ulcerative colitis: past, present, and future. Inflamm. Bowel. Dis. 14, 554-565.

Jeong, B., Kim, S.W., Bae, Y.H., 2002. Thermosensitive sol–gel reversible hydrogels. Adv. Drug Deliver. Rev. 54, 37–51.

Klouda, L., 2015. Thermoresponsive hydrogels in biomedical applications. A seven-year update. Eur. J. Pharm. Biopharm. 97, 338-349.

Lautenschläger, C., Schmidt, C., Fischer, D., Stallmach, A., 2014. Drug delivery strategies in the therapy of inflammatory bowel disease. Adv. Drug Deliver. Rev. 71, 58–76.

Lichtenstein, G.R., Rutgeerts, P., 2010. Importance of mucosal healing in ulcerative colitis. Inflamm. Bowel. Dis. 16, 338-346.

Makó, Á., Csóka, G., Pásztor, E., Marton, S., Horvai, G., Klebovich, I., 2009. Formulation of thermoresponsive and bioadhesive gel for treatment of oesophageal pain and inflammation. Eur. J. Pharm. Biopharm. 72, 260–265.

Marques, M.R.C., Loebenberg, R., Almukainzi, M., 2011. Simulated biological fluids with possible application in dissolution testing. Dissolut. Technol. 18, 15-28.

Mølgaard, P., Holler, J.G., Asar, B., Liberna, I., Rosenbæk, L.B., Jebjerg, C.P., Jørgensen L., Lauritzen J., Guzman A., Adsersen A., Simonsen H.T., 2011. Antimicrobial evaluation of Huilliche plant medicine used to treat wounds. J. Ethnopharmacol. 138, 219–227.

Mori, M., Rossi, S., Ferrari, F., Bonferoni, M.C., Sandri, G., Chlapanidas, T., Torre, M.L., Caramella, C., 2016. Sponge-like dressings based on the association of chitosan and sericin for the treatment of chronic skin ulcers. I. Design of experiments-assisted development. J. Pharm. Sci. 105, 1180-1187.

Neurath, M.F., Travis, S.P.L., 2012. Mucosal healing in inflammatory bowel diseases: a systematic review. Gut 61, 1619–1635.

Parekh, H.B., Rishad, J., Jivani, N.P., Patel, L.D., Makwana, A., Sameja, K., 2012. Novel *in situ* polymeric drug delivery system: a review. J. Drug Deliv. Ther. 2, 136-145.

Pásztor, E., Makó, Á., Csóka, G., Fenyvesi, Z., Benko, R., Prosszer, M., Marton, S., Antal, I., Klebovich, I., 2011. New formulation of *in situ* gelling Metolose-based liquid suppository. Drug Dev. Ind. Pharm. 37, 1-7.

Peng, Y., Zhang, H., Liu, R., Mine, Y., McCallum, J., Kirby, C., Tsao, R., 2016. Antioxidant and anti-inflammatory activities of pyranoanthocyanins and other polyphenols from staghorn sumac (*Rhus hirta L.*) in Caco-2 cell models. .J Funct. Foods. 20: 39–147.

Piberger, H., Oehme, A., Hofmann, C., Dreiseitel, A., Sand, P.G., Obermeier, F., Schoelmerich, J., Schreier, P., Krammer, G., Rogler, G., 2011. Bilberries and their anthocyanins ameliorate experimental colitis. Mol. Nutr. Food Res. 55, 1724-1729.

Rossi, S., Ferrari, F., Bonferoni, M.C., Sandri, G., Faccendini, A., Puccio, A., Caramella, C., 2014. Comparison of poloxamer- and chitosan-based thermally sensitive gels for the treatment of vaginal mucositis, Drug Dev. Ind. Pharm. 40, 352- 360.

Rossi S., Marciello M., Bonferoni M.C., Ferrari F., Sandri G., Dacarro C., Grisoli P., Caramella C., 2010. Thermally sensitive gels based on chitosan derivatives for the treatment of oral mucositis, European Journal of Pharmaceutics and Biopharmaceutics 74, 248–254.

Rubilar, M., Jara, C., Poo, Y., Acevedo, F., Gutierrez, C., Sineiro, J., Shene, C., 2011. Extracts of Maqui (*Aristotelia chilensis*) and Murta (Ugni molinae Turcz.): souces of antioxidant compounds and α-glucosidase/α-amylase inhibitors. J. Agric. Food Chem. 59, 1630-1637.

Ruel-Gariépy, E., Leroux, J.C., 2004. *In situ*-forming hydrogels—review of temperature-sensitive systems. Eur. J. Pharm. Biopharm. 58, 409–426.

Ruiz, A., Hermosín-Gutiérrez, I., Mardones, C., Vergara, C., Herlitz, E., Vega, M., Dorau, C., Winterhalter, P., Von Baer, D., 2010. Polyphenols and antioxidant activity of calafate (Berberis microphylla) fruits and other native berries from Southern Chile. J. Agric. Food Chem. 58, 6081–6089.

Sandri, G., Rossi, S., Ferrari, F., Bonferoni, M.C., Zerrouk, N., Caramella, C., 2004. Mucoadhesive and penetration enhancement properties of three grades of hyaluronic acid using porcine buccal and vaginal tissue, Caco-2 cell lines, and rat jejunum. J. Pharm. Pharmacol. 56, 1083–1090.

Schmaljohann, D., 2006. Thermo- and pH-responsive polymers in drug delivery. Adv. Drug Deliver. Rev. 58, 1655-1670.

Schreckinger, M., Wang, J., Yousef, G., Lila, M., De Mejia, E., 2010. Antioxidant capacity and *in vitro* inhibition of adipogenesis and inflammation by phenolic extracts of *Vaccinium floribundum* and *Aristotelia chilensis*. J. Agric. Food Chem. 58, 8966–8976.

Shimokawa, K., Saegusa, K., Ishii, F., 2009. Rheological properties of reversible thermo-setting *in situ* gelling solutions with the methylcellulose–polyethylene glycol–citric acid ternary system (2): Effects of various water-soluble polymers and salts on the gelling temperature. Colloids Surf. B Biointerfaces. 74, 56–58.

Suwalsky, M., Vargas, P., Avello, M., Villena, F., Sotomayor, C.P., 2008. Human erythrocytes are affected *in vitro* by flavonoids of *Aristotelia chilensis* (Maqui) leaves. Int. J. Pharm. 363 (1–2), 85–90.

Tadros, T., 2004. Application of rheology for assessment and prediction of the long-term physical stability of emulsions. Advances in Colloid and Interface Sciences 108-109, 227- 258

Taylor, K.M., Irving, P.M., 2011. Optimization of conventional therapy in patients with IBD. Nat. Rev. Gastroenterol. Hepatol. 8, 646–656.

Tenci, M., Rossi, S., Bonferoni, M.C., Sandri, G., Boselli, C., Di Lorenzo, A., Daglia, M., Icaro Cornaglia, A., Gioglio, L., Perotti, C., Caramella, C., Ferrari, F., 2016. Pectin/chitosan particles for the delivery of platelet lysate and manuka honey in chronic skin ulcers. Int. J. Pharm. 509: 59- 70.

Van Tomme, S.R., Storm, G., Hennink, W.E., 2008. *In situ* gelling hydrogels for pharmaceutical and biomedical applications. Int. J. Pharm. 355, 1–18.

Van Vlierberghe, S., Dubruel, P., Schacht, E., 2011. Biopolymer-based hydrogels as scaffolds for tissue engeneering applications: a review. Biomacromolecules. 12, 1387-1408.

Ward, M.A., Georgiou, T.K., 2011. Thermoresponsive polymers for biomedical applications. Polymers. 3, 1215-1242.

Yoshioka, Y., Akiyama, H., Nakano, M., Shoji, T., Kanda, T., Ohtake, Y., Takita, T., Matsuda, R., Maitani, T., 2008. Orally administered apple procyanidins protect against experimental inflammatory bowel disease in mice. Int. Immunopharmacol. 8, 1802–1807.

Yuan, Y., Ying, C., Li, Z., Hui-ping, Z., Yi-Sha, G., Bo, Z., Xia, H., Ling, Z., Xiao-hui, W., Li C., 2012. Thermosensitive and mucoadhesive *in situ* gel based on poloxamer as new carrier for rectal administration of nimesulide. Int. J. Pharm. 430, 114– 119.

Chapter 4

Carvacrol/clay hybrids as antibacterial/antioxidant agents in wound healing. Loading into *in situ* gelling viscoelastic films

4.1 ABSTRACT

The aim of the present work was the development of hybrids/polymers films for the delivery of carvacrol (CRV) in the treatment of infected skin ulcers. To reduce CRV volatility, its incorporation in clays such as montmorrilonite (MMT), halloysite (HAL) and paligorskite (PHC) was considered. Two different methods, shear mixing and adsorption in saturation conditions, were employed. Hybrid (HYBD) obtained by shear mixing CRV with PHC showed the highest loading capacity (21% w/w). HYBD was able to reduce CRV cytotoxicity and antimicrobial properties and to maintain antioxidant properties. HYBD was loaded into polymeric films based on poly(vinyl alcohol) (PVA), polyvinylpyrrolidone k90 (PVP) and chitosan glutamate (CS). Films contained also glycerin as plasticizer and sericin to strengthen CRV antioxidant properties. Film optimization was supported by a DoE approach. In a screening phase, a "full factorial design" (FFD) was employed. The following three factors were investigated at two levels: PVA (12% - 14% w/w), PVP (2% - 4% w/w) and CS (0.134% - 0.5% w/w) concentrations. In the optimization phase, FFD was expanded to a "central composite design" (CDD). The response variables considered were: film mechanical properties expressed by % elongation and tensile strength, film hydration propensity expressed as buffer (PBS) absorption and durability of the gel formed upon film hydration.

Due to its elastic properties, hydrated film was able to provide a high protection of the lesion area. Both gel formed upon film hydration and HYBD were able to control CRV release.

4.2 INTRODUCTION

Wound healing is a complex dynamic process involving several inter-related biological and molecular factors, aimed to tissue regeneration. Haemostasis, inflammation, proliferation, migration and remodelling/maturation are the five phases of the wound healing process. Chronic wounds, such as diabetic foot ulcers, pressure ulcers and venous leg ulcers are a worldwide health problem. Such wounds fail to heal due to repeated trauma to the lesion area or underlying pathological conditions, which compromise or delay the physiologic events during the wound healing process (Boateng et al., 2008; Boateng and Catanzano, 2015). In this perspective, advanced therapeutic dressings, designed to take an active role during the wound healing process, represent a relatively new interesting approach in the treatment of chronic wounds. Their biological properties are related not only to the bioactive agents loaded into the dressing, but also to the presence of biomaterials able to improve tissue repair (Boateng and Catanzano, 2015). Among these biomaterials, chitosan, a linear polysaccharide obtained by chitin deacetylation, has been recognized as a biopolymer able to promote tissue repair and to avoid the onset of infections (Rossi et al., 2010; Rossi et al., 2013; Mori et al., 2016; Tenci et al., 2016a).

Various mechanisms have been reported in literature to explain chitosan activity on wound healing process. Chitosan acts as a chemo-attractant for neutrophilis and macrophages, promotes granulation tissue formation, accompanied by angiogenesis and collagen fiber deposition. Chitosan also shows an inhibition effect on metalloproteinases (MMPs), a family of enzymes responsible for the degradation of extracellular matrix components (Muzzarelli, 2009).

The association of synthetic and naturally polymers in composite dressings has been recognized as useful to control drug delivery to wound site (Boateng et al., 2008). Among synthetic polymers poly (vinyl alcohol) (PVA) and polyvinylpyrrolidone (PVP) are largely employed for biomedical applications, such as controlled release systems and tissue engineering (Vicentini et al., 2010; Li et al., 2010).

In the last decades, essential oils (EOs), hydrophobic, aromatic and volatile liquids obtained from plants, have attracted a considerable interest for their biological properties (Bakkali et al., 2008). EOs are considered GRAS (Generally Regarded as Safe) ingredients for food use by the Food and Drug Administration (FDA) (Higueras et al., 2013). Due to their antibacterial, antifungal, antiviral and antioxidant properties, EOs use is widespread also in the pharmaceutical field (Bakkali et al., 2008). EOs have a complex composition, containing from a dozen to several hundred of components at different concentrations. Among EOs components, it is possible to distinguish two or three major components at high concentration, ranging from 20 to 80%, compared to others ones present in trace amounts. Generally, these major components, such as terpenes (oxygenated or not)

and terpenoids, are characterized by low molecular weight and are responsible for the biological properties of EOs (Edris, 2007; Bakkali et al., 2008, Miguel, 2010). In particular, carvacrol (CRV), a monoterpene phenolic compound, is the major component (up to 80%) of oregano essential oil (*Origanum vulgare*) (Burt, 2004). It possesses antioxidant, antifungal and antimicrobial properties (Safaei-Ghomi et al., 2009; Ben Arfa et al., 2006; Tunç and Duman, 2011).

Due to the volatile nature of EOs, different strategies have been proposed to reduce their evaporation. One of these provides the inclusion of EOs in montmorrilonite and halloysite clays. Recently, some authors proposed the use of such clays as packaging materials and demonstrated their capability to enhance the thermal stability and to preserve antimicrobial properties of EOs (Efrati et al., 2014; Shemesh et al., 2015). Gorrasi (2015) proved that packaging hybrid/polymer films were able to control the release of EOs.

On the basis of their chemical composition, clay minerals can be classified in eight major groups, including smectites (e.g. montomorillonite), micas, kaolin (e.g. halloysite), talcum, chlorites, vermiculites, interstratified and fibrous clays (e.g palygorskite and sepiolite) (López-Galindo et al., 2007). So far, to the best of our knowledge, no papers have been published on the use of EOs/clay hybrids loaded into film for cutaneous application. Clays generally employed in the pharmaceutical and cosmetic fields belong to smectites, kaolin and fibrous clay groups.

Given these premises, the aim of the present work was the preparation of clay/CVR hybrids to be loaded into *in situ* gelling viscoelastic films for the treatment of skin lesions. Hybrids should prevent CVR evaporation, maintaining its antioxidant and antimicrobial properties. Three different commercial clays have been considered: montmorrilonite (MMT), halloysite (HAL) and a commercial palygorskite (PHC).

In a first phase of the research, CVR and CVR/clay hybrids were prepared using two different approaches: adsorption in saturated atmosphere and shear mixing. Hybrids were subjected to thermal analysis in order to study the effect of clay type and of preparation method on CRV volatility. On the basis of the results obtained, clay and preparation method which allowed the highest CRV loading were chosen for the continuation of the research. The chosen CRV/clay hybrid (HYBD) was also investigated for *in vitro* cell viability and antioxidant activity on human fibroblasts and for antimicrobial properties towards *E. coli* and *S. aureus* in comparison with pure CRV.

A second phase of the research was devoted to the preparation and optimization of films to be used as vehicle for HYBD. Films should be characterized by suitable mechanical properties (high flexibility and resistance to rupture) and by the capability to absorb wound exudate forming a viscoelastic persistent gel, able to protect the lesion area without impairing CRV release.

Films were composed by poly(vinyl alcohol) (PVA), polyvinylpirrolidone (PVP) and chitosan glutamate (CS). They were prepared by casting HYBD 2.6% (w/w) suspension in the polymer mixture. Sericin (SER) was added at 0.8% (w/w) concentration to improve HYBD antioxidant properties (Mori et al., 2016). To obtain films of optimized composition, a DoE approach was employed. The experimental design provided a screening and an optimization phase. In the screening phase a two full factorial design (FFD) was used not only to investigate the effect of each factor (PVA, PVP and CS concentrations) on the response variables considered (flexibility, mechanical strength, hydration capability of film and gel durability), but also to individuate the main influencing factors. To determine the optimized formulation the screening design was expanding to a central composite design (CDD) by adding a star design and a central point. The experimental results obtained for the optimized formulation were compared to those predicted in order to confirm the predictive power of the model. Rheological (viscoelastic) properties of the gel obtained from film hydration in a medium mimicking wound exudate were also assessed.

4.3 MATERIALS AND METHODS

4.3.1 Materials

The following materials were used: antibiotic antimycotic solution (100×), stabilized with 10,000 units penicillin, 10 mg streptomycin and 25 μg amphotericin B per ml (Sigma Aldrich, Milan, I); carvacrol (CVR) (natural, 99%, FG; CRV) (Sigma Aldrich, Milan, I); chitosan low MW (DD: 80%) (Sigma Aldrich, Milan, I); dimethyl sulfoxide (DMSO) (Sigma Aldrich, Milan, I); Dulbecco's Modified Eagles Medium (DMEM) (Lonza, BioWhittaker, Walkersville, MD, USA); Dulbecco's Phosphate Buffer Solution (Sigma Aldrich, Milan, I); glutamic acid (Sigma Aldrich, Milan, I); glycerol (Carlo Erba, Milan I); halloysite nanoclay (HAL) (Sigma Aldrich, Milan, I); Hank's balance salt solution (HBSS) (Sigma Aldrich, Milan, I); inactivated foetal calf bovine serum (Biowest, Nuaillé, F); montmorillonite (VeegumHS©, MMT) was kindly gifted by Vanderbilt Minerals (USA); MTT (3-(4,5-dimethylthiazol-2-yl)-2,5-diphenyltetrazolium bromide) (Sigma Aldrich, Milan, I); $NaH_2PO_4 \cdot H_2O$ (Carlo Erba, Milan I); $Na_2HPO_4 \cdot H_2O$ (Carlo Erba, Milan, I); NaCl (Carlo Erba, Milan, I); n-hexane (Carlo Erba, Milan I); Pharmasorb© colloidal (PHC) (BASF Aktiengesellschaft, Ludwigshafen, G); poly(vinyl alcohol) (PVA) (Sigma Aldrich, Milan, I); polyvinylpyrrolidone K90 (PVP) (BASF Aktiengesellschaft, Ludwigshafen, G); trypan blue solution (Biological Industries, Beit-Haemek, IL); trypsin–EDTA solution (Sigma Aldrich, Milan, I).

4.3.2 Preparation of CVR/clays hybrids

Three different clays, halloysite (HAL), montmorillonite (MMT) and a commercial palygorskite (PHC), were considered. CVR/clay hybrids were prepared according two different methods: adsorption in saturation conditions and shear mixing.

The first method provides to create an ambient saturated with CVR. At this aim, a beaker containing 5 ml of CVR was put in the centre of a hermetically sealed glass chamber (489 cm^3 volume). 50 mg of each clay was layered on a watch glass inside of the chamber. The chamber was thermostatated at a constant temperature (20, 40, 60, 80 and 120°C) for a fixed time period (48 h).

Shear mixing technique provides to disperse clay in CVR (2: 1 w/w ratio) by ultra-sonication at room temperature for 1 h (Shemesh et al., 2015). CVR not adsorbed on clay was removed by centrifugation (4218 centrifuge, ALC International s.r.l., Milan, I) at 3000 rpm for 15 min and by evaporation in an oven for 24 h at 80°C (Vismara Laselelettronics s.r.l., Lodi, I).

To assess the amount of CRV loaded, CVR/clay hybrids were subjected to thermogravimetric analysis (TGA). Pure CVR and clays were used as references. TGA analysis was carried out by using a Shimadzu mod. TGA-50H apparatus, working over the temperature range 36–950°C at a

heating rate of 10°C/min. The results were expressed as % mass loss as a function of temperature. From the comparison of hybrid TGA profiles with those obtained for pure CVR and clays, % CRV loaded into hybrids was calculated (see Eq. 1).

$$\% \text{ LC} = \frac{\text{CVR loaded (mg)}}{\text{hybrid (mg)}} \times 100 \qquad \text{Eq. (1)}$$

TGA analysis was also used to assess HYBD stability upon storage for 1 month at 20°C in dessicator.

To confirm the data obtained from TGA analysis, the amount of CRV loaded into CVR/PHC hybrid (HYBD) prepared by shear mixing was assessed by an extraction method. In particular, 2 mg of HYBD was weight and added to 10 ml of n-hexane (Tunç and Duman, 2011). The dispersion was maintained under stirring overnight, centrifuged at 3000 rpm for 20 min and then filtered (cellulose acetate, 0.45 μm; Sartorius, Muggiò, I). The supernatant was recovered and analyzed for CRV content by means of a UV-vis spectrophotometer (Perkin Elmer, Lambda 25) setting wavelengths ranging from 200 to 500 nm. A calibration curve was prepared by using CRV hexane solutions at the following concentrations: 50, 25, 20, 10 and 5 μg/ml.

4.3.3 *In vitro* assessment of cytocompatibility of CRV and HYBD

NHDF fibroblasts (Promocell GmbH) from 6th to 16th passage were used. Cells were cultured in a polystyrene flask (Greiner bio-one, PBI International, Milan, I) with 13-15 ml of complete culture medium (CM), consisting of Dulbecco's modified Eagles medium with 4.5 g/l glucose and l-glutamine supplemented with 1% (v/v) antibiotic antimycotic solution (100×), stabilized with 10,000 units penicillin, 10 mg streptomycin and 25 μg amphotericin B per ml and 10% (v/v) inactivated foetal calf bovine serum. Cells were maintained in incubator (Shellab® Sheldon® Manufacturing Inc., Oregon, USA) at 37°C with 95% air and 5% CO_2 atmosphere. All the operations required for cell culture were carried out in a vertical laminar air flow hood (Ergosafe Space 2, PBI International, Milan, I). When cells had reach 80-90% of confluence in the flask, a trypsinization was performed as described by Tenci et al. (2016b). The amount of viable cells in the suspension recorded after trypsinization, was determined in a counting chamber (Hycor Biomedical, Garden Grove, California, USA), using 0.5% (w/v) trypan blue solution.

To assess the biocompatibility of the CRV and CRV/clay hybrid with human fibroblasts, cell viability tests were performed. Such *in vitro* assays were used to estimate the number of viable cells after a prefixed time-contact with the samples considered.

For cell viability tests, $3.5 \cdot 10^4$ cell/well (0.35 cm^2 area) were seeded in 96-well plate (Greiner bio-one, VWR International, Milan, I) with culture medium (CM) and let to grow to reach confluence. When the medium was removed, cells were put in contact for 24 h with 200 µl of CRV solutions. CRV aqueous solution (1 mg/ml) was diluted in CM; the final concentrations upon dilution were: 5, 10, 25 and 50 µg/ml. As for CRV/clay hybrid, the powder was dispersed into CM in order to obtain final concentrations of CRV equal to: 5, 10, 25 and 50 µg/ml. CM was used as positive control. After 24 h, cells were washed with 100 µl of HBSS (pH 7.4) and then put in contact for 3 h with a 8 mM MTT (3-(4,5-dimethylthiazol-2-yl)-2,5-diphenyltetrazolium bromide) solution in HBSS (150 µl/well). Finally, 100 µl of dimethyl sulfoxide was added to each well, to allow the complete dissolution of formazan crystals, obtained from the reduction of the dye MTT into cells by dehydrogenase enzyme. The solution absorbance was determined at a wavelength of 570 nm, with a 690 nm reference wavelength, by means of an IMark® Microplate reader (Bio-Rad Laboratories S.r.l., Segrate, Milan, I) after 60 s shaking. Results were expressed as % viability, normalizing absorbance measured after contact with samples with that measured after contact with CM.

4.3.4 *In vitro* assessment of antioxidant properties of CRV and HYBD

CVR and CVR/clay hybrid antioxidant properties were investigated using fibroblasts as biological substrate. NHDF fibroblasts (Promocell GmbH) from 6^{th} to 16^{th} passage were used. Cells were seeded (3.5×10^4 cells/cm^2) overnight into a 96-well plate (Greinerbio-one, VWR International, Milan, I) and then put in contact for 6 h with samples (200µl). CRV and CRV/clay hybrid were diluted/dispersed into complete medium (CM) in order to obtain final concentrations of CRV equal to 5, 10 and 25 µg/ml. Subsequently, 10 µl of 10.5 mM H_2O_2 (Carlo Erba, Milan, I) was added in each well (the final H_2O_2 concentration, upon dilution with 200 µl of CM or sample solution/dispersion, was equal to 1 mM) and incubated for 18h (Mori et al. 2016; Peng et al. 2016). Then, cells were washed with a HBSS (pH 7.4) and a MTT test was performed (as described in section 4.3.3).

4.3.5 Antimicrobial activity

To evaluate the antimicrobial properties of CRV and HYBD, the following reference bacterial strains were used: *Staphylococcus aureus* ATCC 6538 and *Escherichia coli* ATCC 10536. Before testing, bacteria were grown overnight in Tryptone Soya Broth (Oxoid, Basingstoke, UK) at 37°C. The cultures were centrifuged at 2000 rpm for 20 min to separate cells from culture broth and then washed with purified water. Washed cells were resuspended in Dulbecco's PBS and optical density

(OD) was adjusted to 0.1, corresponding approximately to 1×10^8 colony forming units (CFU) /ml at 650 nm wavelength.

The antimicrobial activity was tested both on CRV and on HYBD and was determined with the macrodilution broth method, according to Clinical and Laboratory Standards Institute (*Clinical and Laboratory Standards Institute, Methods for Dilution Antimicrobial Susceptibility Tests for Bacteria That Grow Aerobically-Eighth Edition: Approved Standard M7-A8, Clinical and Laboratory Standards Institute, Wayne, PA, USA, 2009*), with some modifications reported in this paragraph. The desired concentration of CRV was achieved through the addition of an appropriate CRV volume to 1 ml of double-concentrate Iso-Sensitest broth (ISB, Oxoid) in 15 mm × 100 mm test tubes. Bacterial suspensions were added to the test tubes.

The minimum inhibitory concentration (MIC) was evaluated after a 24h incubation at 37°C, as the lowest concentration that completely inhibited the formation of visible microbial growth. Control test tubes containing broth without CRV for each organism tested were used. The same experiment was performed suspending an appropriate quantity of HYBD in 1 ml of double-concentrate Iso-Sensitest broth (ISB, Oxoid). In this case control test tubes containing broth with unloaded clay for each organism tested were used as control. Various concentrations of CRV and HYBD were tested, starting from 0.4 mg/ml. Incubating temperature was 37°C; MIC was detected after 24 h.

Minimum bactericidal concentration (MBC) was evaluated by inoculating aliquots of culture medium in which the inhibition of bacterial proliferation was observed. MBC was the lowest concentration capable of killing the microbial cells (*Clinical and Laboratory Standards Institute, Methods for Determining Bactericidal Activity of Antimicrobial Agents: Approved Guideline M26-A, Clinical and Laboratory Standards Institute, Wayne, PA, USA, 1999*). Incubating temperature was 37°C. MBC was detected after 24 h. Bacteria-free broth was included as control.

4.3.6 Experimental design

4.3.6.1 Screening of independent variables

A screening design is used to determine which factors and their interactions significantly affect the response variables. Such factors will be subsequently considered in the optimization phase. Full or fractional two-level factorial designs may be employed for this purpose, because they are efficient and economical (Dejaegher B. and Vander Heyden Y, 2011).

In the present work a "2^3 full factorial design" (FFD) was chosen. Three factors, (corresponding to the polymers PVA, PVP and CS, at two different concentrations (levels), were investigated. The polymer concentrations considered were: 12%, 14% w/w for PVA (x_1), 2%, 4% for PVP (x_2) and 0.134%, 0.5% w/w for CS (x_3). Eight film formulations, relating to the different experimental

points, were prepared. In Table 1 polymer concentrations employed for film preparation are reported: for each polymer the upper level is indicated as +1 and the lower one as -1.

Table 1 - Experimental points of "full factorial design".

	PVA	**PVP**	**CS**
1	+1	+1	+1
2	+1	+1	-1
3	+1	-1	+1
4	+1	-1	-1
5	-1	+1	+1
6	-1	+1	-1
7	-1	-1	+1
8	-1	-1	-1

PVA: level -1 (12%); level +1 (14%);

PVP: level -1 (2%); level +1 (4%);

CS: level -1 (0.134%); level +1 (0.5%).

The response variables considered were: percent elongation (%E), tensile strength (TS), hydration properties (buffer amount absorbed per unit weight) and gel durability. The experiments were performed in random sequence. Design generation and statistical analysis were carried out using a statistical software package (Statgraphics 5.0 Statistical Graphics Co., Rockvillle, MD, USA).

4.3.6.2 Optimization design

For the optimization of film formulation, a response surface design, in particular a randomized "central composite design" (CDD), was applied.

A response surface design, such as CDD, is carried out to optimize the level of each factor considered. In this type of design the dependent variables are modeled as function of the independent parameters. Response surface designs are divided into 2 categories, symmetrical and asymmetrical designs; in particular the CDD is a symmetrical response surface design and covers a symmetrical experimental domain (Dejaegher and Vander Heyden, 2011). This design consists of three parts: (1) a full factorial design (2^f experiments), (2) an additional design, a star design ($2*f$ experiments), and (3) a central point. N experiments ($N=2^f+(2*f)+1$) are required to examine the most important factors (f) identified by the screening design.

In a CDD the experimental points of the full factorial design correspond to the levels -1 and +1, those of the star design at the levels 0, $-\alpha$ and $+\alpha$ ($\alpha \geq 1$), and the central point at the level 0. Depending on α value, two different CCDs exist: a face-centred CCD ($\alpha=1$), a simplified CDD, in

which three levels for each factor are considered, and a circumscribed CCD (α>1), examining the factors at five levels (Dejagher and Vander Heyden, 2011).

For our purpose, a CDD with α>0, examining five levels for each factor, was considered and seven additional dressing formulations were investigated with respect to a FFD (Table 2).

Table 2 – Additional experimental points investigated to expand "full factorial" to "central composite" design.

	PVA	**PVP**	**CS**
9	0	-1.73	0
10	0	+1.73	0
11	+1.73	0	0
12	-1.73	0	0
13	0	0	+1.73
14	0	0	-1.73
15	0	0	0

PVA: level -1 (12%); level +1 (14%); level -1.73 (11.27%); level +1.73 (14.73%); level 0 (13%).

PVP: level -1 (2%); level +1 (4%); level -1.73 (1.27%); level +1.73 (4.73%); level 0 (3%).

CS: level -1 (0.134%); le**v**el +1 (0.5%); level -1.73 (0%); level +1.73 (0.634%); level 0 (0.317%).

The factors and the response variables considered in the CDD were the same of the screening phase. The experiments were performed in random sequence. Design generation and statistical analysis were carried out using a statistical software package (Statgraphics 5.0 Statistical Graphics Co., Rockvillle, MD, USA).

4.3.7 Films preparation and characterization

HYBD at 2.6% w/w concentration was dispersed into a sericin (Ser) (1.6% w/w)/glycerol (Gly) (20% w/w) aqueous solution. Ser was used to strengthen CRV antioxidant properties (Mori et al. 2016a), whereas Gly acted as plasticizer (Rossi et al., 2013). Such dispersion was diluted 1:1 w/w with a polymeric aqueous solution, contained PVA, PVP and CS. The final polymer concentrations corresponded to the different points of the experimental design. Upon overnight stirring, 6.7 g of diluted dispersion was layered on a circular teflon plate (30.25 cm^2 area) and dried at 50°C in an oven (Vismara Laselelettronics s.r.l., Lodi, I) for 24 h. After drying, films were recovered and stored in a desiccator until characterization.

Dried films were characterized for mechanical properties, buffer absorption capability and for the durability of gel formed upon hydration in a medium mimicking wound exudate.

4.3.7.1 Assessment of films mechanical properties

Mechanical properties were measured using a TA-XT plus Texture Analyzer (ENCO, Spinea, Venice, I) equipped with 5 kg load cell. Before testing, dried films were cut 40 mm x 20 mm and the strips obtained were clamped between A/TG tensile grips probe, setting an initial distance between the grips of 20 mm. Then, the upper grip was raised at a constant speed of 5 mm/s up to a distance of 20 mm, corresponding to 100% elongation. Films were visually inspected in order to observe the occurrence of a physical damage (break) during the test. % elongation (%E, mm/mm) corresponding to film break was recorded together with the related tensile strength applied (TS, N/mm^2). In absence of film damage, TS value corresponding to 100% elongation was recorded.

TS is an index of film strength, while %E indicates film flexibility that is the capability of the film to deform without breaking when subjected to increasing strengths (El-Malah and Nazzal, 2008).

Percent elongation was calculated as follows:

$$\%\ E = \frac{\text{final lenght - initial lenght}}{\text{initial lenght}} \times 100 \quad \text{Eq. (2)}$$

4.3.7.2 Assessment of films hydration properties and gel durability

Films were subjected to hydration measurements at 32°C by means of Franz diffusion cells (PermeGear, Bethlehem (PA)). A circular films, having a diameter of 20 mm and weight of 200 ± 10 mg, was layered on a pre-hydrated dialysis membrane (Mires Emanuele, MWCO 12-14000 Da; Ø 36/32″ - 28.6 mm), used to separate the donor and the receptor chambers of a Franz diffusion cell. The receptor chamber was filled with a pH 7.4 buffer (phosphate buffered saline (PBS); $NaH_2PO_4 \cdot H_2O$ 0.036% w/w, Na_2HPO_4 H_2O 0.137% w/w, NaCl 0.850% w/w), chosen to mimic wound exudate. After prefixed time (4 and 8 h), films were weighted (Tenci et al., 2016b).

The PBS amount uptaken by the film was normalized for film weight (gPBS/g) to obtain amount of PBS uptaken per film weigth (gPBS/g):

$$\text{gPBS/g} = \frac{\text{weight of the film after 4 h of hydration - weight of the dry film}}{\text{weight of the dry film}} \quad \text{Eq. (3)}$$

The gel durability, expressed as the amount of gel present in the donor chamber over dialysis membrane after 8 h of hydration, was calculated. Such parameter is an index of the dressing resistance against the degradation/erosion process, upon contact with wound exudate.

4.3.8 Optimization procedure

In the optimization phase, experimental data obtained for each response variable (%E, TS, gPBS/g and gel durability) of the experimental design were fitted to a multiple regression model, described below:

$$y = \beta_0 + \sum_{i=1}^{f} \beta_i x_i + \sum_{1 \le i < f}^{f} \beta_{ij} x_i x_j + \sum_{i=1}^{f} \beta_{ii} x_i^2 \quad \text{Eq.(4)}$$

where y is the response, β_0 the intercept, β_i the main coefficients, β_{ij} the two-factor interaction coefficients, and β_{ii} the quadratic coefficients (Dejaegher and Vander Heyden, 2011; Ćurić et al., 2013).

Such model is useful to predict the value of each response variable, related to any combination of factors within the experimental region, by means of a software package (Statgraphics 5.0, Statistical Graphics, Rocknille, MD). It was also possible to compare the predicted values with the experimental data employing the Analysis of Variance (ANOVA) (Dejagher and Vander Heyden, 2009; Dejagher and Vander Heyden, 2011).

4.3.9 Characterization of optimized film formulation

Films of optimized composition, chosen on the basis of the results obtained, were prepared by casting and subjected to the same characterization previously effected on the formulations of FFD and CCD (as described in the section 4.3.7). The experimental results obtained for the film of optimized composition were compared with those provided by the model, in order to confirm its predictive power.

4.3.9.1 Assessment of CRV-loading into films

In order to quantify the amount of CRV loaded into the film, 100 mg of formulation was dissolved in 1 ml of distilled water. After that, 10 ml of n-hexane were added. To allow the complete CRV extraction the aqueous-organic mixture was maintained under magnetic stirring overnight (Campos-Requena, 2015).

The mixture was centrifuged at 3000 rpm for 20 min to separate the organic phase from the aqueous one. Finally, the organic phase was filtered (cellulose acetate membrane, 0.22 μm; Sartorius, Muggiò, I) and analyzed with a UV-vis spectrophotometer (Perkin Elmer, Lambda 25) setting a wavelength ranging from 200 to 500 nm. A calibration curve was prepared by using CRV solutions at the following concentrations: 50, 25, 20, 10 and 5 μg/ml. Finally the loading capacity (LC) of CRV was calculated from Eq. (5):

$$\%\ \text{LC} = \frac{\text{loaded CRV (mg)}}{\text{sample mass (mg)}} \times 100 \quad \text{Eq. (5)}$$

4.3.9.2 Rheological properties

After hydration for 4 h, film of optimized composition was subjected to dynamic viscoelastic analysis by means of a rotational rheometer (Rheostress 600, Haake, I), equipped with a cone plate

combination (C20/1: Ø 20 mm; angle=1°) apparatus. Oscillation measurements were performed. They provide to apply a fixed stress, chosen in the linear viscoelastic region, previously determined, at increasing frequency values (ranging from 0.1 to 10 Hz) and to measure the viscoelastic response of the sample, expressed as loss tangent parameter, calculated as ratio between loss modulus (G″) and storage modulus (G′).

4.3.9.3 Assessment of *in vitro* release properties

CRV release profile of film in comparison with HYBD was evaluated at 32°C by means of Franz diffusion cells (Permeager, Bethlehem, PA, USA) with a 20 mm diameter orifice (3.14 cm^2). In particular, dried films with a diameter of 10 mm and a weight of 100 ± 5 mg were considered. To assess HYBD release properties, 10.0 ± 0.5 mg of HYBD was layered on a filter membrane (cellulose acetate, 0.22 μm; Sartorius, Muggiò, I), using to separate the donor and the receptor chambers of Franz cell (Mori et al. 2014). The receptor chamber was filled with pH 7.4 PBS. At fixed time periods (4, 8, 24 and 48 h), 1 ml of medium was collected and analyzed by UV-vis spectrophotometric method at 273 nm.

4.4 RESULTS AND DISCUSSION

4.4.1 Choice of clay type and hybrid preparation method

Figure 1 reports % CRV loading capacity values of the different CVR/clay hybrids prepared by adsorption in saturated atmosphere after 48h at different temperatures. For all the three clays, an increase in CRV loading on increasing temperature was observed. HAL was able to adsorb CVR at temperature higher than 40°C. Among the three clays considered, PHC was characterized by the highest values of % LC. PHC, being a fibrous clay, was characterized by a higher surface available for adsorption. The highest %LC value was observed at 120°C.

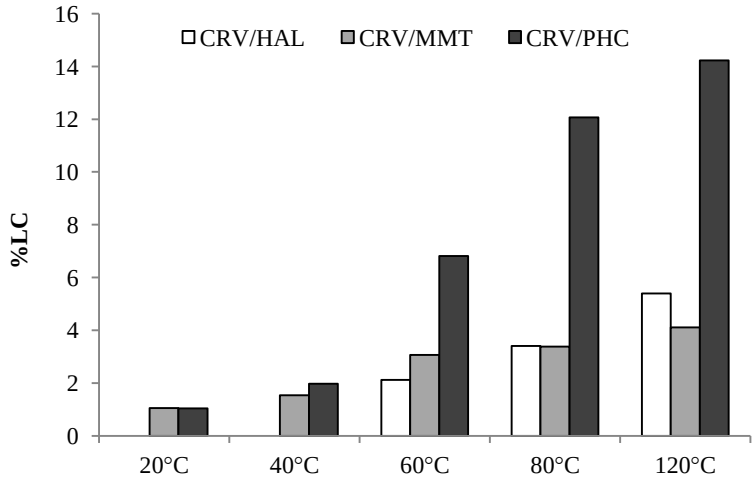

Figure 1 - % CRV loading capacity (%LC) of the different CRV/clay hybrids prepared by adsorption in saturated atmosphere technique at different temperatures (20, 40, 60, 80, 120°C) for 48 h (mean values n= 3; CV% < 10%)

In Figure 2 %LC values of the three different CRV/clay hybrids prepared by shear mixing are reported. Also for this preparation technique, %LC was affected by clay structure: the highest value was observed for the fibrous PHC, followed, in decreasing order, by the tubular HAL and by the lamellar MMT. CVR/PHC hybrid (HYBD) prepared by shear mixing was characterized by a % CRV loading capacity equal to 20% (w/w) in comparison to 14% w/w obtained with adsorption in saturated atmosphere technique. The comparison of the results obtained addressed the choice on PHC and shear mixing technique.

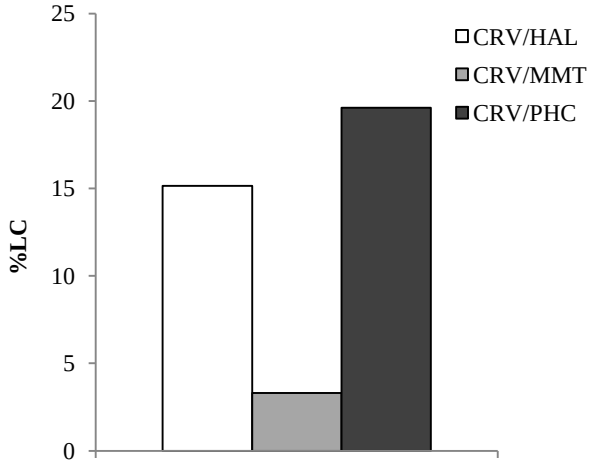

Figure 2 - % CRV loading capacity (%LC) of the different CRV/clay hybrids prepared by shear mixing (mean values n= 3; CV% < 10%)

As an example, in Figure 3 TGA profiles of HYBD was compared with those of pure CRV and PHC. CRV showed a clear weight loss process, relating to CRV evaporation, which started at 36°C and concludes at 191°C. PHC appeared as a thermostable clay, characterized by a weight loss step (150°C), corresponding to evaporation of superficial humidity (7.6% w/w), with a solid residue at 950°C of approximately 83% with respect to the initial mass. In TGA profile of HYBD three different steps were distinguished. The first one (80-286°C) was associated to a 17% weight loss, that was attributable to 9.5% w/w CRV loss, taking into account a PHC loss of 7.5% w/w (see TGA profile of pure PHC). In the second step (260-554°C) HYBD lost a further 16% weight, corresponding to 7.5% w/w PHC loss and to 8.5% w/w CRV loss (calculated as difference). Finally the increase in temperature from 505° to 708°C produced a HYBD % weight loss equal to 5% w/w, related to a CRV loss of 2% w/w. Total % CRV loss from HYBD was about 20%, corresponding to the total % CRV loaded.

The successful loading of CRV on PHC was confirmed by UV spectrophotometer analysis of the supernatant obtained after CRV extraction from HYBD in hexane. The supernatant showed a maximum absorption peak at 275 nm. A CRV-hexane solution showed a maximum absorption peak at 275 nm, which is very close to the wavelength reported by Tunç and Duman (λ_{max} in n-hexane= 273 nm) (Tunç and Duman, 2011). The amount of loaded CRV in 2g of HYBD was 0.43 ± 0.02 g, corresponding to 21 ± 1 % w/w.

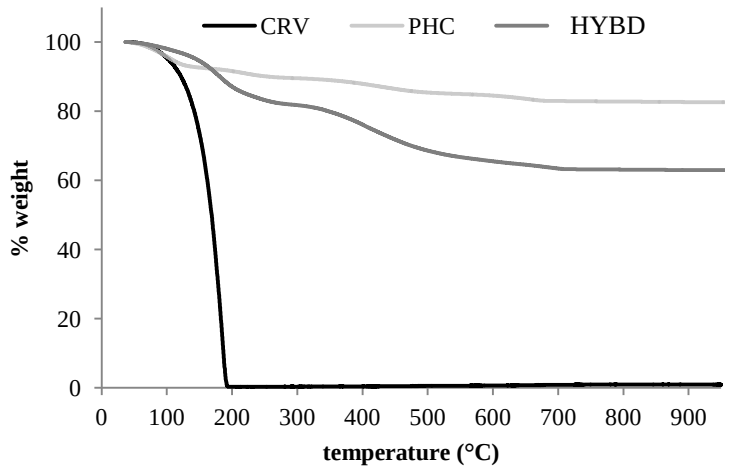

Figure 3 - % weight of PHC, CRV, and HYBD as a function of temperature obtained from TGA analysis

Figure 4 reports TGA curves for HYBD obtained at time 0 and after storage for 1 month at 20°C in dessicator. Storage conditions did not produce any change in % weight *vs* temperature profile, indicating that in such conditions HYBD was stable: no CVR was lost during storage.

The results so far obtained indicate that PHC was able to reduce CRV volatility and that HYBD was a stable composite for temperature values lower than 80°C.

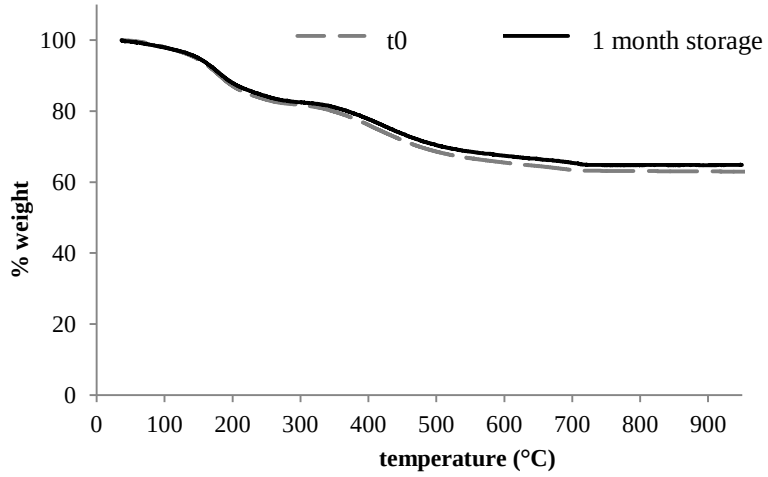

Figure 4 - Comparison of % weight *vs* temperature profiles of HYBD at time 0 and after storage for 1 month in dessicator, at 20°C.

4.4.3 *In vitro* cytocompatibility and antioxidant evaluation

4.4.3.1 Cell viability assessment

In Figure 5 % viability values for CRV and HYBD dissolved/dispersed in complete medium (CM) are reported. Different CRV concentrations, ranging from 10 to 100 μg/ml, were considered.

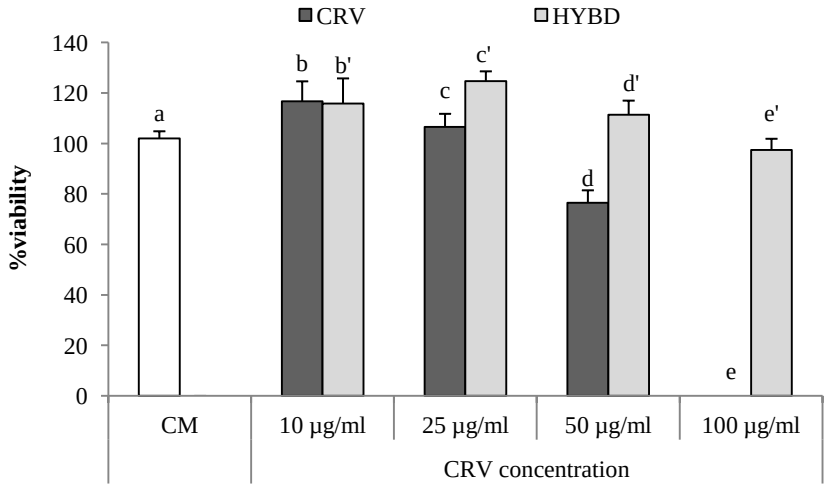

Figure 5 - Comparison of % viability values of CRV (10 - 100 μg/ml) and HYBD dissolved/dispersed in complete medium (CM). HYBD amounts corresponding to 10 -100 μg/ml CVR concentrations were considered. CM was used as reference (mean values ± s.e; n=8). Anova one way - MRT ($p<0.05$): a *vs* d/e; b *vs* d/e; c *vs* d/e; d *vs* e/d′; e *vs* e′; c′ *vs* e′.

CRV at low concentrations (10 and 25 μg/ml) was cytocompatible: it was characterized by % viability values not statistically different from that observed for the reference (CM). At CRV concentrations ≥ 50 μg/ml, a marked reduction in cell viability (76% at 50 μg/ml, and 0% at 100 μg/ml) was observed. On the contrary, HYBD at the concentrations investigated did not show any cytotoxic effect. These results pointed out that the loading of CRV in PHC was able to protect human fibroblasts against CRV cytotoxic effect.

4.4.3.2 Assessment of CRV and HYBD antioxidant activity

In Figure 6, % viability values of fibroblasts treated with H_2O_2, used to produce an oxidative damage, in presence and in absence of CRV pure or loaded in HYBD are compared. Untreated cells, cultured in CM, were used as reference.

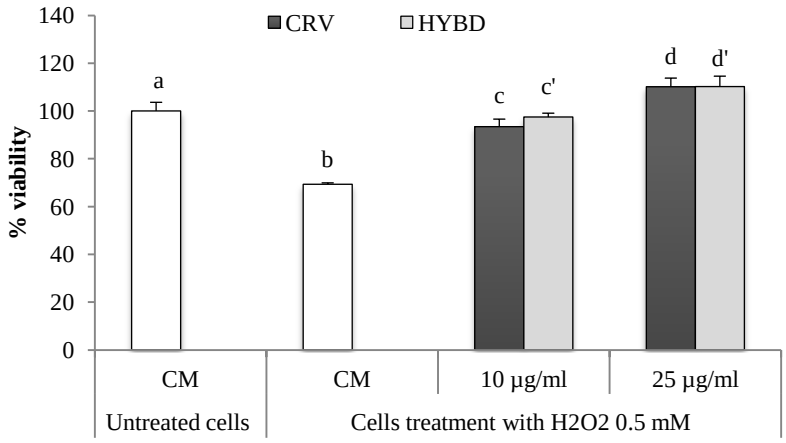

Figure 6 - % cell viability of fibroblasts subjected to oxidative damage (0.5 mM H_2O_2 for 6h), treated or untreated with CRV (10 and 25 µg/ml), either pure or loaded in HYBD. HYBD amounts corresponding to 10 and 25 µg/ml CVR concentrations were considered. Untreated cells cultured in CM were used as reference (mean values ± s.e; n=8). Anova one way - MRT ($p<0.05$): a *vs* b; b *vs* c/d/c´/d´; c *vs* d/d´; c´ *vs* d´.

A significant ($p < 0.05$) decrease of % viability was observed for fibroblasts treated with H_2O_2 in comparison with untreated cells, cultured in CM. This result pointed out the suitability of the experimental conditions (H_2O_2 concentration and contact time) to produce an oxidative damage. A significant ($p < 0.05$) increase in % viability was observed when cells were treated with CRV. As expected, an increase in CRV concentration produced a greater antioxidant effect. No significant differences were observed between CRV and HYBD, when tested at the same CRV concentration. It must be underlined that % viability values of fibroblasts treated with CRV, either pure or loaded in HYBD, were not significantly different from that observed for untreated cells. It indicated CRV capability to protect human fibroblasts from oxidative damage. The results obtained proved that CRV was able to protect human fibroblasts against oxidative stress and its loading on PHC did not disturb such activity.

4.4.4 Antimicrobial activity

In Table 3 MIC and MBC values of free CRV and CRV loaded into HYBD were reported. It can be observed that CRV loading into HYBD produced a decrease of MIC and MBC against both the microorganisms tested. These results indicated a higher antimicrobial activity of CRV when loaded into clay.

Table 3 - MIC (minimum inhibition concentration) and MBC (minimum bactericidal concentration) values of pure CRV and HYBD against *Escherichia coli* and *Staphylococcus aureus*. MIC and MBC are expressed as CRV concentration (mean values (s.d), n=3).

	MIC (mg/ml)		**MBC (mg/ml)**	
	E. coli ATCC: 10536	*S. aureus* ATCC: 6538	*E. coli* ATCC: 10536	*S. aureus* ATCC: 6538
CRV	1.26 (0.81)	0.65 (0.37)	2.75 (1.30)	2.75 (1.30)
HYBD	0.60 (0.28)	0.26 (0.08)	1.18 (0.56)	0.49 (0.42)

4.4.5 Experimental design

4.4.5.1 Full factorial design (FFD)

A full factorial design is useful to study the effect of each factor (X) and their interactions on the response variables (Y) (Dejagher and Vander Heyden, 2011). An analysis of variance was performed to test the statistical significance of the effects (positive or negative) of each factor and interaction on the various response parameters.

Table 4 reports the experimental results obtained for the 8 formulations, relating to the different experimental points of FFD.

Table 4 – % elongation (mm/mm), tensile force (mN/mm^2), buffer (PBS) amount absorbed (g/g) and gel durability (g) of the various films of FFD (mean values ± s.d.; n = 3).

Points of the design	**% elongation (mm/mm)**	**Tensile force (mN/mm^2)**	**PBS amount absorbed (g/g)**	**Gel durability (g)**
1	100.00 ± 0.00 ^{a}	1.230 ± 0.092 $^{a'}$	1.227 ± 0.292 $^{a''}$	0.718 ± 0.057 $^{a'''}$
2	100.00 ± 0.00 ^{b}	2.646 ± 0.317 $^{b'}$	1.541 ± 0.206 $^{b''}$	0.743 ± 0.069 $^{b'''}$
3	100.00 ± 0.00 ^{c}	1.849 ± 0.238 $^{c'}$	1.278 ± 0.081 $^{c''}$	0.637 ± 0.046 $^{c'''}$
4	48.44 ± 13.18 ^{d}	3.282 ± 0.273 $^{d'}$	0.639 ± 0.293$^{d''}$	0.283 ± 0.097 $^{d'''}$
5	38.59 ± 6.49 ^{e}	1.829 ± 0.114 $^{e'}$	1.313 ± 0.408 $^{e''}$	0.680 ± 0.048 $^{e'''}$
6	100.00 ± 0.00 ^{f}	2.638 ± 0.245 $^{f'}$	1.118 ± 0.040$^{f''}$	0.573 ± 0.058 $^{f'''}$
7	80.46 ± 18.28 ^{g}	2.048 ± 0.027 $^{g'}$	1.442 ± 0.088 $^{g''}$	0.669 ± 0.059 $^{g'''}$
8	100.00 ± 0.00 ^{h}	3.077 ± 0.068 $^{h'}$	0.925 ± 0.072$^{h''}$	0.477 ± 0.072 $^{h'''}$

Anova one way - multiple range test ($p<0,05$): a *vs* d/e/g; b *vs* d/e/g; c *vs* d/e/g; d *vs* f/g/h; e *vs* f/g/h; f *vs* g; g *vs* h; a′ *vs* b′/c′/d′/e′/f′/g′/h′; b′ *vs* c′/d′/e′/g′; c′ *vs* d′/f′/h′; d′ *vs* e′/f′/g′; e′ *vs* f′/h′; f′ *vs* g′; g′ *vs* h′; a″ *vs* d″; b″ *vs* d″/f″/ h″; c″ *vs* d″/h″; d″ *vs* e″/f″/g″; e″ *vs* h″; g″ *vs* h″; a‴ *vs* d‴/f‴/h‴; b‴ *vs* d‴/f‴/h‴; c‴ *vs* d‴/ h‴; d‴ *vs* e‴/f‴/g‴/h‴; e‴ *vs* h‴; g‴ *vs* h‴.

It can be observed that all films, except for the formulation 4, characterized by the highest concentration of PVA and the lowest concentrations of PVP and CS, and formulation 5, prepared with the highest concentrations of PVP and CS and the lowest concentration of PVA, were characterized by high elongation capability. High % elongation indicates a high film deformability/flexibility, that is a high capability to deform under stress without breaking. As for tensile strength, formulations characterized by the lowest CS concentrations showed the highest strength values.

All the films prepared, with the exception of formulations 4 and 8, were able to absorb an amount of buffer higher than their weight. Formulations 4 and 8 showed also the lowest value of gel durability. Such formulations were characterized by low levels of both PVP and CS. The results demonstrated that such polymers were responsible for a slow and high hydration, corresponding to a slow erosion/dissolution and then to a high gel durability.

In Table 5, the estimated effects and the relating P-values, obtained from the analysis of variance (Anova), for each factor and their interaction on each response variable, were reported.

Table 5 -Estimated effects and their statistical significance (P-values) for each factor and their interactions on each response variable of FFD.

	% E (mm/mm)		**TS (N/mm^2)**		**gPBS/g**		**Gel durability (g)**	
	Estimated effect	*P-value*	*Estimated effect*	*P-value*	*Estimated effect*	*P-value*	*Estimated effect*	*P-value*
A: PVA	7.34667	0.0418	-0.102667	0.1689	-0.0285	0.7715	-0.00425	0.8935
B: PVP	2.42333	0.4775	-0.462833	0.0000	0.228667	0.0300	0.162083	0.0001
C: CS	-7.34667	0.0418	-1.19383	0.0000	0.259167	0.0157	0.156917	0.0001
AB	23.3583	0.0000	-0.2105	0.0090	0.197167	0.0570	0.108583	0.0029
AC	33.1283	0.0000	-0.332167	0.0002	-0.097	0.3292	0.00741667	0.8154
BC	-23.3583	0.0000	0.0193333	0.7900	-0.318833	0.0042	-0.11625	0.0017

*For p-value lower than 0.05 a statistical significant effect was observed.

It can be observed that PVA and CS had a significant effect on % elongation, in particular an increase in PVA concentration caused an increase in such parameter, on the contrary an increase in CS concentration determined a decrease of film elongation capability. Such response variable was not significantly affected by PVP concentration. All interactions showed a significant effect (Figure 7).

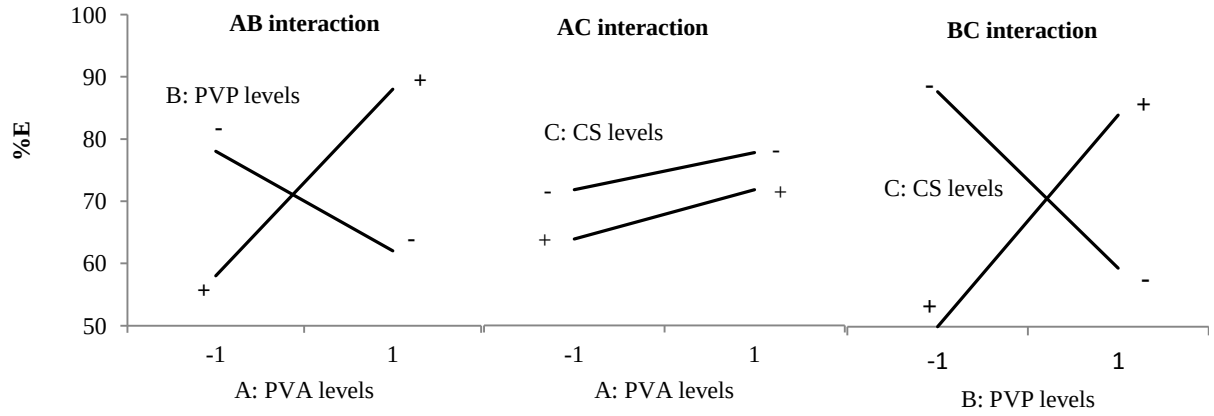

Figure 7 - Interaction plots for the response variable percent elongation of the "full factorial design"

As for PVA-PVP interaction, for the lowest PVA level an increase in PVP concentration was responsible for a decrease of % elongation, while for the highest PVA level an increase in PVP concentration should produce an increase in film deformability. Conversely, for both PVA levels, an increase in CS concentration was expected to cause a decrease of % elongation value. As for PVP-CS interaction, the highest % elongation value was estimated for low levels of both PVP and CS.

As for tensile stress, PVP and CS had a significant negative effect, meaning that an increase in PVP or CS concentrations produced a decrease of such parameter (Table 4), indicating a weakening of film structure. On the contrary PVA level did not affect film mechanical properties. As for PVA-PVP and PVA-CS interactions, the highest tensile strength values was expected for the highest PVA level associated with the lowest PVP or CS levels (Figure 8).

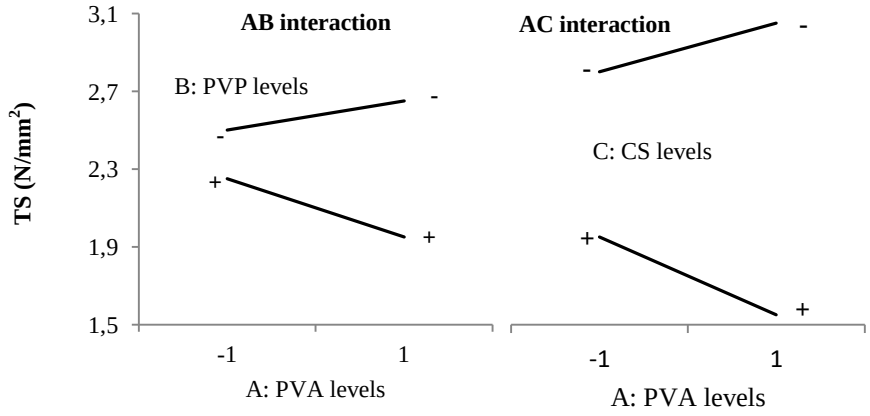

Figure 8 - Interaction plots for the response variable tensile strength of the "full factorial design"

Both PVP and CS concentrations positively affected film capacity to absorb a buffer mimicking wound exudate. As already mentioned, such polymers were responsible for a slow and high film hydration. The effect of PVP level was more pronounced for the highest CS concentration (Figure 9).

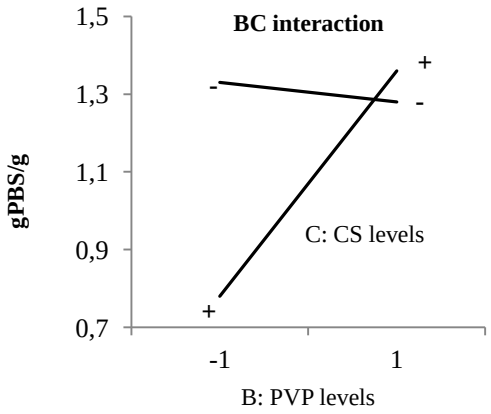

Figure 9 - Interaction plots for the response variable PBS amount absorbed (g/g) per unit weight of the "full factorial design"

When PVP level was fixed at -1, an increase in CS concentration caused a marked decrease in PBS amount absorbed; on the contrary, in the presence of the highest PVP concentration an increase in CS concentration determined a decrease of such parameter, even if of small extent.

PVP and CS concentrations also influenced gel durability, that is gel capability to remain for a prolonged time at the wound site. In particular, an increase in PVP or CS concentrations produced an increase in such parameter. PVA-PVP and PVP-CS interactions showed a significant effect. The highest values of gel durability were expected for the highest PVP level in presence of the highest PVA concentration.

4.4.5.2 Central composite design (CDD)

In Table 6 the experimental results of the additional points investigated to expand FFD to CDD are reported.

Table 6 – % elongation (%E; mm/mm), tensile force (TS; N/mm^2), buffer (PBS) amount absorbed (g/g) and gel durability (g) of the additional films of CCD (mean values ± s.d.; n = 3).

Points of the design	% E (mm/mm)	TS (N/mm^2)	PBS amount absorbed (g/g)	Gel durability (g)
9	64.18 ± 9.72 ^{I}	3.74 ± 0.33 $^{I'}$	0.79 ± 0.12 $^{I''}$	0.29 ± 0.03 $^{I'''}$
10	83.97 ± 10.49 ^{l}	3.12 ± 0.53 $^{l'}$	0.98 ± 0.13 $^{l''}$	0.64 ± 0.03 $^{l'''}$
11	69.13 ± 12.92 ^{m}	3.36 ± 0.11 $^{m'}$	0.88 ± 0.06 $^{m''}$	0.64 ± 0.04 $^{m'''}$
12	100.00 ± 0.00 ^{n}	4.12 ± 0.62 $^{n'}$	0.97 ± 0.08 $^{n''}$	0.56 ± 0.06 $^{n'''}$
13	100.00 ± 0.00 ^{o}	2.74 ± 0.10 $^{o'}$	1.35 ± 0.26 $^{o''}$	0.76 ± 0.06 $^{o'''}$
14	100.00 ± 0.00 ^{p}	3.47 ± 0.08 $^{p'}$	0.30 ± 0.13 $^{p''}$	0.22 ± 0.05 $^{p'''}$
15	100.00 ± 0.00 ^{q}	3.55 ± 0.03 $^{q'}$	1.52 ± 0.35 $^{q''}$	0.69 ± 0.12 $^{q'''}$

Anova one way - multiple range test ($p<0,05$): see also Table 4

a *vs* d/e/g/I/l/m; b *vs* d/e/g/I/l/m; c *vs* d/e/g/I/l/m; d *vs* f/g/h/I/l/m/n/o/p/q; e *vs* f/g/h/I/l/m/n/o/p/q; f *vs* g/I/l/m; g *vs* h/I/n/o/p/q; h *vs* I/l/m; I *vs* l/n/o/p/q; l *vs* m/n/o/p/q; m *vs* n/o/p/q; a′ *vs* b′/c′/d′/e′/f′/g′/h′/I′/l′/m′/n′/o′/p′/q′; b′ *vs* c′/d′/e′/g′/I′/l′/m′/n′/p′/q′; c′ *vs* d′/f′/h′/I′/l′/m′/n′/o′/p′/q′; d′ *vs* e′/f′/g′/n′/o′; e′ *vs* f′/h′/I′/l′/m′/n′/o′/p′/q′; f′ *vs* g′/I′/l′/m′/n′/p′/q′; g′ *vs* h′/ I′/l′/m′/n′/o′/p′/q′; h′ *vs* I′/n′/q′; I′ *vs* l′/n′/o′/p′/q′; l′ vs n′; m′ *vs* n′/o′; n′ vs o′/p′/q′; o′ *vs* p′/q′;

a″ *vs* d″/I″/p″; b″ *vs* d″/f″/h″/I″/l″/m″/n″/p″; c″ *vs* d″/h″/I″/m″/p″; d″ *vs* e″/f″/g″/o″/q″; e″ *vs* h″/I″/m″/p″; f″ *vs* p″/q″; g″ *vs* h″/I″/l″/m″/n″/p″; h″ *vs* o″/p″/q″; I″ *vs* o″/p″/q″; l″ *vs* o″/p″/q″; m″ *vs* o″/p″/q″; n″ *vs* o″/p″/q″; o″ *vs* p″; p″ *vs* q″; a‴ *vs* d‴/f‴/h‴/I‴/n‴/p‴; b‴ *vs* d‴/f‴/h‴/I‴/n‴/p‴; c‴ *vs* d‴/ h‴/I‴/o‴/p‴; d‴ *vs* e‴/f‴/g‴/h‴/ l‴/m‴/o‴/p‴; e‴ *vs* h‴/I‴/n‴/p‴; f‴ *vs* I‴/n‴/p‴; g‴ *vs* h‴/n‴/p‴; h‴ *vs* I‴/l‴/m‴/n‴/p‴; I‴ *vs* l‴/m‴/n‴/o‴/q‴; l″ *vs* o‴/q‴; m‴ *vs* o‴/p‴; n‴ *vs* o‴/p‴/q‴; o‴ *vs* p‴; p‴ *vs* q‴.

Table 7 shows the estimated effects and the relating P-values, obtained from the analysis of variance (Anova), for each factor and their interactions on each response variable.

Table 7 - Estimated effects and their statistical significance (P-values) for each factor and their interactions on each response variable of the "central composite design".

	% E (mm/mm)		**TS (N/mm^2)**		**gPBS/g**		**Gel durability (g)**	
	Estimated effect	*P-value**	*Estimated effect*	*P-value**	*Estimated effect*	*P-value**	*Estimated effect*	*P-value**
A: PVA	-3.43942	0.2935	-0.215376	0.2998	-0.0374002	0.6764	0.0181086	0.5219
B: PVP	6.28152	0.0598	-0.375657	0.0752	0.178422	0.0528	0.179139	0.0000
C: CS	-4.1981	0.2016	-0.837745	0.0003	0.408563	0.0001	0.222457	0.0000
AB	23.3583	0.0000	-0.2105	0.4419	0.197167	0.1028	0.108583	0.0060
AC	33.1283	0.0000	-0.332167	0.2281	-0.097	0.4150	0.00741667	0.8424
BC	-23.3583	0.0000	0.0193333	0.9434	-0.318833	0.0105	-0.11625	0.0035

*For p-value lower than 0.05 a statistical significant effect was observed.

The extension of FFD to CDD, by adding a star design and a central point, showed that no polymer concentration individually affected film elongation. On the contrary, the interactions showed significant effects, in particular a synergic effect for PVA-PVP and PVA-CS interactions and an antagonist one for PVP-CS interaction (Figure 11).

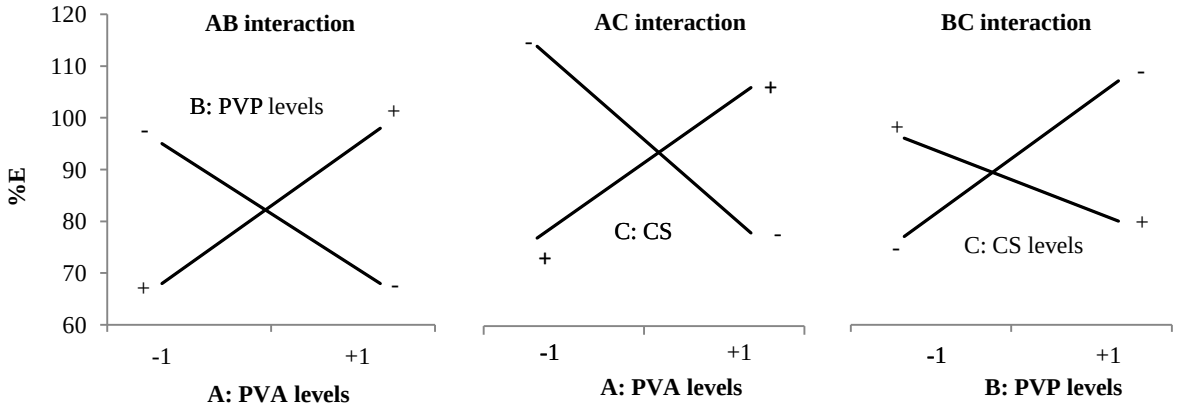

Figure 11 - Interaction plots for the response variable percent elongation of the "central composite design".

As for PVA-PVP and PVA-CS interactions, when a low PVP or CS concentration was considered, an increase in PVA concentration was responsible for a decrease of % elongation; on the contrary, when PVP or CS level was fixed at + 1 an increase in PVA concentration produced an increase in

such parameter. As for PVP-CS interaction, the highest % elongation value is observed for the highest PVP and CS concentrations.

As for tensile stress, the extension of FFD to CDD evidenced a significant effect only for CS. No polymer interaction had a significant effect on such parameter.

As for PBS amount absorbed, no changes on effect of each factor and their interactions were observed upon the extension of FFD to CDD, with the exception of PVP concentration that did not significantly influence film hydration properties.

Also for gel durability no differences were observed upon the extension of FFD to CDD.

Based on the results of the statistical analysis (Anova), an equation of the fitted model for each response variable (percent elongation (%E), tensile strength (TS), hydration properties (gPBS/g) and gel durability) was described. In particular, for each response variable, all the factors and/or their interactions, that did not significantly affect the response parameter considered, were excluded from the general polynomial regression. In such way it was possible to consider the following simplified fitted models (Eq 6-9):

$$\%\,E = 98.8695 - 1.71971 * PVA + 3.14076 * PVP - 2.09905 * CS - 5.33287 * PVA^2 + 11.6792 * PVA * PVP + 16.5642 * PVA * CS - 8.82898 * PVP^2 - 11.6792 * PVP * CS \quad \text{(Eq. 6)}$$

$$TS = 2.97739 - 0.418873 * CS - 0.178079 * CS^2 \quad \text{(Eq. 7)}$$

$$gPBS/g = 1.51733 - 0.0187001 * PVA + 0.0892109 * PVP + 0.204281 * CS - 0.139164 * PVA^2 - 0.151997 * PVP^2 - 0.159417 * PVP * CS - 0.171719 * CS^2 \quad \text{(Eq. 8)}$$

$$\text{gel durability} = 0.657096 + 0.0090543 * PVA + 0.0895696 * PVP + 0.111229 * CS + 0.0542917 * PVA * PVP - 0.0485951 * PVP^2 - 0.058125 * PVP * CS - 0.0426507 * CS^2 \quad \text{(Eq. 9)}$$

These models were graphically interpreted by drawing 2D contour plots and 3D response surface plots. 2D counter plots represent the responses as function of the levels of two factors, while 3D response surface plots showed the responses in third dimension.

From such plots it is possible to derive the best or optimal conditions for each response variable. When the effects of three or more factors are evaluated, bi- and tri-dimensional plots represent only a part of the entire response surface in the experimental domain (Dejaegher and Vander Heyden, 2011).

Moreover, the results of the statistical analysis (Anova) had evidenced that, among the main factors considered, PVA was the less influent on the response variables. For such reason, it was decided to

fix PVA level for the optimization procedure. To choose the PVA concentration to be fixed, the maximum value of each response variable predicted by the simplified fit models for each PVA level, was considered (Table 8).

Table 8 - maximum estimated effects for each PVA level

PVA level	%E (mm/mm)	TS (N/mm^2)	gPBS/g	Gel durability (g)
-1.73	139.454	2.98	1.139	0.65
-1	131.45	3.22	1.458	0.73
0	117.97	3.22	1.578	0.73
+1	117.7	3.22	1.420	0.78
+1.73	80.8	2.98	1.074	0.68

Among PVA levels, only + 1.73 was estimated to produce films characterized by % elongation lower than 100%. High mechanical resistance, hydration propensity and gel durability were observed for +1, 0 and -1 levels. Among these, the lowest PVA level was chosen. For the continuation of the work, PVA level was fixed to -1.

In Figure 12 a, b, c, d, bi- and tri-dimensional plots drawn according to the fit model for each response variable are reported.

a)

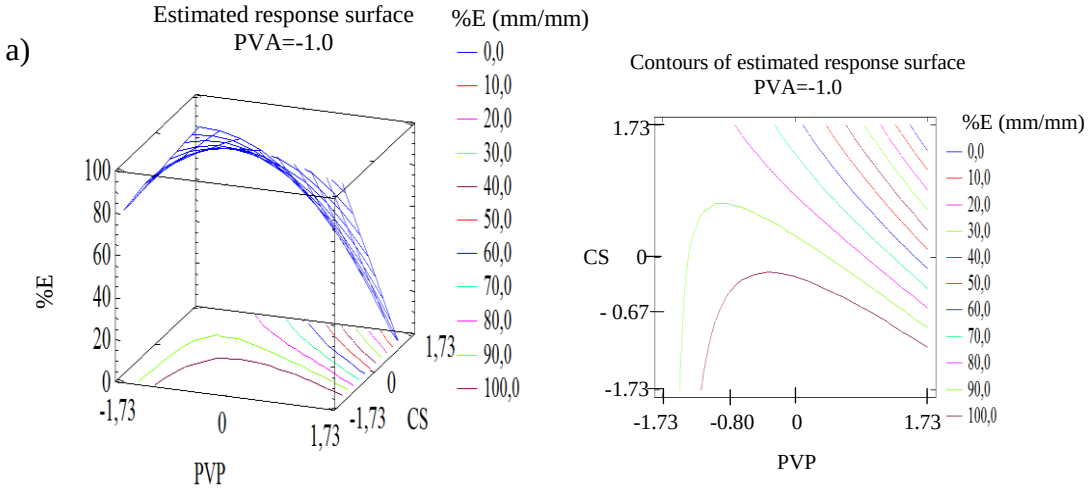

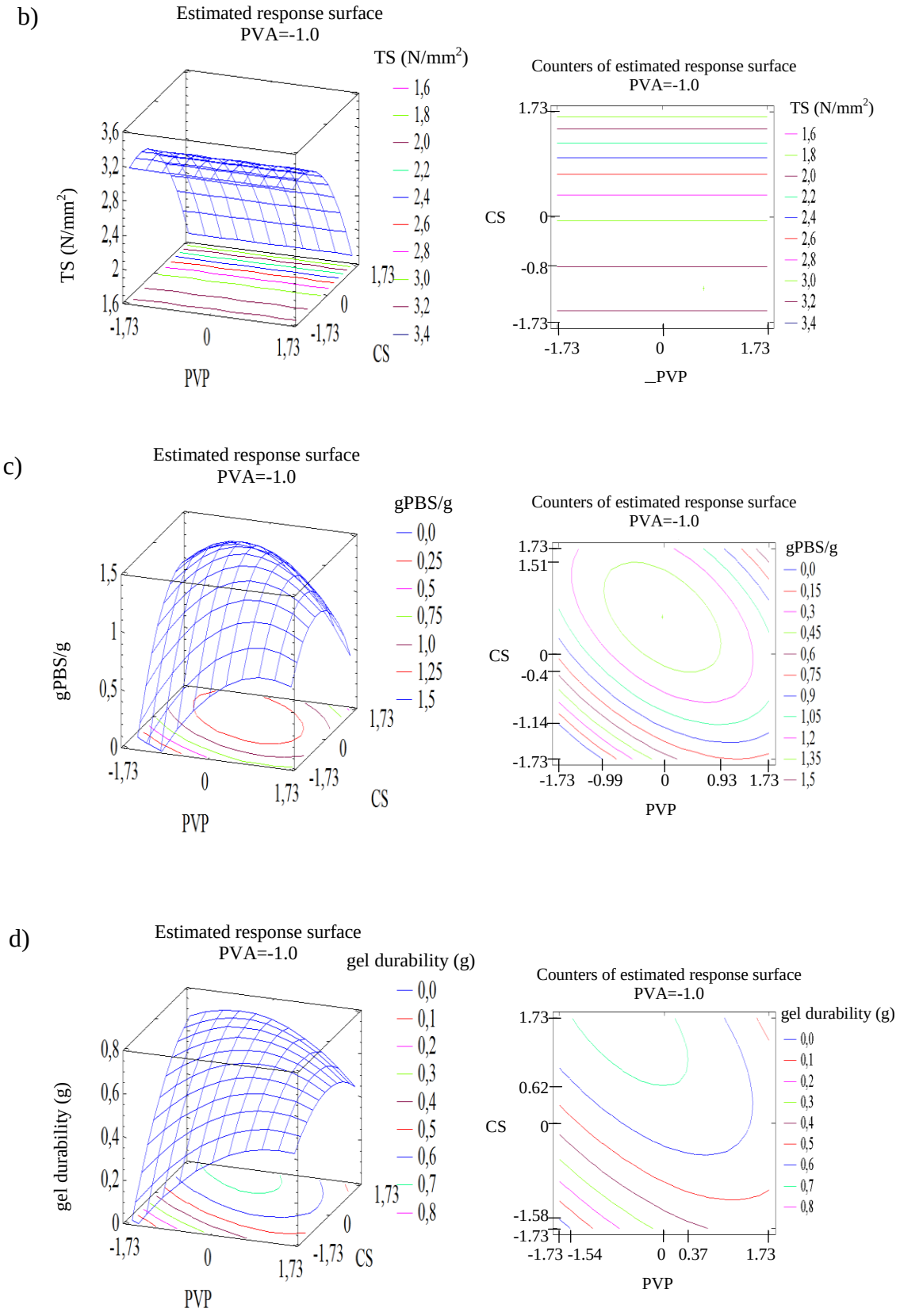

Fig. 12 - Contour plots (in bi- and tri- dimensional projections) drawn according to simplified polynomial model for each response variable of the "central composite design".

The model predicted that the highest value of percent elongation was obtained for PVP and CS concentrations ranging, respectively, into the intervals -0.80 (2.20% w/w) – +1.73 (4.73% w/w) and -0.67 (0.19% w/w) - +1.73 (0.634% w/w) (Figure 12a).

As for tensile strength (Figure 12b), counters plots evidenced the best performance for films characterized by low CS concentration (≤ 0.17% w/w), independently of PVP concentration.

As shown in Figure 12c the model predicted that film formulations, prepared with PVP and CS concentrations ranging, respectively, into the intervals 2.01% w/w (-0.99) – 3.93% w/w (+0.93) and 0.27% w/w (-0.25) – 0.59% w/w (+1.51), were characterized by high capacity to absorb PBS, mimicking wound exudate.

The model, describing the gel durability response, predicted the highest value of such parameter for a PVP concentration between 1.46% w/w (-1.54) and 3.37% w/w (+0.37) and a high CS concentration (≥ 0.431% w/w; +0.62) (Figure 12d).

In general optimal performances do not correspond to a single point but a region of the experimental domain. For this reason, in order to identify the optimal region into the examined domain the individual 2D contour plots were superimposed, satisfying the following constraints: percent elongation ≥ 80%; 3 N/mm^2 ≥ tensile strength ≥ 2.4 N/mm^2 ; (g) of PBS absorbed by unit weight of dressing ≥ 1.0 g/g; gel durability ≥ 0.6 g. The choice of the constrains was based on the following considerations: a high film flexibility is desiderable since an easy film deformation allows a comfortable and simple administration; a suitable mechanical resistance (tensile strength) is required to maintain film integrity during packaging; a good capability to absorb the excess of wound exudate and a prolonged film permanence on the wound site are features useful for the improvement of wound healing. In case of exudative chronic wounds, the use of solid formulations is preferred since they are able to absorb the excess of exudate, rich in metalloproteinases, and to maintain optimal wetting conditions for healing (Boateng and Catanzano, 2015).

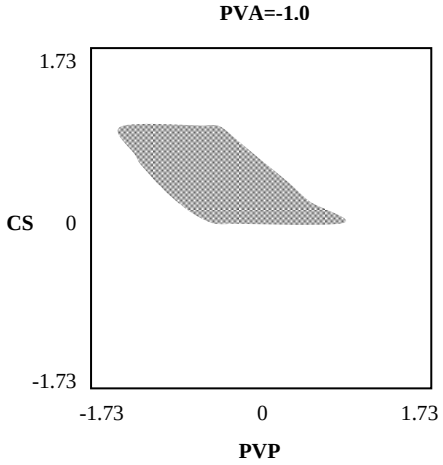

Figure 13 - Combined contour plot showing the region of optimal film composition which satisfies all the constraints of the response variables.

The formulation of optimized composition, chosen inside the region evidenced in Figure 13, was: PVA 11.3% w/w - PVP 2.4% w/w – CS 0.46% w/w – Ser 0.8 % w/w – PHC 2% w/w – Gly 10% w/w.

Table 9 reports the predicted and experimental values obtained for the film of optimized composition.

Table 9 - predicted and experimental values obtained for the formulation of optimized composition (mean values ± ds; n=3)

Response	Predicted values at 95% of confidence	Experimental values
%E (mm/mm)	87 ± 4.3	92 ± 11
TS (N/mm^2)	2.6 ± 0.13	2.7 ± 0.14
gPBS/g	1.44 ± 0.072	1.44 ± 0.080
Gel durability (g)	0.70 ± 0.035	0.703 ± 0.005

It can be observed that the experimental values were comparable to the fitted ones at 95% confidence level. This fact confirmed the prediction power of the regression models.

4.4.6 Characterization of loaded formulation

4.4.6.1 Film CRV-loading capacity

The supernatant gave a maximum absorption peak at 275 nm, as observed for pure CRV and HYBD, confirming the presence of CRV into film.

The loading amount was equal to 100 ± 9 %, with respect to the theoretical one. Such results indicated that the method employed for film preparation did not produce any CRV loss.

4.4.6.2 Rheological properties

Oscillation test is a dynamic method used to for determine elastic (storage modulus G′) and viscous (loss modulus, G″) properties of gel formed upon film hydration (Lippacher et al., 2002).

In Figure 14 loss tangent profile as function of frequency obtained for HYBD- is showed. It can be observed that such parameter, independently of frequency, was lower than 1. This result pointed out that the gel, formed after film hydration, was characterized by a predominance of the elastic properties on the viscous one. High elastic properties are preferred since they are related to gel protective action towards lesion area.

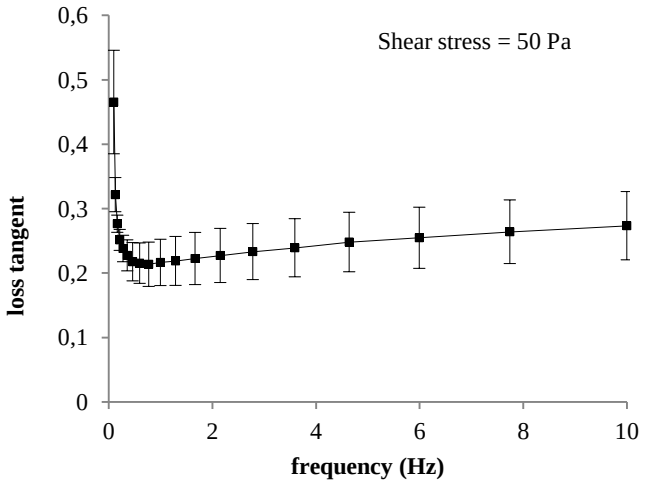

Figure 14 – Loss tangent profiles obtained for HYBD-loaded film. Results are expressed as loss tangent (G″/G′) as a function of frequency (ranging from 0.1 up to 10 Pa) at a constant shear stress (50 Pa).

4.4.6.3 Assessment of *in vitro* release properties

Advanced composite dressings, based on natural and synthetic polymers, have been reported as controlled drug delivery systems (Boateng et al., 2008). Many physical processes are able to control drug release from a polymeric system, such as: hydration polymers by biological fluids, swelling, diffusion of bioactive compounds through the polymeric network and eventual degradation/erosion of the system (Boateng and Catanzano, 2015).

In Figure 15 % CRV released from loaded film and HYBD as a function of time are reported. Statistical ($p<0.05$) differences between % CRV released were observed only at 4 and 8 h: film was characterized by lower values with respect to HYBD. This behavior was due to the formation of a

viscoelastic gel that slowed down CRV diffusion. After 24 h, the superimposition of the released profiles was related to the almost complete dissolution of the polymeric gel: CRV release was only controlled by HYBD.

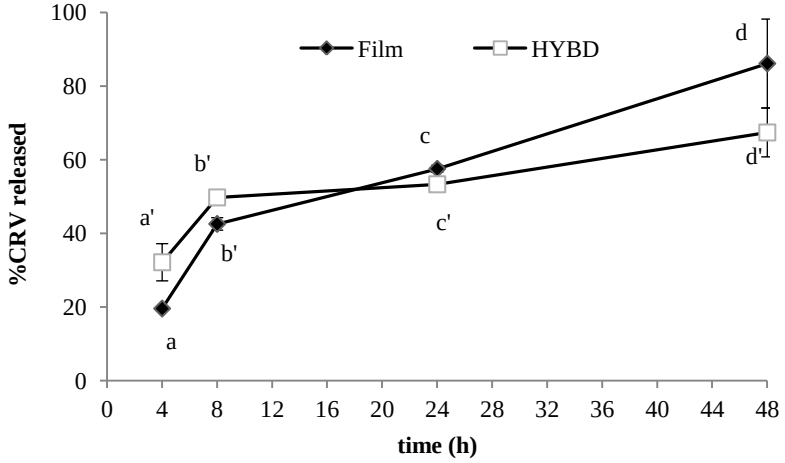

Figure 15 - % CRV released as a function of time (h) for the loaded films and CRV/PHC hybrid (mean values ± s.e.; n=3). T-test ($p<0.05$): a *vs* b/c/d/a′; b *vs* c/d/b′; c *vs* d;. a' *vs* b'/c'/d'; b' *vs* c'/d′; c' *vs* d′.

4.5 CONCLUSIONS

UV-vis spectrophotometry and thermal techniques proved the successful loading of CRV on PHC particles by means of shear mixing method. In particular, TGA analysis pointed out that such a clay was able to protect CRV molecules against evaporation. CRV/PHC hybrid was a stable system at temperature below 80°C. CRV after loading on PHC was able to exert *in vitro* antioxidant and antimicrobial activities. Loading CRV on PHT produced a reduction of CRV cytotoxicity and an increase in CRV antimicrobial activity.

FFD approach allowed to investigate the effects of film composition on the response variables (percent elongation, tensile strength, capability to absorb wound exudate and gel durability) and to determine the main factors. Thanks to the expansion of FFD to CDD, the composition of the film characterized by optimal technological properties was determined.

Film was able upon hydration to form a viscoelastic gel able to protect lesion area and to modulate CRV release up to 8 h. After this time CRV release was controlled by HYBD.

4.6 REFERENCES

Amato, E., Diaz-Fernandez, Y. A., Taglietti, A., Pallavicini, P., Pasotti, L., Cucca, L., Milanese, C., Grisoli, P., Dacarro, C., Fernandez-Hechavarria, J. M., Necchi, V., 2011. Synthesis, characterization and antibacterial activity against gram positive and gram negative bacteria of biomimetically coated silver nanoparticles. Langmuir. 27, 9165−9173.

Bakkali, F., Averbeck, S., Averbeck, D., Idaomar, M., 2008. Biological effects of essential oils − A review. Food Chem. Toxicol. 46, 446−475.

Ben Arfa, A., Combes, S., Preziosi-Belloy, L., Gontard, N., Chalier, P., 2006. Antimicrobial activity of carvacrol related to its chemical structure. Lett. Appl. Microbiol. 43, 149–154.

Boateng, J., Catanzano, O., 2015. Advanced therapeutic dressings for effective wound healing-A review. J. Pharm. Sci. 104, 3653–3680.

Boateng, J.S., Matthews, K.H., Stevens, H.N., Eccleston, G.M.m 2008.Wound healing dressings and drug delivery systems: a review. J. Pharm. Sci. 97, 2892–2923.

Burt, S., 2004. Essential oils: their antibacterial properties and potential applications in foods - a review. Int. J. Food. Microbiol. 94, 223–253.

Campos-Requena, V.H., Rivas, B.L., Pérez, M.A., Figueroa, C.R., Sanfuentes, E.A., 2015. The synergistic antimicrobial effect of carvacrol and thymol in clay/polymer nanocomposite films over strawberry gray mold. LWT-Food Sci. Technol. 64, 390–396.

Ćurić, A., Reul, R., Möschwitzer, J., Fricker, G., 2013. Formulation optimization of itraconazole loaded PEGylated liposomes for parenteral administration by using design of experiments. Int. J. Pharm. 448, 189-197.

Dejagher, B., Vander Heyden, Y., 2009. The use of experimental design in separation science. Acta Chromatogr. 21: 161- 201.

Dejagher, B., Vander Heyden, Y., 2011. Experimental designs and their recent advances in set-up, data interpretation, and analytical applications. J. Pharm. Biomed. Anal. 56: 141-158.

Edris, A,E., 2007. Pharmaceutical and therapeutic potentials of essential oils and their individual volatile constituents: a review. Phytother. Res. 21, 308–323.

Efrati, R., Natan, M., Pelah, A., Haberer, A., Banin, E., Dotan, A., Ophir, A., 2014. The combined effect of additives and processing on the thermal stability and controlled release of essential oils in antimicrobial films. J. Appl. Polym. Sci. 131, 40564-40574.

El-Malah Y., Nazzal S., 2008. Novel use of Eudragit® NE 30D/Eudragit® L 30D-55 blends as functional coating materials in time-delayed drug release applications. Int. J. Pharm. 357, 219–227.

Gorrasi, G., 2015. Dispersion of halloysite loaded with natural antimicrobials into pectins: characterization and controlled release analysis. Carbohyd. Polym. 127, 47–53.

Higueras, L., López-Carballo, G., Cerisuelo, J.P., Gavara, R., Hernández-Muñoz, P., 2013. Preparation and characterization of chitosan/HP-β-cyclodextrins composites with high sorption capacity for carvacrol. Carbohyd. Polym. 97, 262– 268.

Li, J., Zivanovic, S., Davidson, P.M., Kit, K., 2010. Characterization and comparison of chitosan/PVP and chitosan/PEO blend films. Carbohyd. Polym. 79, 786–791.

Lippacher, A., Müller, R.H., Mäder, K., 2002. Semisolid SLN^{TM} dispersions for topical application: influence of formulation and production parameters on viscoelastic properties. Eur. J. Pharm. Biopharm. 53, 155–160.

López-Galindo, A., Viseras, C., Cerezo, P., 2007. Compositional, technical and safety specifications of clays to be used as pharmaceutical and cosmetic products. Appl. Clay Sci., 36: 51–63.

Miguel, M.G., 2010. Antioxidant and anti-inflammatory activities of essential oils: a short review. Molecules. 15: 9252-9287.

Mori, M., Rossi, S., Bonferoni, M.C., Ferrari, F., Sandri, G., Riva, F., Del Fante, C., Perotti, C., Caramella, C., 2014. Calcium alginate particles for the combined delivery of platelet lysate and vancomycin hydrochloride in chronic skin ulcers. Int. J. Pharm. 461, 505–513.

Mori, M., Rossi, S., Ferrari, F., Bonferoni, M.C., Sandri, G., Chlapanidas, T., Torre, M.L., Caramella, C., 2016. Sponge-like dressings based on the association of chitosan and sericin for the treatment of chronic skin ulcers. I. Design of experiments-assisted development. J. Pharm. Sci. 105, 1180-1187.

Muzzarelli, R.A.A., 2009. Chitins and chitosans for the repair of wounded skin nerve, cartilage and bone. Carbohydr. Polym. 76, 167–182.

Pallavicini, P., Taglietti, A., Dacarro, G., Diaz Fernandez, Y. A., Galli, M., Grisoli, P., Patrini, M., Santucci De Magistris, G., Zanoni, R., 2010. Self-assembled monolayers of silver nanoparticles firmly grafted on glass surfaces: Low Ag+ release for an efficient antibacterial activity. J. Colloid Interface Sci. 350, 110-116.

Peng, Y., Zhang, H., Liu, R., Mine, Y., McCallum, J., Kirby, C., Tsao, R., 2016. Antioxidant and anti-inflammatory activities of pyranoanthocyanins and other polyphenols from staghorn sumac (*Rhus hirta L.*) in Caco-2 cell models. .J Funct. Foods. 20, 39–147.

Rossi, S., Faccendini, A., Bonferoni, M.C., Ferrari, F., Sandri, G., Del Fante, C., Perotti, C., Caramella, C., 2013. Sponge-like dressings based on biopolymers for the delivery of platelet lysate to skin chronic wounds. Int. J. Pharm. 440, 207–215.

Rossi, S., Marciello, M., Bonferoni, M.C., Ferrari, F., Sandri, G., Caramella, C., Dacarro, C., Grisoli, P., 2010. Thermally sensitive gels based on chitosan derivatives for the treatment of oral mucositis. Eur. J. Pharm. Biopharm. 74, 248–254.

Safaei-Ghomi, J., Ebrahimabadi, A.H., Djafari-Bidgoli, Z., Batooli, H., 2009. GC/MS analysis and *in vitro* antioxidant activity of essential oil and methanol extracts of *Thymus caramanicus* Jalas and its main constituent carvacrol. Food. Chem. 115, 1524–1528.

Shemesh, R., Krepker, M., Natan, M., Danin-Poleg, Y., Banin, E., Kashi, Y., Nitzan, N., Vaxmanb, A., Segal, E., 2015. Novel LDPE/halloysite nanotube films with sustained carvacrol release for broad-spectrum antimicrobial activity. RSC Adv. 5, 87108 –87117.

Tenci, M., Rossi, S., Bonferoni, M.C., Sandri, G., Boselli, C., Di Lorenzo, A., Daglia, M., Icaro Cornaglia, A., Gioglio, L., Perotti, C., Caramella, C., Ferrari, F., 2016a. Pectin/chitosan particles for the delivery of platelet lysate and manuka honey in chronic skin ulcers. Int. J. Pharm. 509, 59-70.

Tenci, M., Rossi, S., Bonferoni, M.C., Sandri, G., Mentori, I., Boselli, C., Icaro Cornaglia, A., Daglia, M., Marchese, A., Caramella, C., Ferrari, F., 2016b. DoE assisted development of capsules based on biopolymers for the delivery of manuka honey components into skin ulcers. Int. J. Pharm. Available online. http://dx.doi.org/10.1016/j.ijpharm.2016.10.050.

Tunç, S., Duman, O., 2011. Preparation of active antimicrobial methyl cellulose/carvacrol/ montmorillonite nanocomposite films and investigation of carvacrol release. LWT - Food Sci. Technol. 44, 465-472.

Vicentini, D.S., Smania, A., Laranjeira, M.C.M., 2010. Chitosan/poly (vinyl alcohol) films containing ZnO nanoparticles and plasticizers. Mat. Sci. Eng. C. 30, 503-508.

This work was object of a conference presentation:

1. Tenci M., Rossi S., Aguzzi C., Bonferoni M.C., Sandri G., Caramella C.M., Cerezo P., Viseras C., Ferrari F. Development of polymers/hybrids films for the delivery of EOs. 10th A.It.U.N. Annual Meeting "Non-traditional emerging technologies in drug product manufacturing", Parma, May 5-6th 2016 (poster presentation).

Conclusions

In the last decades the therapeutic approaches employed for the wound treatment have progressively changed. Traditional "inert" dressings having as unique target the isolation of the lesion from the infected environment have been replaced by modern ones capable to promote healing. The bioactive properties of modern dressings are due to the use of so-called biopolymers that are able of interacting with tissue components, taking part to the healing process. In the last years, many papers have been published on the use of biopolymers in association with growth factors (GFs), that are recognized as the "leading actors" of wound healing. Since tissue repair cannot be effectively mediated by a single GF, the therapeutic use of hemoderivatives (such as platelet rich preparations) as potential sources of multiple GFs have been recently suggested. This topic has been the object of an active research line of the group where I developed my PhD studies. Starting from this basis, the early two years of my research were devoted to the development of biopolymer-based powders able to deliver a bioactive fraction of manuka honey (MH) in skin ulcers. The biopolymers employed belonged to the class of polysaccharides and included chitosan, hyaluronic acid and pectin. MH fraction, when loaded into the developed formulations, proved to possess an *in vivo* efficacy on animal model comparable to that of the hemoderivative platelet lysate. MH fraction is characterized by undoubted advantages with respect to hemoderivatives, such as an easier availability and manipulation, and a less expensive preparation, that results in an affordable therapy in terms of costs. In addition, the simple methods employed for the production of the developed formulations make them easily obtainable in a hospital pharmacy service and promptly administrable to patients.

Based on polysaccharides (gellan, methyl cellulose and hydroxypropyl cellulose) was also the vehicle developed for the treatment of ulcerative colitis. It was an *in situ* gelling liquid to be locally applied on the damaged mucosa. The innovation of such a vehicle resides in the synergic effect of the polymers employed. While the presence of gellan, responsible for vehicle gelation when in contact with colonic fluid ions, determines a lowering of gelation temperature of methyl cellule in the physiological range, hydroxypropyl cellulose makes the vehicle mucoadhesive. Loading of maqui berry extract into vehicle improves its barrier effect and is responsible for antioxidant properties.

The last year of the research was focused on the development of an *in situ* gelling film loaded with a carvacrol (CRV)/clay hybrid and intended for the treatment of skin ulcers. The combination of CRV with a fibrous clay, paligorskite, protects CVR against evaporation, reduces its cytotoxicity and improves its antimicrobial activity. The developed film was based on polyvinylpyrrolidone, poly (vinyl alcohol) and chitosan glutamate; it formed upon hydration a viscoelastic gel able to protect lesion area and to modulate CRV release up to 8 h.

A “leit motif” of my research has been the employment of DoE approach in the formulation development. Such an approach allowed to save time and efforts in the investigation of the effects of the various excipients on formulation functional properties and in the determination of the optimal formulation composition.

As a final remark, all the formulations developed can be defined “multifunctional” since they combine the bioactive properties of the loaded active principles with those of “enabling” excipients that, acting in synergy, take part to the healing process.